

**MASTER**

**Development of a hysteresis current controller**

Risseeuw, P.M.

*Award date:*  
1998

[Link to publication](#)

**Disclaimer**

This document contains a student thesis (bachelor's or master's), as authored by a student at Eindhoven University of Technology. Student theses are made available in the TU/e repository upon obtaining the required degree. The grade received is not published on the document as presented in the repository. The required complexity or quality of research of student theses may vary by program, and the required minimum study period may vary in duration.

**General rights**

Copyright and moral rights for the publications made accessible in the public portal are retained by the authors and/or other copyright owners and it is a condition of accessing publications that users recognise and abide by the legal requirements associated with these rights.

- Users may download and print one copy of any publication from the public portal for the purpose of private study or research.
- You may not further distribute the material or use it for any profit-making activity or commercial gain

Afstudeerverslag

Development of a hysteresis current  
controller

EMV 98-08

P.M. Risseeuw

Hoogleraar: Prof. dr. ir. A.J.A. Vandenput

Mentor: Dr.-Ing. F. Blaschke

Eindhoven, oktober 1998

## Abstract

In industrial electrical drive systems three-phase asynchronous machines are often used, because they are cheap and robust. To save power in certain applications, it is desirable to change speed, which can be controlled by the frequency of the applied magnetic fields. As a consequence, the speed can be changed by use of an inverter which generates a three-phase supply current, with a variable frequency. The operation of the inverter is based on a kind of pulse width modulation.

For high speed applications (10% to 100% of rated machine speed), commercial inverters are available which operate without use of rotor position encoders. For driving pumps and fans these inverters are suitable.

To operate accurately at lower speed, these inverters need rotor position encoders.

Disadvantage of the use of rotor position encoders is that they are quite expensive and they make the drive system less robust.

At the Eindhoven University of Technology, research has been done on sensorless direct field orientation at zero flux frequency, i.e. controllers which use the measured three stator currents and voltages as feedback only.

For the experimental set-up a current controlled asynchronous machine was required. This can be accomplished by using a hysteresis-controlled current-regulated voltage-sourced inverter.

For the specific application a hysteresis controlled inverter with a stable output current, and low harmonic distortion is necessary.

For this reason, a hysteresis current controller which doesn't use the zero-voltage vector, has been developed. For this purpose a special switching algorithm has been derived. The algorithm uses the six possible voltage vectors equally and always keeps the sequence of switching the same. A big advantage is that the output current shows a very stable, predictable and regular behaviour at low speed. This results then in low harmonic distortion at low speed. At higher speed the hysteresis current controller still shows stable operation, with low harmonic distortion. Estimation of machine parameters is not required.

Zero-voltage vectors are often used to reduce the inverter switching frequency at low speed, because they give a lower current slope, resulting in a longer switching period. Thus avoiding the use of zero-voltage vectors yields an increase of the switching frequency at low speeds.

To reduce the switching frequency to an acceptable value, several measures can be taken:

Reducing the DC-link voltage of the inverter at low speed, increasing the hysteresis band width or connecting inductors between the inverter and machine. The first solution is quite expensive, as a second converter is necessary to get a variable DC-link voltage. The second solution can easily be implemented, but gives a large ripple current at low speed.

Nevertheless a larger ripple current doesn't mean larger harmonic distortion in the frequency band of interest, but gives higher machine losses. A combination of a variable DC-link voltage and variable hysteresis band width gives good results, to keep the switching frequency and ripple current limited.

The effect of connecting inductors between inverter and machine hasn't been investigated.

## Abbreviations

$I_{sa}^*$	[A]	Desired stator current of phase A
$I_{sb}^*$	[A]	Desired stator current of phase B
$I_{sc}^*$	[A]	Desired stator current of phase C
$I_s^*$	[A]	Desired absolute stator current
$I_{sa}$	[A]	Stator current of phase A
$I_{sb}$	[A]	Stator current of phase B
$I_{sc}$	[A]	Stator current of phase C
$I_s$	[A]	Absolute stator current
$I_r$	[A]	Absolute rotor current
$I_{s1}$	[A]	Stator current of phase 1 in a two phase stator reference frame
$I_{s2}$	[A]	Stator current of phase 2 in a two phase stator reference frame
$I_{s0}$	[A]	Stator neutral current
$\Delta I_{sa}$	[A]	Stator current error of phase A
$\Delta I_{sb}$	[A]	Stator current error of phase B
$\Delta I_{sc}$	[A]	Stator current error of phase C
$\Delta I_s^{s1}$	[A]	Stator current error of phase 1 in a two phase stator reference frame
$\Delta I_s^{s2}$	[A]	Stator current error of phase 2 in a two phase stator reference frame
$\Delta I_{s\text{rot}}^{s1}$	[A]	Rotated stator current error of phase 1 in a two phase stator reference frame
$\Delta I_{s\text{rot}}^{s2}$	[A]	Rotated stator current error of phase 2 in a two phase stator reference frame
$I_s^{b*}$	[A]	Desired stator reactive current
$I_s^{w*}$	[A]	Desired stator active current
$I_s^b$	[A]	Stator reactive current
$I_s^w$	[A]	Stator active current
$I_k^w$	[A]	Rotor active current
$U_{sa}$	[V]	Stator voltage of phase A
$U_{sb}$	[V]	Stator voltage of phase B
$U_{sc}$	[V]	Stator voltage of phase C
$U_s$	[V]	Absolute value of stator voltage-vector
$U_r$	[V]	Absolute value of rotor voltage-vector
$U_{dc}$	[V]	DC-link voltage of the inverter
$U_n$	[V]	Neutral voltage of the machine

$E_{sa}$	[V]	Stator EMF voltage of phase A
$E_{sb}$	[V]	Stator EMF voltage of phase B
$E_{sc}$	[V]	Stator EMF voltage of phase C
$E_s^{s1}$	[V]	Stator EMF voltage of phase 1 in a two phase reference frame
$E_s^{s2}$	[V]	Stator EMF voltage of phase 2 in a two phase reference frame
$E_s^s$	[V]	Stator EMF voltage-vector in two phase stator reference frame
$E_s$	[V]	Absolute value of stator EMF voltage vector
$E_r^r$	[V]	Rotor EMF voltage-vector in two phase rotor reference frame
$E_r$	[V]	Absolute value of rotor EMF voltage vector
$\Psi^s$	[Wb]	Flux-vector in stator reference frame
$\Psi^r$	[Wb]	Flux-vector in rotor reference frame
$\Psi^\Psi$	[Wb]	Absolute value of flux-vector
$\varphi^s$	[rad]	Angle between the flux-vector and stator reference axis
$\varphi^r$	[rad]	Angle between the flux-vector and rotor reference axis
$R(\varphi)$	[rad]	Rotation of a vector with an angle $\varphi$
$\varepsilon_s^{r*}$	[rad]	Desired angle between the stator current-vector and rotor reference axis
$\varepsilon_s^r$	[rad]	Angle between the stator current-vector and rotor reference axis
$\varepsilon_s^{s*}$	[rad]	Desired angle between the stator current-vector and stator reference axis
$\varepsilon_s^s$	[rad]	Angle between the stator current-vector and stator reference axis
$\rho^s$	[rad]	Rotor position in stator reference frame
$R_{sa}$	[ $\Omega$ ]	Stator resistance of phase A
$R_{sb}$	[ $\Omega$ ]	Stator resistance of phase B
$R_{sc}$	[ $\Omega$ ]	Stator resistance of phase C
$R_s$	[ $\Omega$ ]	Stator resistance
$R_r$	[ $\Omega$ ]	Rotor resistance
$R_k$	[ $\Omega$ ]	Rotor resistance transformed to stator side
$\hat{R}_k$	[ $\Omega$ ]	Estimated rotor resistance transformed to stator side
$L_{osa}$	[H]	Stator stray inductance of phase A
$L_{osb}$	[H]	Stator stray inductance of phase B
$L_{osc}$	[H]	Stator stray inductance of phase C
$L_{os}$	[H]	Stator stray inductance
$L_{or}$	[H]	Rotor stray inductance
$L_\sigma$	[H]	Stray inductance
$L$	[H]	Main machine inductance
$\hat{L}$	[H]	Estimated main machine inductance

$\delta_1$	[rad]	Angle deviation of current-slope-vector 1
$\delta_2$	[rad]	Angle deviation of current-slope-vector 2
$\delta_3$	[rad]	Angle deviation of current-slope-vector 3
$\delta_4$	[rad]	Angle deviation of current-slope-vector 4
$\delta_5$	[rad]	Angle deviation of current-slope-vector 5
$\delta_6$	[rad]	Angle deviation of current-slope-vector 6
$\gamma$	[rad]	Rotation angle of current-error-vector
$\Delta x_1$	[A]	Current limit cross place shift of current-slope-vector 1
$\Delta x_2$	[A]	Current limit cross place shift of current-slope-vector 2
$\Delta x_3$	[A]	Current limit cross place shift of current-slope-vector 3
$\Delta x_4$	[A]	Current limit cross place shift of current-slope-vector 4
$\Delta x_5$	[A]	Current limit cross place shift of current-slope-vector 5
$\Delta x_6$	[A]	Current limit cross place shift of current-slope-vector 6
$d_1$	[-]	Deflection factor of current-slope-vector 1
$d_2$	[-]	Deflection factor of current-slope-vector 2
$d_3$	[-]	Deflection factor of current-slope-vector 3
$d_4$	[-]	Deflection factor of current-slope-vector 4
$d_5$	[-]	Deflection factor of current-slope-vector 5
$d_6$	[-]	Deflection factor of current-slope-vector 6
$C_1$	[-]	Current limit cross place shift factor
$C_2$	[-]	Current limit cross place shift factor
$n$	[-]	Turns ration of asynchronous machine
$T$	[Nm]	Torque of asynchronous machine

# Contents

<b>1. Introduction</b>	<b>1</b>
<b>2. Hysteresis current controller</b>	<b>3</b>
2.1. Introduction and requirements	3
2.2. Concept new hysteresis current controller	11
2.3. Influence of asymmetry	15
2.4. Producing hexagonal trajectories	23
<b>3. Current control at higher speed</b>	<b>31</b>
3.1. Calculation of EMF	31
3.2. Influence of EMF on the average switching frequency	35
3.3. Influence of EMF on the momentary switching frequency	37
3.4. Harmonic distortion	39
3.5. Constant average switching frequency	42
<b>4. Drive control system</b>	<b>43</b>
4.1. Slip control	43
4.2. Machine parameter identification	46
4.3. Adjusting slip controller based on the load	50
<b>5. Practical set-up</b>	<b>53</b>
5.1. Entire set-up	53
5.2. PCB 1, the hysteresis current controller	53
5.3. PCB 2, the 3-2 converter	54
5.4. PCB 3, the vector rotator	55
5.5. PCB 4, the 2-3 converter	56
5.6. PCB 5, the vector driver	56
5.7. PCB 6, the switching frequency controller	58
<b>6. Conclusion</b>	<b>71</b>
<b>References</b>	<b>73</b>
<b>Appendix</b>	
<b>A. Circuit lay-out of PCB 1: Hysteresis current controller</b>	<b>75</b>
<b>B. Circuit lay-out of PCB2: 3-2 converters</b>	<b>81</b>
<b>C. Data sheet of the D/A converter AD7541A</b>	<b>87</b>
<b>D. Digital Signal Processor routines of the Slip-Controller</b>	<b>95</b>
<b>E. Simulation software for simulation of the hysteresis current controller</b>	<b>103</b>
<b>F. Program to transfer measured data from a Nicolet Oscilloscope to a Personal computer.</b>	<b>109</b>

# 1. Introduction

In industrial electric drive systems, used for pumps and fans for example, asynchronous motors are often used, because they are cheap and reliable. To save power, one has to be able to vary speed. This can be done by use of an inverter between the electricity grid and the machine, which varies the machine's speed by changing the current frequency. Commercially available sensorless drive systems, which operate without use of rotor position encoders, work properly between 10% and 100% of the rated machine speed. At low speed and especially at zero speed, these drive systems need rotor position encoders, which are expensive and make the system less robust.

At the Eindhoven University of Technology, Department of Electrical Engineering, investigation has been done at a drive system which works properly at very low speed, without use of a rotor position encoder, but only with the measured stator currents and voltages as feedback for the controller (Sensorless Direct Field Orientation) [1]. An experimental set-up has been built for this investigation. It consists of a current controlled asynchronous machine, driven by an inverter. The required current controller has to provide low harmonic distortion (in the frequency band between 0 and 300Hz) over the whole speed range. A hysteresis current controller has been chosen for this purpose, because of its simplicity. Nevertheless a classic hysteresis current controller gives too much distortion, especially at higher speed.

This report describes the development of a novel hysteresis current controller. The controller doesn't use zero-voltage vectors, which gives a decrease of harmonic distortion. Due to the stable, predictable and regular behaviour the designed controller meets the requirements.

First the controller has been investigated at low speed conditions. A theoretical analysis of the hysteresis current controller has been made, and the results have been compared with experimental data (chapter 2). After the required behaviour at low speed had been accomplished, the hysteresis controller's behaviour at higher speed has been investigated. The relationship between switching frequency, DC-link voltage and speed is described. The frequency spectrum of the output current has been measured under different conditions, and the resulting line current of the novel current controller has been compared with that of a classic current controller, to establish the improvement (chapter 3).

For investigation of the hysteresis current controller in the practical set-up, it was necessary to keep the machine flux as constant as possible, to exclude its influence on the behaviour of the hysteresis current controller, especially at higher speeds. For this reason a slip controller has been implemented in a DSP system, to drive the current controlled asynchronous machine. For a proper operation of a slip controller, some machine parameters have to be known, i.e. the main inductance and the rotor resistance. Usually it is difficult to determine these parameters, because the inductance is dependent of saturation and the resistance is dependent of temperature. Therefore a relatively easy method to determine the required parameters with use of the load of the experimental set-up is described (chapter 4). Finally, chapter 5 describes the practical set-up, of which one part has been implemented in a digital signal processor and the second part has been build on printed circuit boards.



## 2. Hysteresis current control

### 2.1. Introduction and requirements

The overall drive control system requires a current controlled ac machine, which can be achieved in different ways. A hysteresis current controller, which is a kind of current regulated voltage source, has been chosen because of its simplicity. The asynchronous machine is fed by an inverter, which is connected to a DC voltage source. Figure 2.1 shows such an inverter, which is controlled by a simple hysteresis current controller. Every phase current is measured and subtracted from the desired current signal. The current error is compared with the hysteresis bands. If a phase current is too high the inverter leg of that phase will be switched to the negative voltage rail. If the current is too low the inverter leg will be switched to the positive voltage rail. In this way the three phase currents are controlled independent of each other.

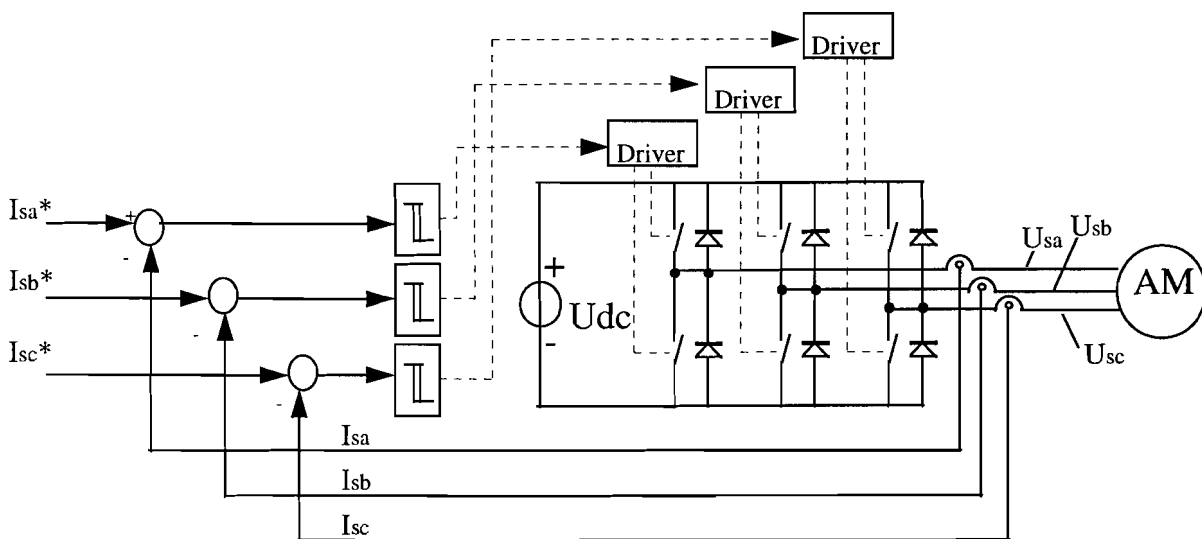


**Figure 2.1: Inverter with hysteresis controller**

Every inverter leg can be switched to the positive or to the negative rail. This results in 8 ways (inverter states) the inverter can be switched (Table 2.1).

**Table 2.1: Eight ways to switch the inverter.**

Inverter state	$U_{sa}$	$U_{sb}$	$U_{sc}$
1	P	N	N
2	P	P	N
3	N	P	N
4	N	P	P
5	N	N	P
6	P	N	P
7	P	P	P
8	N	N	N

If all the inverter legs are switched to the positive rail or to the negative rail at the same time, then the machine terminals are short circuited, which gives a decaying current in all phases (inverter state 7 and 8). This is caused by the floating star point of the three phase stator winding, i.e. the star point is not connected to a fixed potential, for example ground. This makes the three phase currents dependent of each other.

A hysteresis controller in its easiest form (Figure 2.1) attempts to regulate the three phase currents independent of each other. For each phase a hysteresis band is formed around the desired current. If the current is too high in a certain phase, then that phase will be switched to the negative voltage rail, and when the lower current limit is crossed, the phase will be switched back to the positive rail. When the desired current is sinusoidal, the resulting current gets a sinusoidal shape, with a triangular current error. Figure 2.2 shows for a sinusoidal current the hysteresis bands and the current with a triangular current error added. In most cases the hysteresis controller will work correctly, in such a way that the phase current will increase if the corresponding inverter leg is switched to the positive voltage rail, and will decrease if the inverter leg is switched to the negative voltage rail. However, if for example, phase A and phase B are switched to the positive rail and phase C to the negative rail (state 2, Table 2.1), the current in phase C will decrease. If the lower current limit of phase C is crossed, phase C will be switched to the positive voltage rail as well. This means, all the phases are switched to the positive voltage rail (state 7 of Table 2.1), which gives an absolute decreasing current in all the phases. So the phase current of phase C, which crossed the lower current limit is not increasing by switching to the positive rail, but still decreasing, and will leave the hysteresis band. This goes on till the leg of an other phase is switched to the negative rail.

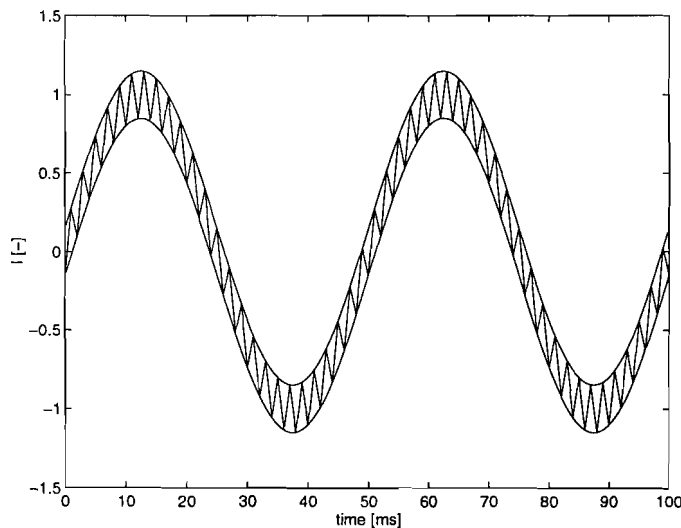


**Figure 2.2: Output current of a hysteresis controlled inverter.**

The three phase stator current system can be transformed into a two coordinate stator current system, by the matrix given in equation ( 2.1). [3]

$$(2.1) \quad \begin{bmatrix} I_{s1} \\ I_{s2} \end{bmatrix} = \begin{bmatrix} 1 & -\frac{1}{2} & -\frac{1}{2} \\ 0 & \frac{\sqrt{3}}{2} & -\frac{\sqrt{3}}{2} \end{bmatrix} \begin{bmatrix} I_{sa} \\ I_{sb} \\ I_{sc} \end{bmatrix}$$

After this transformation the stator current can easily be represented in a current vector diagram.

Figure 2.3 shows an example of a desired current vector in the stator coordinate system, with the corresponding hysteresis current limits of the three phases. Labels have been placed, near each current limit showing, whether it is the upper or the lower limit, and of which phase. Normally the hysteresis controller will take care of keeping the current in the hexagon, formed by the current limits.

In case the machine is fed with a sinusoidal current, the current vector with the hysteresis bands will rotate. The orientation of the hysteresis bands is fixed in the stator coordinate system, which means that the hexagon, formed by the current limits, doesn't rotate, but only shifts to follow the desired current vector.

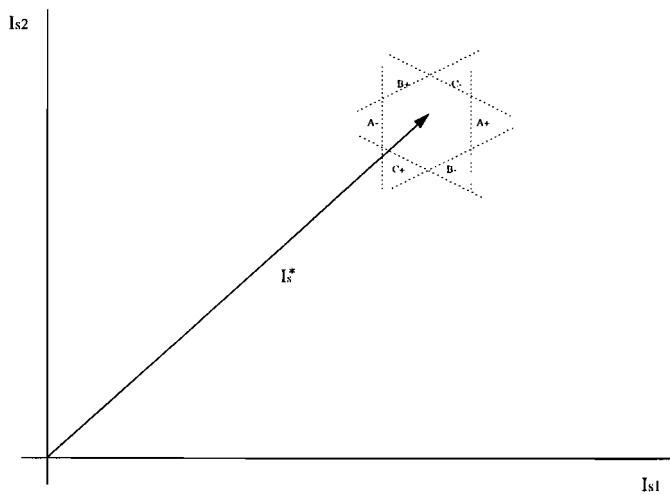


**Figure 2.3: Desired current vector in the stator coordinate system, with the hysteresis bands.**

In order to study the system behaviour further, the model shown in Figure 2.4 has been used for the AC machine. [2]

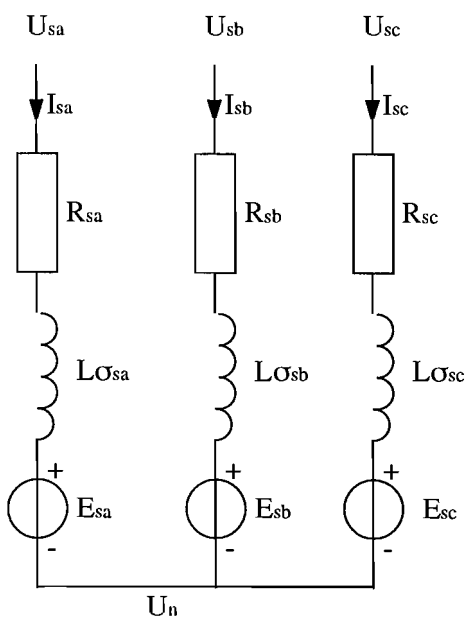


**Figure 2.4: Used machine model.**

This model results in the differential equations ( 2.2) to ( 2.5).

$$( 2.2) \quad \frac{dI_{sa}}{dt} = \frac{U'_{sa} - U_n}{L_{osa}}$$

$$( 2.3) \quad \frac{dI_{sb}}{dt} = \frac{U'_{sb} - U_n}{L_{osb}}$$

$$( 2.4) \quad \frac{dI_{sc}}{dt} = \frac{U'_{sc} - U_n}{L_{osc}}$$

$$( 2.5) \quad I_{sa} + I_{sb} + I_{sc} = 0$$

With:

$$( 2.6) \quad U'_{sa} = U_{sa} - I_{sa} \cdot R_{sa} - E_{sa}$$

$$( 2.7) \quad U'_{sb} = U_{sb} - I_{sb} \cdot R_{sb} - E_{sb}$$

$$( 2.8) \quad U'_{sc} = U_{sc} - I_{sc} \cdot R_{sc} - E_{sc}$$

After differentiating equation ( 2.5) we get:

$$( 2.9) \quad \frac{dI_{sa}}{dt} + \frac{dI_{sb}}{dt} + \frac{dI_{sc}}{dt} = 0$$

Substituting equations ( 2.2) to ( 2.4) into ( 2.9) gives:

$$( 2.10) \quad \frac{U'_{sa} - U_n}{L_{osa}} + \frac{U'_{sb} - U_n}{L_{osb}} + \frac{U'_{sc} - U_n}{L_{osc}} = 0$$

And from equation ( 2.10) can be derived that:

$$( 2.11) \quad U_n = \frac{U'_{sa} \cdot L_{osb} \cdot L_{osc} + U'_{sb} \cdot L_{osa} \cdot L_{osc} + U'_{sc} \cdot L_{osa} \cdot L_{osb}}{L_{osb} \cdot L_{osc} + L_{osa} \cdot L_{osc} + L_{osa} \cdot L_{osb}}$$

At low speed the EMF voltages  $E_{sa}$ ,  $E_{sb}$  and  $E_{sc}$  of the machine can be neglected. As a first approximation the stator resistance will be neglected as well, which makes  $U'_{sa} = U_{sa}$ ,  $U'_{sb} = U_{sb}$  and  $U'_{sc} = U_{sc}$ . Also the stray inductances of the three phases are assumed to be equal. Substituting this in equation ( 2.11) and ( 2.2), ( 2.3) and ( 2.4) gives:

$$( 2.12) \quad U_n = \frac{1}{3}U_{sa} + \frac{1}{3}U_{sb} + \frac{1}{3}U_{sc}$$

$$(2.13) \quad \frac{dI_{sa}}{dt} = \frac{U_{sa} - U_n}{L_\sigma} = \frac{\frac{2}{3}U_{sa} - \frac{1}{3}U_{sb} - \frac{1}{3}U_{sc}}{L_\sigma}$$

$$(2.14) \quad \frac{dI_{sb}}{dt} = \frac{U_{sb} - U_n}{L_\sigma} = \frac{\frac{2}{3}U_{sb} - \frac{1}{3}U_{sa} - \frac{1}{3}U_{sc}}{L_\sigma}$$

$$(2.15) \quad \frac{dI_{sc}}{dt} = \frac{U_{sc} - U_n}{L_\sigma} = \frac{\frac{2}{3}U_{sc} - \frac{1}{3}U_{sa} - \frac{1}{3}U_{sb}}{L_\sigma}$$

From the differential equations (2.13) to (2.15) it can be derived that the current slope for each phase is dependent of the phase voltages. Therefore it is possible to derive in which direction the current vector in the stator coordinate system will move, for the first six ways (states) the inverter can be switched (Table 2.1). The voltage  $U_n$  will be  $1/3U_{dc}$  if two inverter legs are connected to the negative voltage rail and will be  $2/3U_{dc}$  if only one inverter leg is connected to the negative voltage rail. The length of the current slope vectors can be derived from the equations (2.13) to (2.15).

Figure 2.5 shows the construction of the six current slope vectors in the stator coordinate system, which is a sum of the current slope of each phase into the direction of that corresponding phase. The numbers correspond with the inverter state numbers of Table 2.1. The amplitude of each slope vector is given by (2.13)-(2.15).

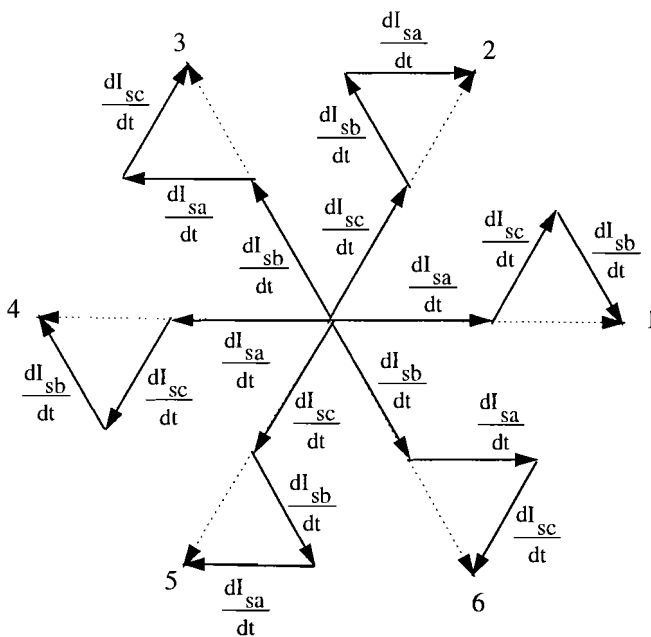


**Figure 2.5: Current slope vectors for six inverter states, neglecting EMF voltages.**

The angle between two adjacent vectors is 60 degrees.

A hysteresis current controller in its easiest form, as described before, switches the three inverter legs independent of each other, depending on which current limits are crossed. If the current vector crosses a current limit of a certain phase, the inverter leg of that phase will be switched to the opposite voltage rail.

Figure 2.6 shows an example how this hysteresis current controller works. The way the current vector goes in case a certain desired current vector is given, is drawn in this figure.

The dashed vector represents the desired current vector  $I_s^*$  and the solid lines represent the real output current of the inverter.

The starting point is at current zero. In practice this situation can occur when the desired current vector is already set at the moment the inverter is switched on. At the starting point three current limits are crossed:

The current limit A-, the current limit B- and the current limit C+. This means the hysteresis controller will switch the A phase and B phase to the positive rail and the C phase to the negative rail. From Table 2.1, can be derived that this corresponds with state 2. Figure 2.5 shows the direction the current vector will follow in the stator coordinate system.

After a while, the current limit B+ is crossed, and the B phase will be switched to the negative voltage rail, resulting in inverter state 1.

The current limits which are crossed after each other, and the corresponding switching of the inverter is given in Table 2.2. A “-” means the negative current limit of that phase is crossed, and a “+” means the positive current limit is crossed. The direction of the current vector can be derived from Figure 2.5. From Figure 2.6 can be concluded that a hexagon-shaped trajectory will appear in this particular case.

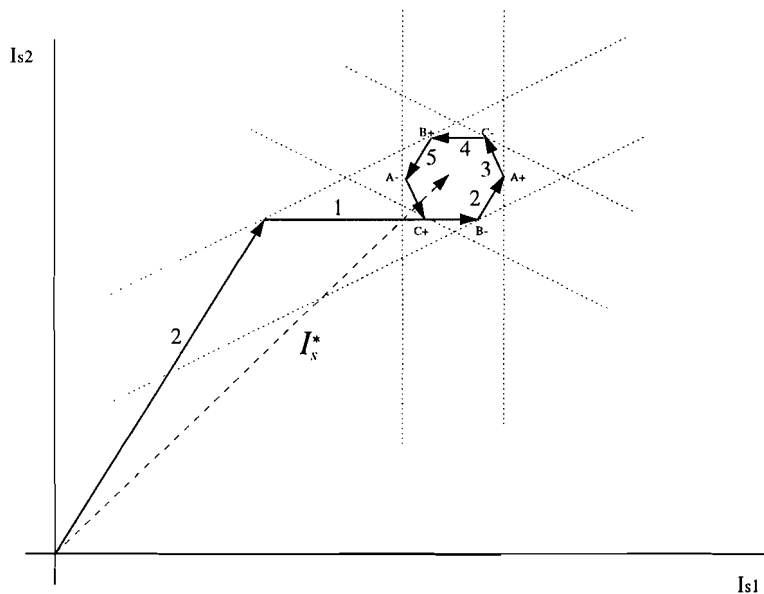


Figure 2.6: A hexagon appears in the ideal case.

Table 2.2: Switching of the hysteresis controller.

Current limits crossed			Output inverter			Inverter state
A	B	C	A	B	C	
-	-	+	P	P	N	2
-	+	+	P	N	N	1
	-		P	P	N	2
+			N	P	N	3
		-	N	P	P	4
	+		N	N	P	5
-			P	N	P	6
		+	P	N	N	1

Notice that the so-called zero-voltage vectors are not switched, i.e. inverter state 7 and 8 are not used in this example. But sometimes it can happen that these vectors are switched. This will be shown in the next example. Figure 2.7 shows again the output current of the inverter. The starting point is again zero current and at that point the current limit A-, the current limit B- and the current limit C+ are crossed. This makes that the hysteresis controller switches into state 2 (Table 2.3). All the next steps are given in Table 2.3. When the current limit C- is crossed, phase C will be switched to the positive voltage rail. As the other two phases were already connected to the positive rail, all phases are connected to the positive rail, which means the inverter is in state 7, and a zero-voltage vector is switched at the machine. This means the current will slowly decrease to zero, which is represented with the dashed vectors in Figure 2.7, till the current limit C+ is crossed. After that, the inverter switches back into state 2 and the current vector goes again in the direction of the current limit C-. After the upper story is repeated once, the current vector crosses the current limit B+ and starts to run in a hexagon. In comparison with Figure 2.6, now the current error runs in clockwise direction, instead of running in counter clockwise direction.

From this example can be concluded that the zero-voltage vectors can be switched if a current limit out of the expected sequence is crossed when the converter is switched in a certain state.

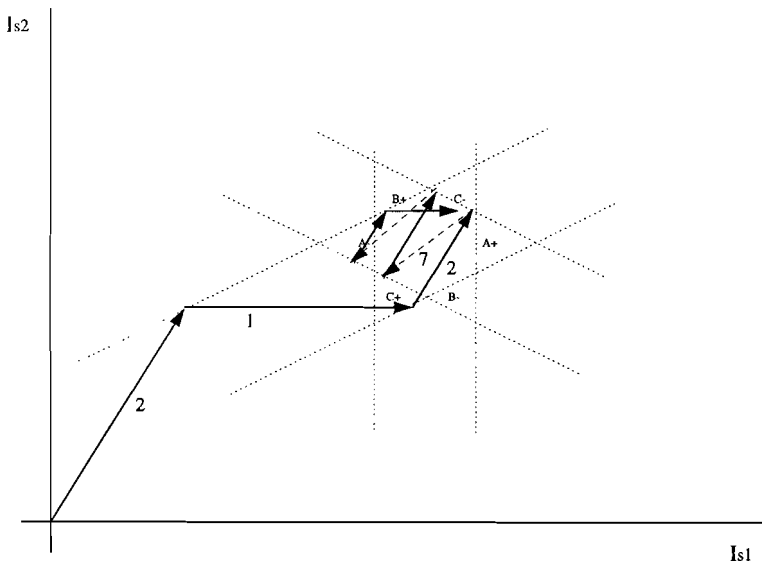


Figure 2.7: Switching with zero-voltage vectors.

Table 2.3: Switching of the inverter, with zero voltage vectors.

Current limits crossed			Output inverter			Inverter state
A	B	C	A	B	C	
-	-	+	<b>P</b>	<b>P</b>	<b>N</b>	2
-	+	+	<b>P</b>	<b>N</b>	<b>N</b>	1
	-		<b>P</b>	<b>P</b>	<b>N</b>	2
		-	<b>P</b>	<b>P</b>	<b>P</b>	7
		+	<b>P</b>	<b>P</b>	<b>N</b>	2
	+	-	<b>P</b>	<b>P</b>	<b>P</b>	7
-		+	<b>P</b>	<b>P</b>	<b>N</b>	2
	+		<b>P</b>	<b>N</b>	<b>N</b>	1

Table 2.4 shows the cases where the zero-voltage vector will be activated, depending on the starting state of the inverter. If the inverter is in the state 1, for example, and the current limit A+ is crossed, then the inverter will switch into state 8.

**Table 2.4: Switching zero voltage vectors.**

Start state	U <sub>sa</sub>	U <sub>sb</sub>	U <sub>sc</sub>	Current limit	Next state	U <sub>sa</sub>	U <sub>sb</sub>	U <sub>sc</sub>
1	P	N	N	A+	8	N	N	N
2	P	P	N	C-	7	P	P	P
3	N	P	N	B+	8	N	N	N
4	N	P	P	A-	7	P	P	P
5	N	N	P	C+	8	N	N	N
6	P	N	P	B-	7	P	P	P

If we compare Table 2.4 with Figure 2.6, we can draw some conclusions:

Normally the current vector will stay in the hexagon formed by the current limits. The current error will have the shape of a hexagon as well, if no zero-voltage vectors are switched. Comparing Table 2.4 and Figure 2.6, shows us that a zero-voltage will be switched if one current limit is skipped in sequence, while the current runs in the hexagon. For example when the inverter state 1 is switched on, normally the current limit B- should be crossed and the inverter would switch into state 2. But if due to an error, the current limit A+ is crossed, a zero-voltage vector is switched on.

When the current error runs in the shape of a hexagon, the average current error will be around zero, which means that the desired current and the real average current match. In practice the switching frequency of the inverter should be about 2 kHz, while line currents up to a frequency of 300Hz will be taken into account. This means the current error will not be noticed, the machine's behaviour will not be affected by this current error, and the machine will act according to the average current.

But if now and then a zero-voltage vector is switched on (which could be the case when a classic controller would be in use), with a corresponding low current slope, the average current error will not stay constant. As it can be derived from Figure 2.7, the current shape is not predictable anymore. Harmonic distortion with low frequencies has been introduced, by means of the low current slope caused by the zero-voltage vectors and by the irregular shape of the current error. In this case the machine's behaviour will be affected by the distorted current error.

In order to be applied in the motor control system, which has been specially designed for research at low speeds, a current control system which gives no harmonic distortion under 300Hz, is required. This can be achieved by keeping the switching frequency of the inverter as constant as possible, and even more important, the error current shape as regular as possible. Therefore the zero-voltage vectors, which give a longer period time and irregular shape, must be excluded.

An other requirement is that the six voltage vectors, which are left, have to be switched equally, i.e. a current error with the shape of a hexagon is desired.

To achieve these requirements, a new hysteresis current controller has been developed.



## 2.2. Concept new hysteresis current controller

The new hysteresis current controller, which has been developed and implemented, consists of two main parts (Figure 2.8).

First of all, we can distinguish the part which compares the measured phase currents with the wished ones. Therefore the measured phase current is subtracted from the wished phase current, which gives the current error for that phase. This is done for all three phases, which gives three current errors. The current errors are compared with the hysteresis current limits, and so can be seen whether a phase current is too high or too low.

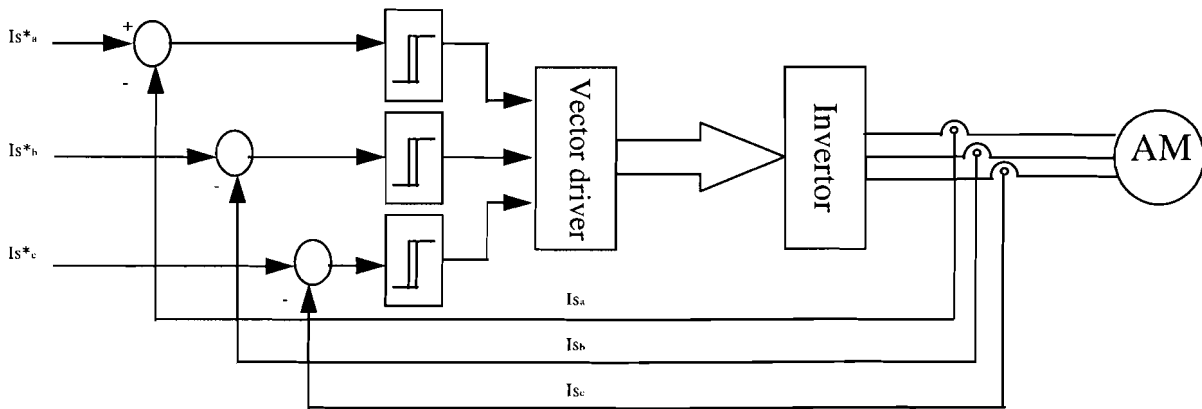


**Figure 2.8: New designed hysteresis controller.**

Second is the so called vector driver, which switches the IGBT's in such a way that the current error stays between the hysteresis bands of the phase currents. No zero-voltage vectors are allowed, and at low speed, i.e. when there is almost no EMF, all six possible voltage vectors have to be switched equally.

This can be achieved by using a driver which can only be switched into six states instead of eight, one for each non-zero voltage vector. In this way the zero-voltage vectors are excluded, because the driver only knows the six non-zero voltage vectors.

The next problem is how to switch the six states (=voltage vectors) in such a way that the shape of the current error trajectory in the stator coordinate system gives a hexagon.

From Figure 2.5 it can be derived, that it is possible to push the current into a certain direction. It should be possible to get a current error with the shape of a hexagon, if the inverter is controlled correctly.

One solution is as follows (Figure 2.9):

Switch the inverter into a certain state if a certain current limit is crossed. If a hexagon, which "runs counter clockwise" is desirable, then the inverter has to switch as given in Table 2.5.

**Table 2.5, switching criterion.**

Current limit crossed	Switch into state
C+	1
B-	2
A+	3
C-	4
B+	5
A-	6

If the current vector crosses the current limit C+ for example, then state 1 will be switched on. The current vector will move towards the current limit B-, and after crossing that vector 2 will be switched. In the same way state 3,4,5 and 6 will be switched after each other if the current limits A+, C-, B+ and A- are crossed. This will result in a hexagon shaped current error and the current error will make cycles counter clockwise.

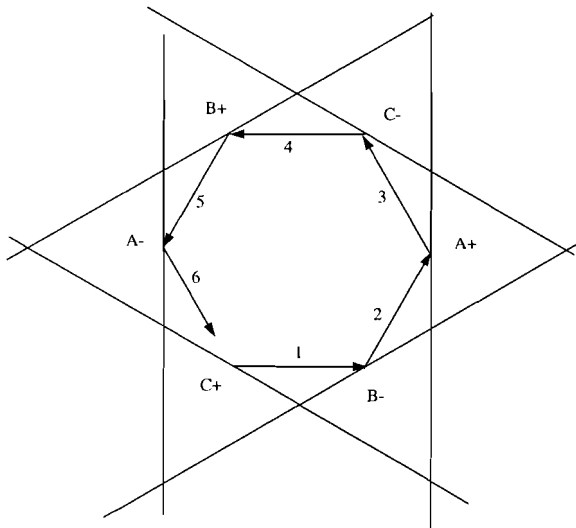


**Figure 2.9: Desired switching, with one current limit crossed.**

So a controller is desired, which provides the right state when the current limits are crossed. But it can occur that two, or even three current limits are crossed, out of the normal hexagonal sequence. More than one limit can be crossed, if the desired current vector makes a step or if the inverter is switched on and there is already a desired current vector. When the machine is running at high speed it is also possible that the current error leaves the hysteresis bands due to the EMF, and more than one current limit will be crossed. In all these cases it has also to be clear which state the inverter has to switch into.

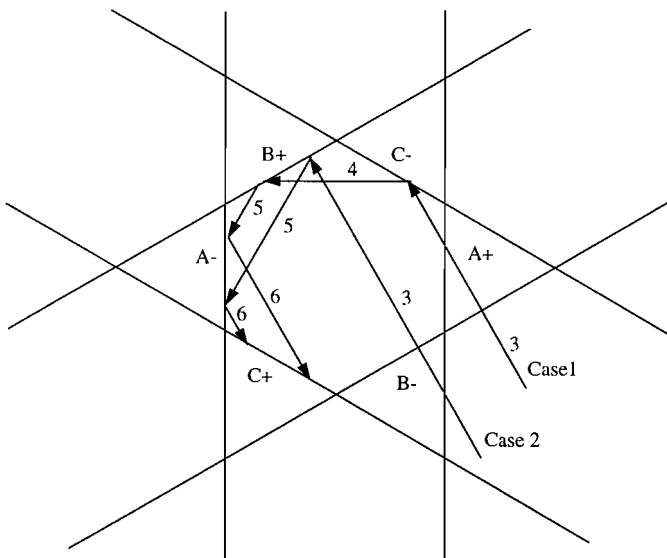


**Figure 2.10: Desired switching, when two current limits are crossed.**

Figure 2.10 shows two examples for the case that two current limits are crossed (case 1 and 2). For both situations the current limit A+ and the current limit B- are crossed at the start. Normally the inverter would switch into state 2 when the current limit B- is crossed, and would switch into state 3 when the current limit A+ is crossed (Table 2.5).

So the situation at the start is undefined and another criterion is required. This criterion is as follows: It is impossible to switch one state back, which means switching back from state 3 to state 2 is excluded. This will result for these particular situations that the inverter will switch into state 3.

For case 1 the current moves towards the current limit C-. After a while, only the current limit A+ is crossed. When the current limit A+ is crossed, state 3 of the inverter is desired (Table 2.5), and so nothing changes while the current moves on towards the current limit C-. When the current limit C- is crossed, the current starts to run in a hexagon.

For case 2 the inverter starts also in state 3. After a while, when the current vector is between the current limits A- and A+, only the current limit B- will be crossed. In that case it is not desirable that the inverter switches back to state 2, because the current would cross the current limit A+ soon again. This would cause the inverter switches back to state 3. An oscillating inverter between state 2 and 3 would be the result, till the current enters the hexagon, formed by the current limits.

But as switching back has been excluded, the inverter doesn't switch back and the current moves towards the current limit C+, where it starts running in a hexagon.

We can conclude that one state switching back of the inverter is not desirable, for two reasons: First one state switching back would give undefined states when two current limits are crossed and second it would cause oscillation of the inverter under certain circumstances.

It is also possible that three current limits are crossed, when the inverter is switched on (if a desired current vector is already applied for example). Figure 2.11 shows two cases. At the starting point the current limits A+, B- and C- are crossed. This would mean that the inverter should switch into state 2, 3 and 4 respectively. If "one and two states switching back" is excluded, then the inverter will switch automatically into state 4 and there will be no undefined state.

In case 1 the inverter starts in state 4, and the current vector moves on, till the current limit B+ is crossed. Then the inverter switches into state 5 and enters the hysteresis bands. Again it is not desirable to switch one state back.

In case 2 the inverter starts with state 4 as well. After a while the current vector is in between the current limit C- and C+. But “switching one state back” has been excluded and the current vector moves on. Next the current limit C+ will be crossed. The vector driver (Figure 2.8) will switch into state 1, because this is not one or two states back. But as the current limit A+ is still crossed, the vector driver will switch immediately from state 1 into state 3. This goes very fast and the inverter hasn't time to switch the IGBT's into state 1, but immediately switches them into state 3. This phenomenon can clearly be seen in Figure 2.12, the resulting logic state diagram of the hysteresis current controller: The vector driver goes from state 4 into state 1 when the current limit C+ is crossed and goes from state 1 immediately into state 3 as the current limit A+ is still crossed.

After switching into state 3, again the current limit C- will be crossed, the inverter will switch into state 4 and will start running in a hexagon.

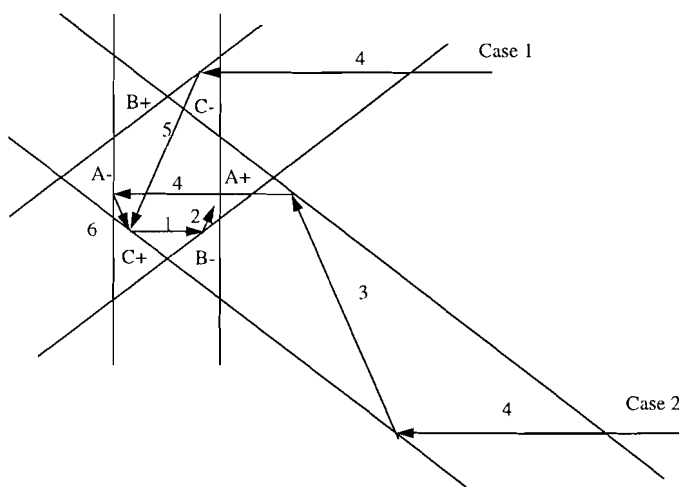


**Figure 2.11: Switching, when the current value at start is outside three current limits.**

In general, when a current limit is crossed, a corresponding voltage vector will be switched. If no current limit is crossed, the controller stays at its former state.

When the current is outside the hexagon, and is moving towards the center of it, along a current limit, fast switching between two states can occur. To avoid this negative effect, “switching one and two steps back” has been excluded. For example switching from 3 to 2 and from 3 to 1 is not possible. This exclusion also makes the driver switches into one defined state if more than one current limit is crossed.

In Figure 2.12 the resulting logic state diagram of the hysteresis current controller is given.

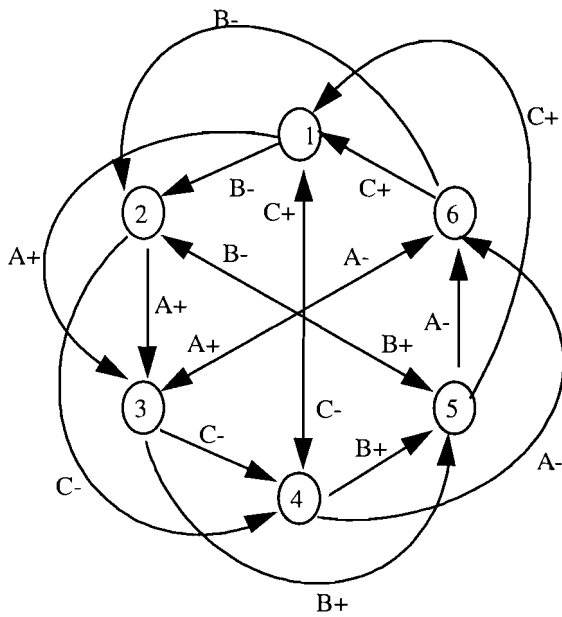


Figure 2.12: The logic state diagram of the hysteresis current controller.

### 2.3. Influence of asymmetry.

To check the performance of the hysteresis current controller, as described in 2.2, the total system has been simulated. First the behavior at low speed has been investigated. For these simulations the influences of the stator resistance and the EMF are neglected and the stray inductances are assumed to be equal. This means that the simplified equations ( 2.13) to ( 2.15) have been used.

The simulated result, given in Figure 2.13, shows that in the ideal case a current error with the shape of a hexagon in the stator coordinate system appears.

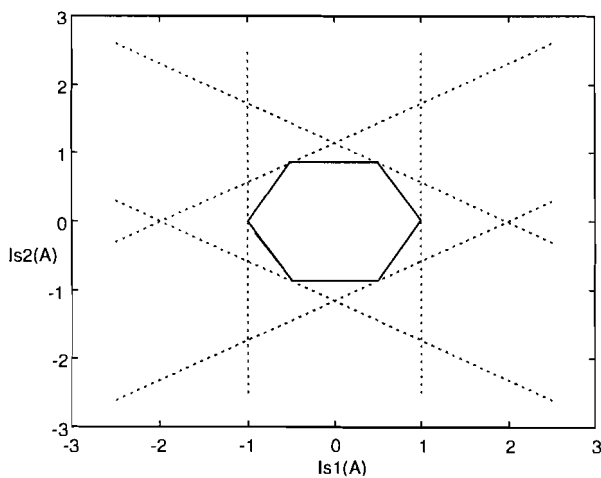
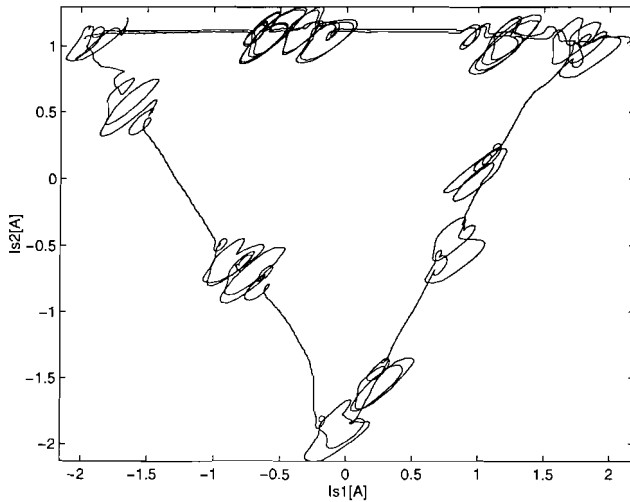


Figure 2.13: Simulated current error, with ideal machine and controller.

The hysteresis current controller, as described in 2.2, has been built and some measurements have been done. The measured current error, given in Figure 2.14, has a triangular shape. This means that only three of the six possible voltage vectors are being activated. In this case the vectors 2, 4 and 6.



**Figure 2.14: Measured current error.**

From the measurements it has been determined that the orientation of the triangle is independent of the desired current, i.e. when the machine rotates slowly the triangular shaped current error doesn't rotate in the stator coordinate system. The explanation for this triangular shaped current error lies on the deflection of the current slope vectors, as follows. For the ideal case, the angles between the different current slope vectors (Figure 2.5) is 60 degrees. There are three main causes which can introduce a deviation at these angles:

- \* Influence of the stator resistances of the three stator phases.
- \* Differences in the stray inductances of the three stator phases.
- \* Asymmetry in the hysteresis band widths.

Figure 2.15 shows what happens when an angle deviation in one current slope vector is introduced. The dashed lines represent the current when no errors are introduced. In that case the current always arrives at the starting point. The solid line is drawn for the case that current slope vector 1 (state 1 of the inverter) is rotated with a negative angle deviation. From the figure can be derived that the current doesn't arrive at the starting point, but below it. This will result in the current error running into a triangular shape as given in Figure 2.14.

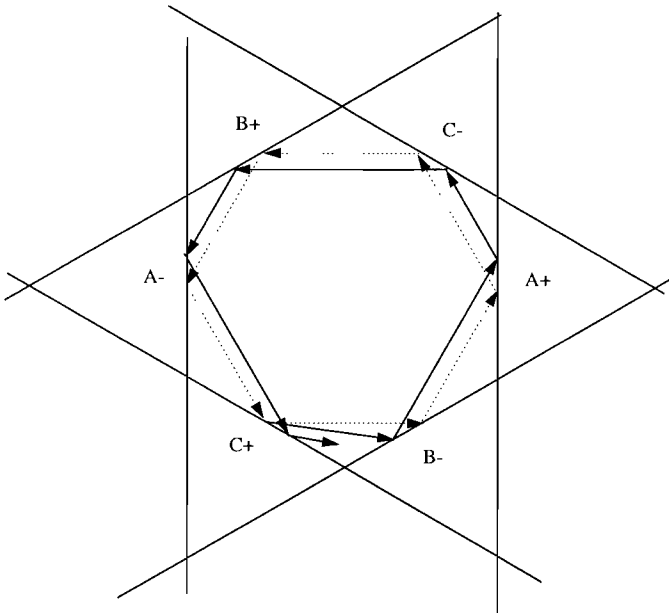


**Figure 2.15: Influence of angle deviations at the current error shape.**

To investigate the influence of the three main causes of the deflection of the current slope vectors, some simulations with equal stator resistance's, asymmetric stray inductances and asymmetric hysteresis bands have been carried out.

First of all, the influence of the stator resistance of the machine at the stator current has been investigated. Three equal stator resistances have been taken into account. From the differential equations ( 2.2) to ( 2.4), it can be derived what happens to the current slope vectors. Figure 2.16 shows for a particular case, a certain DC-link voltage and a certain stator current vector, what happens to the current slope vectors. For this example the following stator phase currents have been chosen:  $I_{sa} = I$ ,  $I_{sb} = -\frac{1}{2}I$  and  $I_{sc} = -\frac{1}{2}I$ . The positive phase current  $I_{sa}$  gives a positive voltage drop over  $R_{sa}$ . This results in a decreasing current slope  $\frac{dI_{sa}}{dt}$  for a positive phase voltage  $U_{sa}$ , and an increasing current slope for a negative phase voltage.

The negative phase currents  $I_{sb}$  and  $I_{sc}$  give a negative voltage drop over  $R_{sb}$  and  $R_{sc}$ . This results in an increasing current slope for a positive phase voltage of the corresponding phase, and results in a decreasing current slope for a negative phase voltage. The influence of these changes in current slope on the direction of the current slope vectors is given in Figure 2.16. This figure shows that the resulting current slope vectors (dashed vectors, Figure 2.16) deflect due to the stator resistance's influence. The deflection is given by the so called angle deviations  $\delta_1$  to  $\delta_6$ . The angles are both positive and negative and are dependent on the stator currents as given by the differential equations ( 2.2) to ( 2.4). So the current slope vectors are not constant, because the current is not constant when the hysteresis current controller is switching between the hysteresis bands.

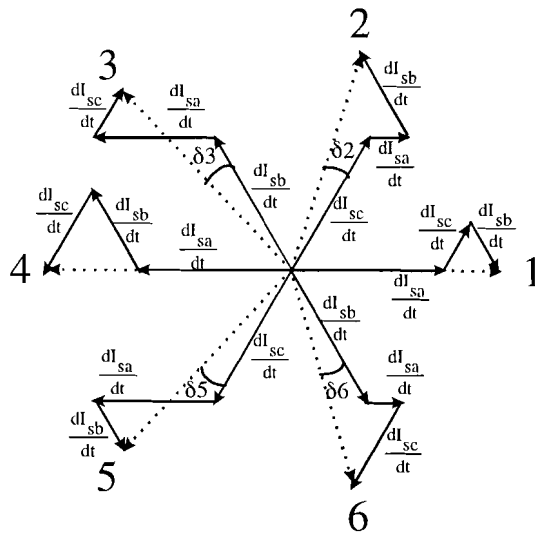


**Figure 2.16: Current slope vectors, taking equal stator resistances into account.**

When we have a look at the differential equations ( 2.2) to ( 2.4), it is obvious that the angle deviations given in Figure 2.16 change when the desired current vector (and the real one) changes, either in direction (rotation) or length.

Simulations have been carried out, without neglecting the stator resistances

( $R_{sa}=R_{sb}=R_{sc}=0.228\Omega$ ). The simulations have been done for several desired current vectors.

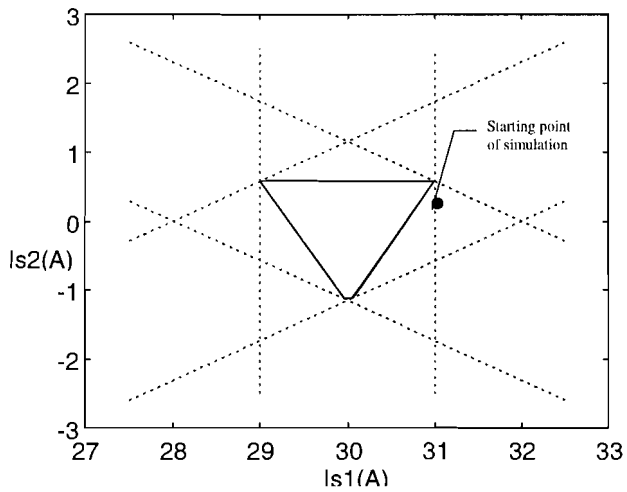
From the simulations it can be derived that the influence of the stator resistance doesn't count that much when the applied phase voltage is much higher than the voltage drop over the resistance. The current slope sets the direction of the current vector. If the phase voltage is high, then the influence of the stator resistance at this slope is low (equations ( 2.2) to ( 2.4)). That's the reason it takes a certain time till the current error gives a stable shape.

After a while, a triangular shaped current error appears. Figure 2.17 shows a simulation with the stator resistances taken into account. The starting point of the current vector is also given. Several simulations with a changing desired current vector have been carried out. The orientation of the triangle seems to be independent of the desired current vector. This means that the triangle doesn't rotate when the desired current vector rotates.

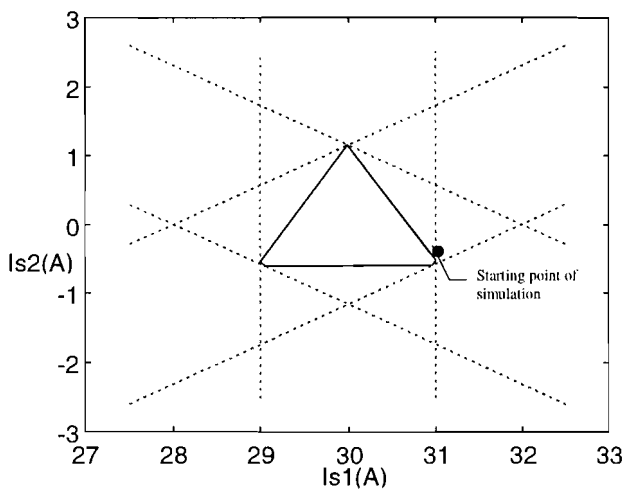
The orientation of the triangle is only dependent on the starting point of the simulation.

Figure 2.18 shows a result of a simulation with the same desired current vector, but with an other starting point as used in the simulation of Figure 2.17.





**Figure 2.17: Simulation with stator resistances.**



**Figure 2.18: Simulation with stator resistance's and another starting point.**

From these simulations it can be derived that the influence of the stator resistances gives a triangular shaped current error.

Next the influence of asymmetric stray inductances has been investigated. From equations ( 2.2) to ( 2.4) can be derived that the current slope

$\frac{dI}{dt} \sim \frac{1}{L\sigma}$  for each phase. This suggests that asymmetry in stray inductances has strong influence on the current slope vectors.

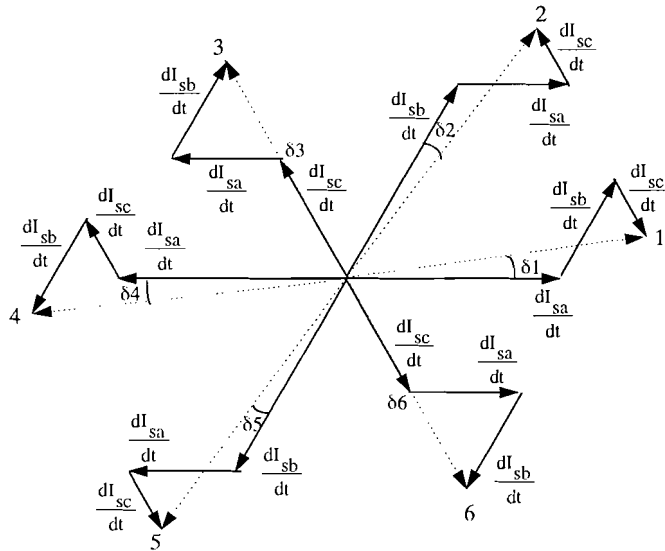


**Figure 2.19: Current slope vectors, with asymmetric stray inductances.**

Figure 2.19 shows the current slope vectors in the case that  $L_{\sigma sb}$  is larger than  $L_{\sigma sa}$  and  $L_{\sigma sc}$ .

This results in a decreasing current slope  $\frac{dI_{sb}}{dt}$ . From the figure can be derived that this

decrease of current slope gives a rotation of the current slope vectors 1, 2, 4 and 5. For the so called angle deviations can be written:  $\delta_1 = \delta_4$  and  $\delta_2 = \delta_5$ .

Some simulations have been carried out with an increased  $L_{\sigma sb}$ . For the simulations the next parameters are chosen:

$$L_{\sigma sb} = 1.1 L_{\sigma sa}$$

$$L_{\sigma sc} = L_{\sigma sa}$$

Figure 2.20 shows a result of the simulations with the chosen parameters. The influence of the stator resistances has been neglected by assuming the resistances to be zero in the model. From these simulations can be derived that asymmetry in stray inductances doesn't give a triangular shaped current error in the stator coordinate system, but an irregular hexagon.

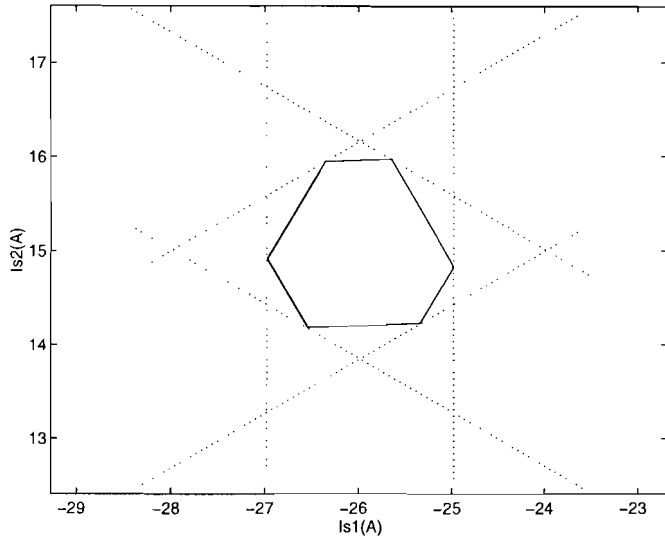


**Figure 2.20: Simulation with asymmetric stray inductances.**

The reason is that the angles  $\delta_1 = \delta_4$  and  $\delta_2 = \delta_5$ . The rotation introduced by the current slope vectors compensates each other, i.e. the rotation of current slope vector 1 gives a certain error which is compensated by the error given by current slope vector 4. This makes the current vector always arrives at its starting point, which gives a stable, but irregular hexagonal shaped current error.

At last the influence of asymmetry in hysteresis band widths has been investigated by doing simulations. For the simulations the current limit  $A_+$  has been increased with 5% to 105% (Figure 2.22). This means when the current error vector reaches the current limit  $A_+$ , it takes a longer way and therefore more time, till the controller switches. In Figure 2.21 it can be seen clearly what the influence at the current error vector is. Due to the larger current limit, the current error vector shifts up every time it crosses this current limit. This goes on till the current current vector “walks” in a triangle in steady-state operation. There is no influence of the initial conditions.

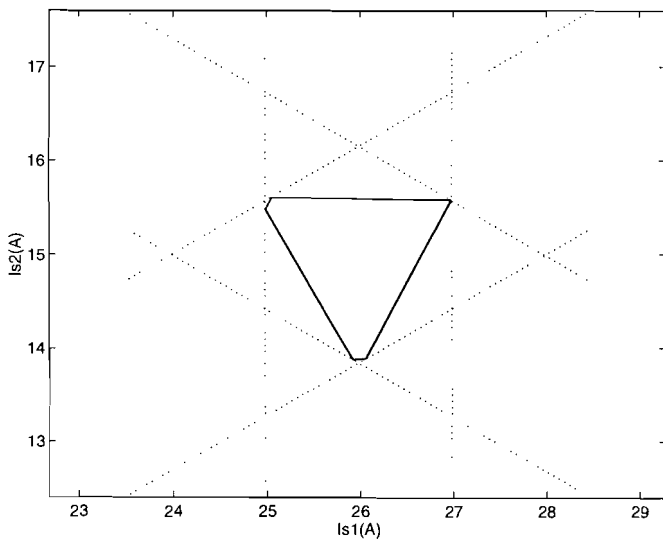


**Figure 2.21: Current error with asymmetric hysteresis bands.**

In this case the orientation of the triangle is independent of the desired current vector, because the asymmetry, which causes this shape, is coupled with the hysteresis bands. And these don't rotate in the stator coordinate system, as the desired current vector rotates.

An increase of the current limit  $A+$  has the same effect as rotating the current slope vector 1 with a positive angle. Figure 2.22 shows what happens in this case. The dashed vectors are the ones without rotation, but in case of an increased current limit  $A+$ . The solid vector is rotated over an angle  $\delta_2$  and crosses, after switching into state 3, the current limit  $C-$  at the same place. Increasing a current limit gives the same result as rotating the current slope vector with a positive angle and decreasing gives the same result as rotating the current slope vector with a negative angle.

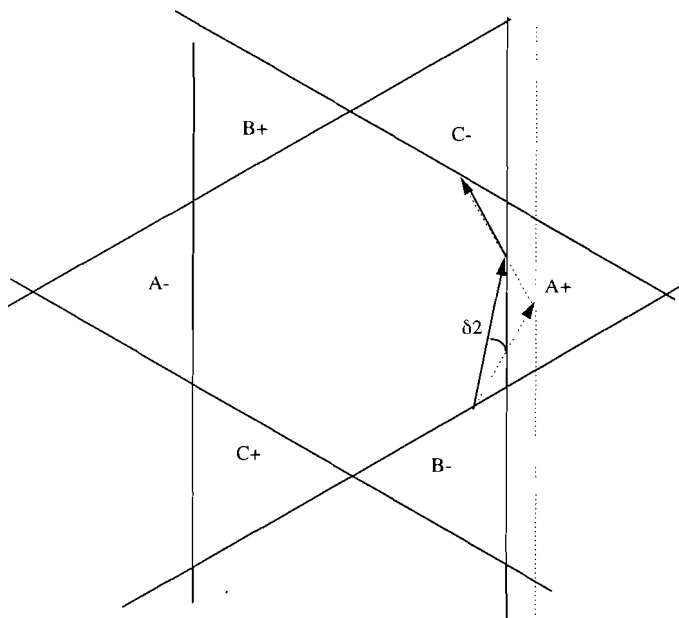


**Figure 2.22: Asymmetric hysteresis band has the same effect as rotation.**

We can conclude that deflection of the current slope vectors in general can cause a triangular shaped current error instead of a hexagonal shaped one.

The influence of the stator resistances and asymmetry of hysteresis bands causes a triangular shaped current error as well. But when only asymmetry of the stray inductances is taken into account, an irregular hexagonal current error is the result. In the latter case the influences of the angle deviations introduced by the asymmetry seem to compensate each other.

From the simulations we can conclude that the orientation of the triangle can change when the influence of the stator resistances is taken into account. The orientation of the triangle is fixed if there is only asymmetry in the hysteresis bands.

The measurements show that the orientation of the triangle is fixed as well. Of course the stator resistances have to be taken into account, and there will be some asymmetry of the stray inductances, but the influence of the asymmetric hysteresis bands seems to be dominant.

## 2.4. Producing hexagonal trajectories.

The next step is to determine under which circumstances the current error will run in a hexagon. For this purpose we have to know what happens if an angle deviation  $\delta$  is applied to a certain current slope vector. If a deviation is applied the current vector will cross the next current limit at another place in regard to the original case. The shift between these two places is called  $\Delta x$ , which will be negative if  $\delta$  is negative. Figure 2.23 shows a part of the hexagon, formed by the current limits. The two current limits with a current slope vector form a triangle.

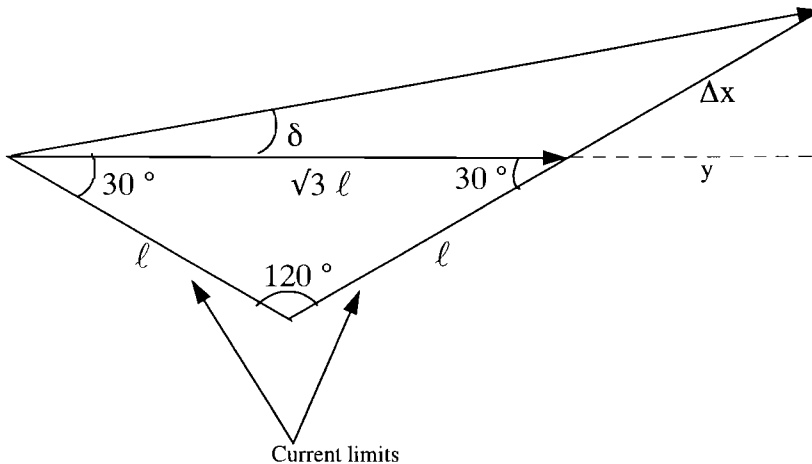


Figure 2.23: Influence of the angle deviation at current limit cross place.

The “current limit cross place shift”,  $\Delta x$ , can be calculated as follows:

$$(2.16) \quad y \cdot \tan(30^\circ) = [\sqrt{3} \cdot l + y] \tan(\delta)$$

$$(2.17) \quad y = \frac{\sqrt{3} \cdot l \cdot \tan(\delta)}{\tan(30^\circ) - \tan(\delta)}$$

$$(2.18) \quad \Delta x = \frac{y}{\cos(30^\circ)} = \frac{2 \cdot \tan(\delta)}{\tan(30^\circ) - \tan(\delta)} \cdot l$$

This can be written as

$$(2.19) \quad \Delta x = l \cdot d$$

with “d” being a function of “ $\delta$ ”.

$$(2.20) \quad d = \frac{2 \cdot \tan(\delta)}{\tan(30^\circ) - \tan(\delta)}$$

Figure 2.24, shows the current error, which runs in a hexagon for a particular case. Now it is possible to calculate the “current limit cross place shift” for the six current slope vectors with

equation ( 2.19). The first shift,  $\Delta x_1$ , can easily be calculated with equation ( 2.19). For the next shifts the former shift also has to be taken into account, by means of subtracting it. If there is only an angle deviation at the first current slope vector, then this will still have influence at the final  $\Delta x_6$ . The calculation of each shift is given by equation ( 2.21). Finally it can be derived that  $\Delta x_6$  is dependent on  $\Delta x_1$  to  $\Delta x_5$  and also on  $d_1$  to  $d_6$  and  $\delta_1$  to  $\delta_6$ . At the starting point 'a' and 'b' (Figure 2.24) can be determined. After calculating one cycle ( $\Delta x_1$  to  $\Delta x_6$ ) 'a' and 'b' have to be determined again for the next cycle because the starting point has changed.

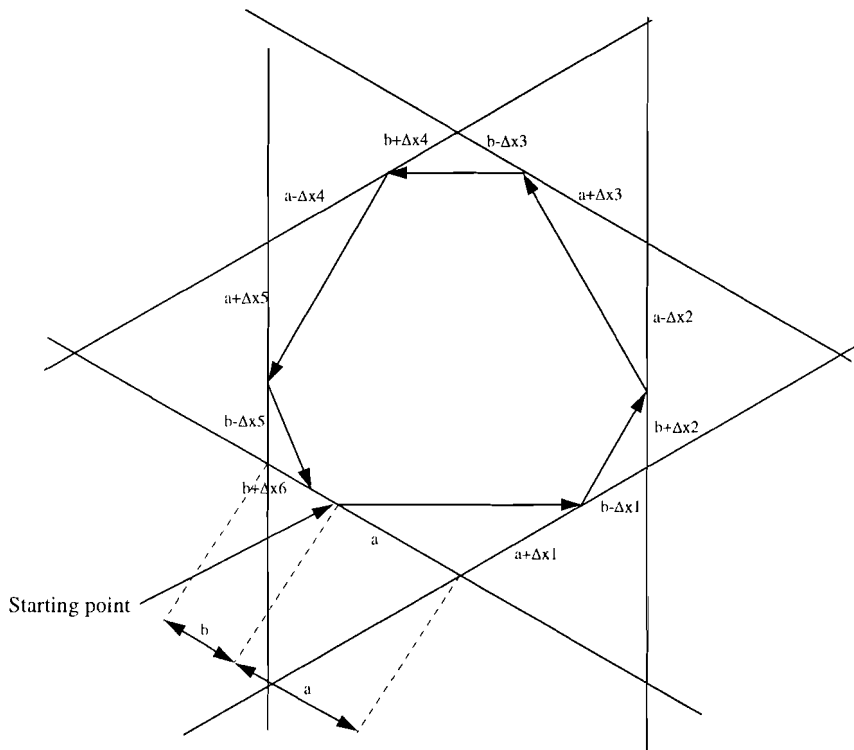


**Figure 2.24: Calculation of the “current limit cross place” for each current slope vector.**

$$\begin{aligned}
 (2.21) \quad \Delta x_1 &= a \cdot d_1 \\
 \Delta x_2 &= (b - \Delta x_1) d_2 - \Delta x_1 \\
 \Delta x_3 &= (a - \Delta x_2) d_3 - \Delta x_2 \\
 \Delta x_4 &= (b - \Delta x_3) d_4 - \Delta x_3 \\
 \Delta x_5 &= (a - \Delta x_4) d_5 - \Delta x_4 \\
 \Delta x_6 &= (b - \Delta x_5) d_6 - \Delta x_5
 \end{aligned}$$

with  $a + b = \text{constan } t$

It is possible to write  $\Delta x_6$  as a function of  $d_1$  to  $d_6$  as given in equation ( 2.22).

( 2.22)

$$\begin{aligned}\Delta x_6 = & -[d_1 + d_3 + d_5 \\ & +d_1d_2 + d_1d_3 + d_1d_4 + d_3d_4 + d_1d_5 + d_3d_5 + d_1d_6 + d_3d_6 + d_5d_6 \\ & +d_1d_2d_3 + d_1d_2d_4 + d_1d_3d_4 + d_1d_2d_5 + d_1d_3d_5 + d_1d_4d_5 \\ & +d_3d_4d_5 + d_1d_2d_6 + d_1d_3d_6 + d_1d_4d_6 + d_3d_4d_6 + d_1d_5d_6 + d_3d_5d_6 \\ & +d_1d_2d_3d_4 + d_1d_2d_3d_5 + d_1d_2d_4d_5 + d_1d_3d_4d_5 + d_1d_2d_3d_6 \\ & +d_1d_2d_4d_6 + d_1d_3d_4d_6 + d_1d_3d_4d_6 + d_1d_2d_5d_6 + d_1d_3d_5d_6 + d_1d_4d_5d_6 + d_3d_4d_5d_6 \\ & +d_1d_2d_3d_4d_5 + d_1d_2d_3d_4d_6 + d_1d_2d_3d_5d_6 + d_1d_2d_4d_5d_6 + d_1d_3d_4d_5d_6 \\ & +d_1d_2d_3d_4d_5d_6] \cdot a \\ & +[d_2 + d_4 + d_6 \\ & +d_2d_3 + d_2d_4 + d_2d_5 + d_4d_5 + d_2d_6 + d_4d_6 \\ & +d_2d_3d_5 + d_2d_4d_5 + d_2d_3d_6 + d_2d_4d_6 + d_2d_5d_6 + d_4d_5d_6 \\ & +d_2d_3d_4d_5 + d_2d_3d_4d_6 + d_2d_3d_5d_6 + d_2d_4d_5d_6 \\ & +d_2d_3d_4d_5d_6] \cdot b\end{aligned}$$

This can also be written as:

( 2.23)  $\Delta x_6 = C_1 \cdot a + C_2 \cdot b$

with  $C_1$  and  $C_2$ :

( 2.24)

$$\begin{aligned}C_1 = & -d_1(1 + d_2 + d_4 + d_6) - d_3(1 + d_1 + d_4 + d_6) - d_5(1 + d_1 + d_3 + d_6) \\ & -d_1d_2d_3(1 + d_4) - d_1d_2d_4(1 + d_5) - d_1d_2d_5(1 + d_3) \\ & -d_1d_3d_5(1 + d_4) - d_1d_4d_5(1 + d_6) - d_3d_4d_5(1 + d_6) \\ & -d_1d_2d_6(1 + d_3) - d_1d_3d_6(1 + d_4) - d_1d_4d_6(1 + d_2) \\ & -d_1d_5d_6(1 + d_2) - d_3d_5d_6(1 + d_1) \\ & -d_1d_3d_4 - d_3d_4d_6 \\ & -d_1d_2d_3d_4d_5(1 + d_2) \\ & -d_1d_2d_3d_4d_5 - d_1d_2d_3d_4d_6 - d_1d_2d_3d_5d_6 - d_1d_2d_4d_5d_6\end{aligned}$$

$$\begin{aligned}
C_2 &= d_2(1+d_3+d_5)+d_4(1+d_2+d_5)+d_6(1+d_2+d_4) \\
(2.25) \quad & d_2d_3d_5(1+d_4)+d_2d_3d_6(1+d_5)+d_2d_4d_6(1+d_3)+d_2d_5d_6(1+d_4) \\
& +d_2d_3d_4+d_2d_4d_5+d_4d_5d_6 \\
& +d_2d_3d_4d_5d_6
\end{aligned}$$

For a stable operation  $\Delta x_6$  has to be zero, which means that the current vector arrives at the starting point after one cycle. Under these conditions the current error will run in a hexagon and the lengths “a” and “b” will have a constant value.

If the current doesn't end at the starting point then “a” and “b” will change for the calculations of the next cycle. It is possible that the current error leaves its stable mode which results in a change of “a” and “b”. If “a” is too large and “b” too small then  $\Delta x_6$  has to be positive to make the current runs back into its stable mode. For the other case, when “a” is too small and “b” is too large,  $\Delta x_6$  has to be negative. This can be achieved if  $C_1$  is positive and  $C_2$  is negative. If  $C_1$  is negative and  $C_2$  is positive, then from equation (2.23) can be derived that for stable operation both ‘a’ and ‘b’ have to be negative, which is impossible. This involves an unstable operation and the current error will run into a triangle, because the current error is pushed into a corner of the hexagon formed by the current limits. If both  $C_1$  and  $C_2$  are negative then for stable operation ‘b’ has to be negative and ‘a’ positive (2.23). The current error will still run in a hexagon, but will leave the hysteresis bands. Figure 2.25 shows the result of a simulation with both  $C_1$  and  $C_2$  negative, by means of  $\delta_1 = \delta_2 = \delta_3 = \delta_4 = \delta_5 = \delta_6 = \gamma = -50$  degrees.

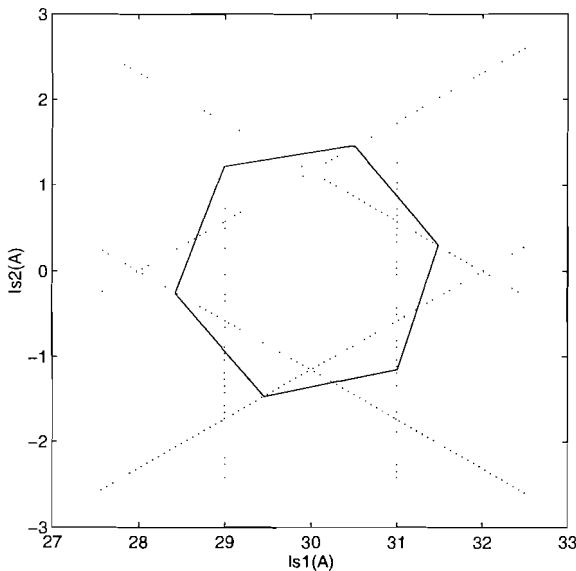


**Figure 2.25: Simulated current error, with both  $C_1$  and  $C_2$  negative,  $\gamma = -50$  degrees.**

To investigate under which angles  $C_1$  is positive and  $C_2$  negative the angles  $\delta_1$  to  $\delta_6$  are assumed to be equal to  $\gamma$ . Figure 2.26 shows a plot of  $C_1$  and  $C_2$  for different  $\gamma$ . From this plot



can be concluded that the current error will run into a stable hexagonal shape if the angle deviations  $\delta_1$  to  $\delta_6$  are between -30 degrees and 0 degrees.

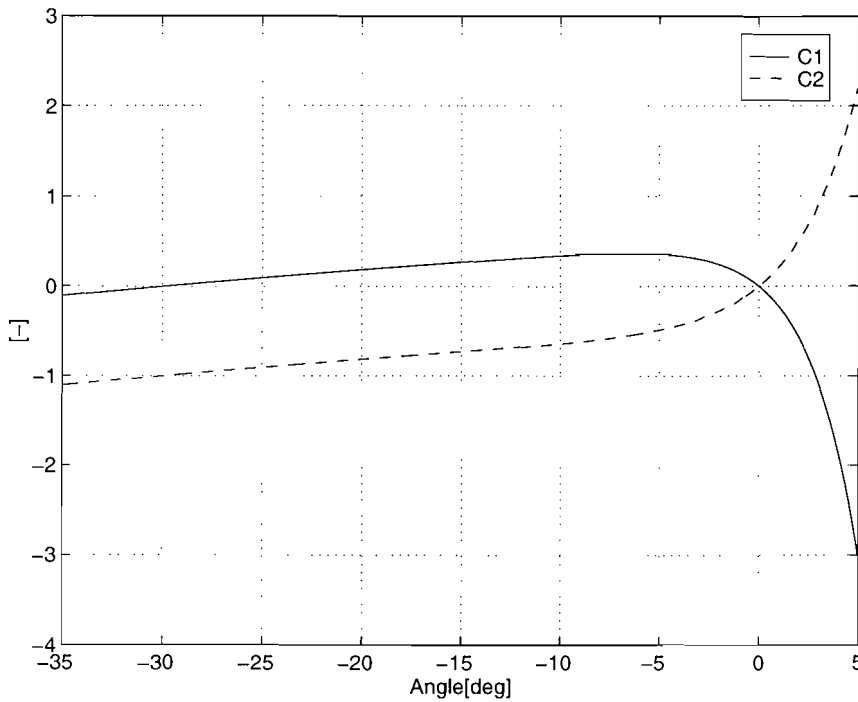


**Figure 2.26:  $C_1$  and  $C_2$  as a function of  $\gamma$**

In normal operation, at low speed the angle deviations  $\delta_1$  to  $\delta_6$ , given by the machine (due to asymmetry in stator resistances and stray inductances) will be small and so  $C_1$  and  $C_2$  will be around zero. This means unstable operation can occur, and will result in a triangular shaped current error. If all the angle deviations are between -30 degrees and 0 degrees, the hysteresis current controller will operate in a stable mode. If the angle deviations, given by the machine, would be increased in an artificial way, stable operation would be guaranteed. This can be done by rotating the current error with a negative angle  $\gamma$ , before comparing it with the hysteresis bands

Figure 2.27 shows a possible solution: First the current error is transformed from a three phase system to a two axis system. This is done to make it easier to rotate the current error vector. After rotating the current error over a certain angle  $\gamma$  (with  $\gamma$  negative), it is transformed back to a three phase system, to be able to compare the three phase currents with the three hysteresis bands. In this way an angle deviation is effectively applied to the six current slope vectors.

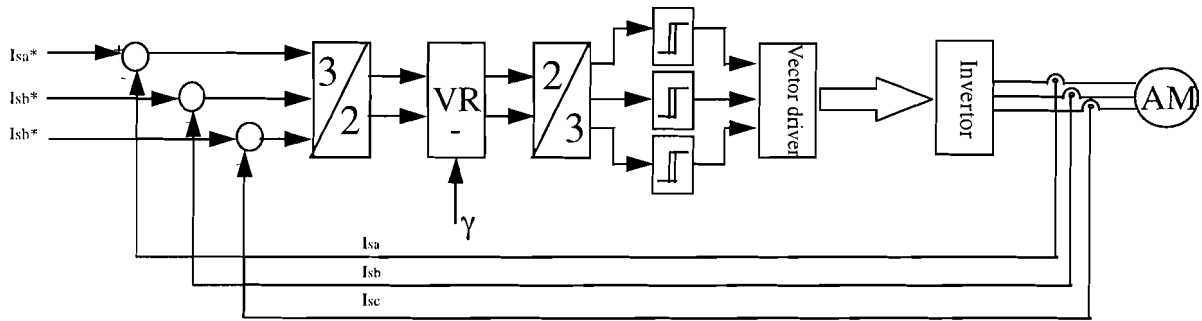


**Figure 2.27: Hysteresis current controller with vector rotator.**

From Figure 2.26 it can be derived that a stable operation is guaranteed if  $\gamma$  is between -30 degrees and 0 degrees. If  $\gamma$  is chosen small about -6 degrees, the individual angle deviations  $\delta_1$  to  $\delta_6$  will have their influence in regard to  $\delta$ , and an irregular shaped current error hexagon will be the result. If  $\gamma$  is chosen larger, about -15 degrees, the individual influence of the angles  $\delta_1$  to  $\delta_6$  will be less in regard to  $\delta$  and a more regular shaped current error hexagon will be the result. If the rotation angle  $\gamma$  is chosen too large, unstable operation can occur at higher speed, when the EMF has to be taken into account. This EMF also has its influence at the angle deviations  $\delta_1$  to  $\delta_6$  and when  $\gamma$  is too large, the total angle deviation could be more than -30 degrees, which means the current error leaves the hysteresis bands. This can give problems, as the real current goes in an other direction as the one projected by the hysteresis bands, and in reality other current limits will be crossed as it is seen by the hysteresis current controller. In the extreme case, when the total angle deviation is 180 degrees, for example, the hysteresis current controller can't work properly at all, because every time a wrong current slope vector will be switched on. So it may be clear that the angle deviation introduced by the vector rotator has to be as small as possible, but on the other hand not too small, to avoid an irregular shaped current error. In the experimental set up a rotation angle  $\gamma$  of -15 degrees has been chosen.

Figure 2.28 and Figure 2.29 show the simulated and measured stator current for  $\gamma = -15$  degrees. In comparison with Figure 2.14, the current error now runs in the shape of a hexagon if the current error vector is rotated with a negative angle.

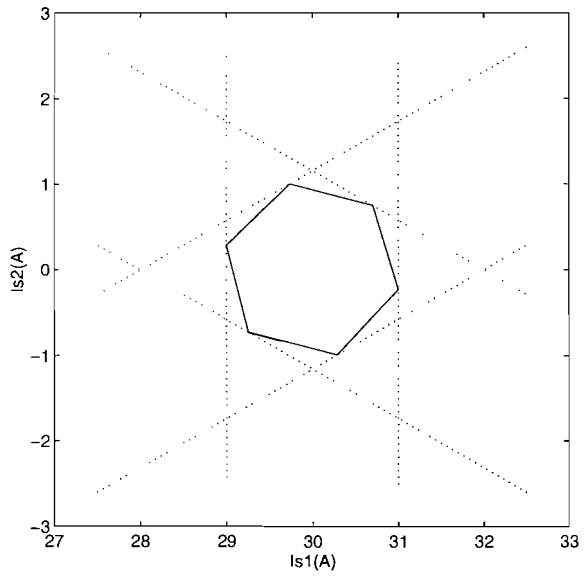


**Figure 2.28: Simulated stator current, with  $\gamma = -15$  degrees**

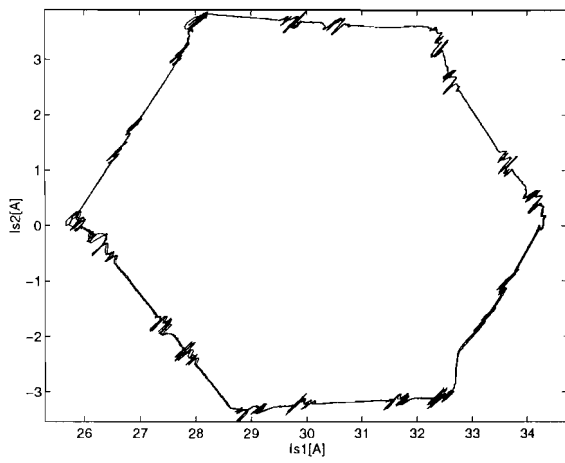


**Figure 2.29: Measured stator current, with  $\gamma = -15$  degrees.**

### 3. Current control at higher speed

#### 3.1. Influence of EMF on current error trajectory

At higher speed the EMF of the machine can't be neglected anymore and has to be taken into account considering the hysteresis current controller.

The EMF can be calculated in vector coordinates as follows [3]:

$$(3.1) \quad E_s^s = \dot{\Psi}^s = R(\varphi^s) \cdot \dot{\Psi}^\psi + R(\varphi^s) \cdot R\left(\frac{\pi}{2}\right) \cdot \Psi^\psi \cdot \dot{\varphi}^s$$

with

$$(3.2) \quad R(\varphi) = \begin{bmatrix} \cos(\varphi) & -\sin(\varphi) \\ \sin(\varphi) & \cos(\varphi) \end{bmatrix}$$

$E_s^s$  represents the EMF voltage vector in stator coordinates,  $\psi$  is the flux vector and  $\varphi^s$  is the angle of the flux vector with regard to the stator main axis. The EMF voltage is the differential of the flux vector in time.

From equation (3.1) can be derived that the EMF is dependent on the rotational speed of the flux vector and the change of its length.

In normal operation the flux will be constant, which involves that the first term of (3.1) will be zero and makes the EMF only dependent on the rotational speed.

Equation (3.1) can be written as follows in a two phase system:

$$(3.3) \quad \Psi^\psi = L \cdot I_s^b$$

$$(3.4) \quad \begin{aligned} E_s^{s1} &= \cos(\varphi^s) \cdot L \cdot \frac{dI_s^b}{dt} - \sin(\varphi^s) \cdot L \cdot I_s^b \cdot \frac{d\varphi^s}{dt} \\ E_s^{s2} &= \sin(\varphi^s) \cdot L \cdot \frac{dI_s^b}{dt} + \cos(\varphi^s) \cdot L \cdot I_s^b \cdot \frac{d\varphi^s}{dt} \end{aligned}$$

Figure 3.1 shows the used model of the AC machine, with the stator resistances and the stray inductances. The EMF is represented by three voltage sources.

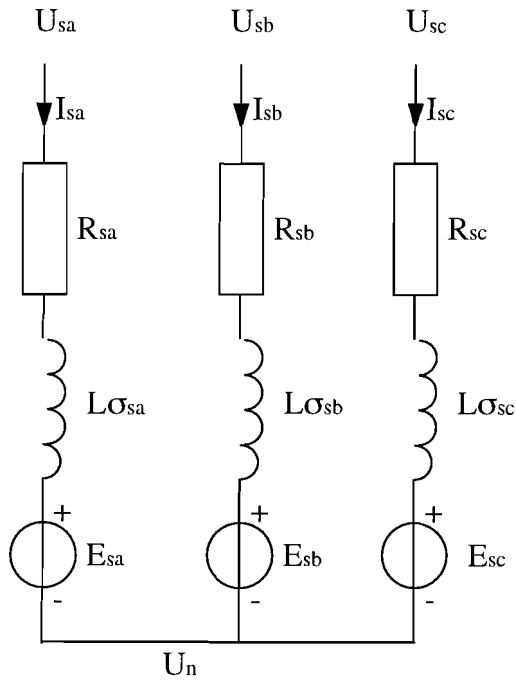


**Figure 3.1: Model of a AC machine.**

Equation ( 3.4) can be transformed from a two phase system into a three phase system as shown in Figure 3.1:

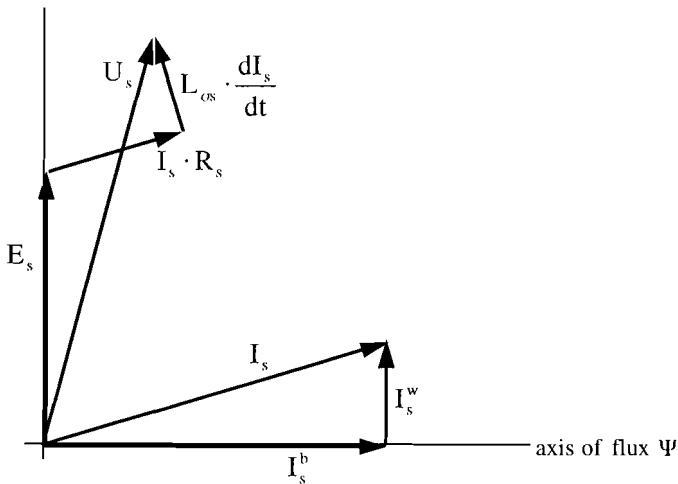
$$\begin{aligned}
 E_{sa} &= \text{Cos}(\varphi^s) \cdot L \cdot \frac{dI_s^b}{dt} - \text{Sin}(\varphi^s) \cdot L \cdot I_s^b \cdot \frac{d\varphi^s}{dt} \\
 \text{( 3.5)} \quad E_{sb} &= \text{Cos}(\varphi^s + \frac{2}{3}\pi) \cdot L \cdot \frac{dI_s^b}{dt} - \text{Sin}(\varphi^s + \frac{2}{3}\pi) \cdot L \cdot I_s^b \cdot \frac{d\varphi^s}{dt} \\
 E_{sc} &= \text{Cos}(\varphi^s + \frac{4}{3}\pi) \cdot L \cdot \frac{dI_s^b}{dt} - \text{Sin}(\varphi^s + \frac{4}{3}\pi) \cdot L \cdot I_s^b \cdot \frac{d\varphi^s}{dt}
 \end{aligned}$$

Figure 3.2 shows a phasor diagram of the stator current and voltages.  $I_s$  consists of two components: The reactive current  $I_s^b$ , responsible for the machine flux and the active current  $I_s^w$ , responsible for the torque. The reactive current is parallel to the flux axis and the active current perpendicular to it. The applied stator voltage vector  $U_s$  can be constructed as follows:

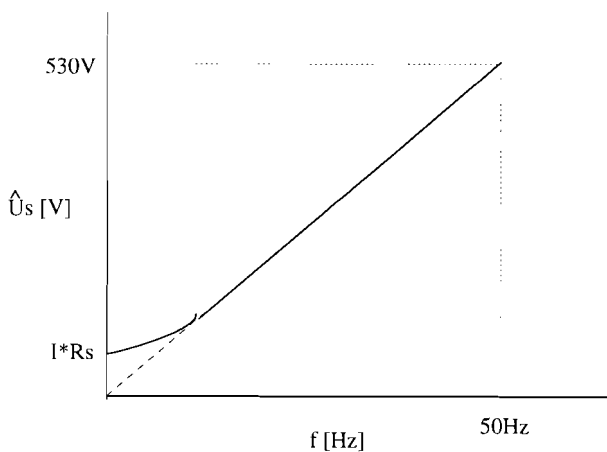
First of all the EMF  $E_s$  is taken into account, which is perpendicular to the flux axis. The voltage drop over the stator resistances is parallel to the stator current  $I_s$  and the voltage drop over the stray inductance is perpendicular to the stator current. The sum of these three voltages is the applied stator voltage  $U_s$ .

A voltage source controlled machine can also be driven by an inverter. The applied frequency (not switching frequency, but machine frequency) and stator voltage can be controlled by means of pulse width modulation. The relation between voltage and frequency is given by the so called volt per hertz characteristic, in order to keep the flux constant (Figure 3.3). At low speed the applied voltage does not go to zero, because the voltage drop over the stator resistance has to be compensated. The EMF voltage  $E_s$  goes to zero of course.

In our case the stator current is controlled by a hysteresis current controller and the flux is also kept constant. That means the applied stator voltage will also follow the so called volt per hertz characteristic automatically. This means, when the stator voltage will be measured and filtered by a low pass filter, a voltage signal conform the volt per hertz characteristic will be also measured.

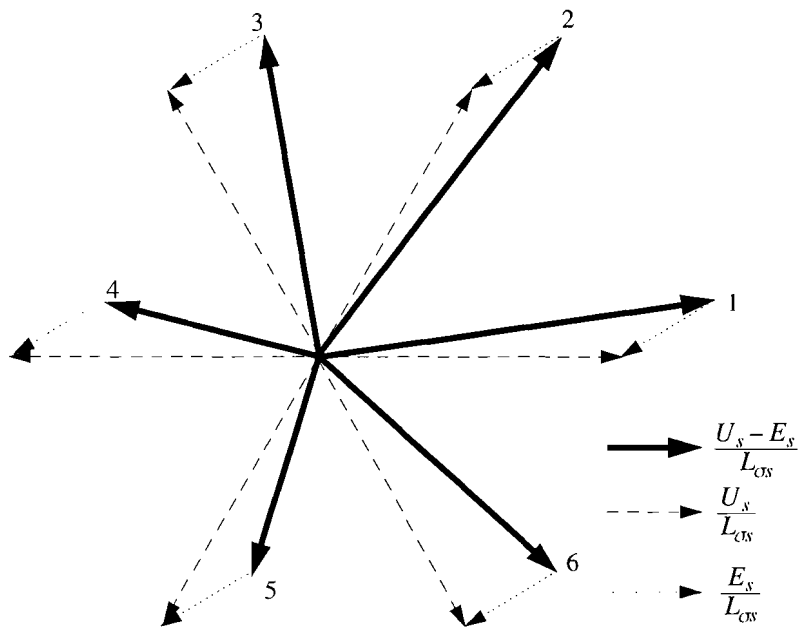


**Figure 3.2: Phasor diagram.**



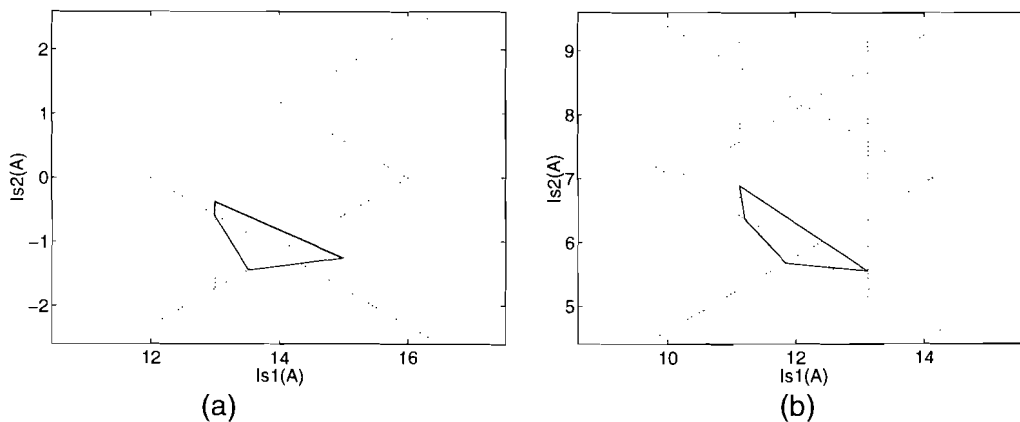
**Figure 3.3: Volt per Hertz characteristic.**

The EMF of the machine also has influence at the length of the current slope vectors and the angle deviations of the current slope vectors. This is illustrated in Figure 3.4 for a particular situation. The dashed vectors represent the six current slope vectors at low speed, which can be switched, since there is no EMF. The dotted vectors are the changes of the current slope vectors introduced by the EMF at a higher speed. The dotted vectors are all parallel to each other. The direction is dependent on the EMF voltage and will rotate synchronously with the machine. The sum of these two vectors gives the solid ones, the current slope vectors which can be applied by the inverter. When the current vector together with the EMF vector rotates in the stator reference frame, the current slope vectors will change as well in length and phase, because the EMF voltage vector rotates as well.



**Figure 3.4: Influence of EMF at the current slope vectors.**

These changes of the current slope vectors also have influence on the shape of the current error. At low speed it has the shape of a hexagon, but when the EMF becomes too high at higher speed, a hexagonal shaped current error can't stand any longer. The current error will move to one side of the hexagon formed by the hysteresis bands, and the average current error moves from the center of the hysteresis bands. This is shown in Figure 3.5. The current error is shown for different positions of the desired current vector (Figure 3.6), with the coupled EMF voltage equal to 90% of the d.c. link voltage. From the plots it can be derived that the shape of the current error changes as the desired current vector rotates and that the current error also shifts to one side of the hysteresis bands. However, at every position of the desired current vector, the current error runs in a stable figure, which gives at least a stable average current. There is no random behaviour. Only the average value doesn't fit the desired value. This error can easily be compensated by applying an additional feedback current control system. This will be discussed in chapter 4.



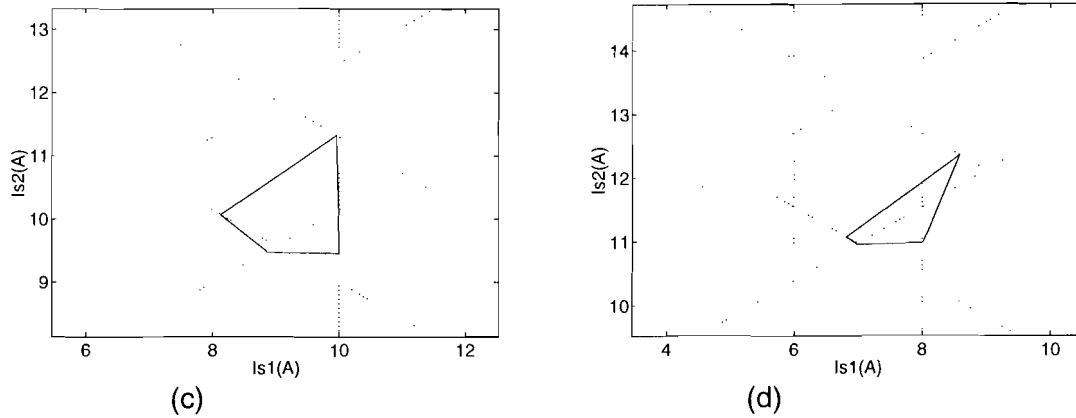


**Figure 3.5: Current error at high speed with influence of EMF.**

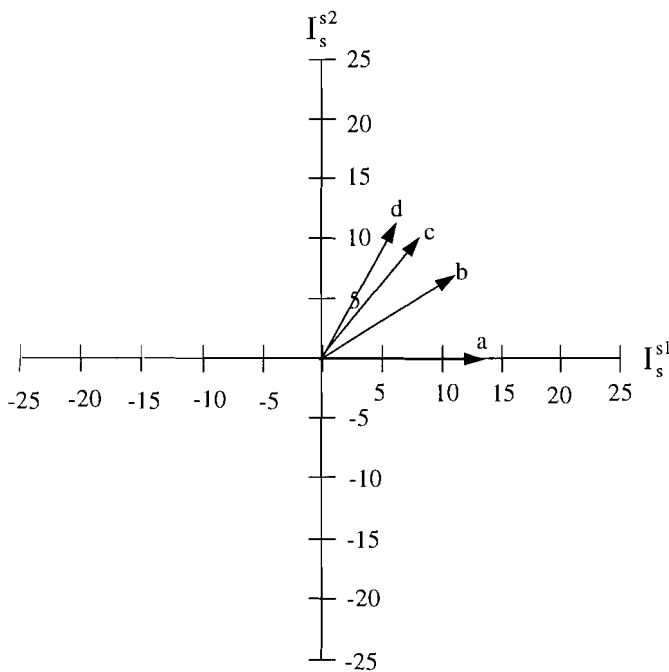


**Figure 3.6: Four different desired stator current vectors, related to Figure 3.5.**

### 3.2. Influence of EMF on the average switching frequency

At higher speed, the EMF of the machine, also has influence on the switching frequency of the inverter. The length of the current slope vector is a measure for the speed of the current error vector, moving towards a current limit. As the length of the current slope vectors changes when the EMF increases, the period time and thus the switching frequency will change as well. At higher speed the trajectory the current error describes isn't hexagonal shaped anymore. That implies that it is difficult to calculate the switching frequency in an analytic way, as the trajectory is unknown.

Figure 3.7 shows the average switching frequency of the inverter as a function of the EMF voltage  $E_s$ , for different dc link voltages  $U_{dc}$ . The figure is the result of simulations which have been carried out. If the machine flux is constant, then the EMF voltage  $E_s$  is proportional with the machine's speed. The hysteresis band width has been kept constant during the simulations. From the figure can be concluded that an increasing EMF voltage gives a

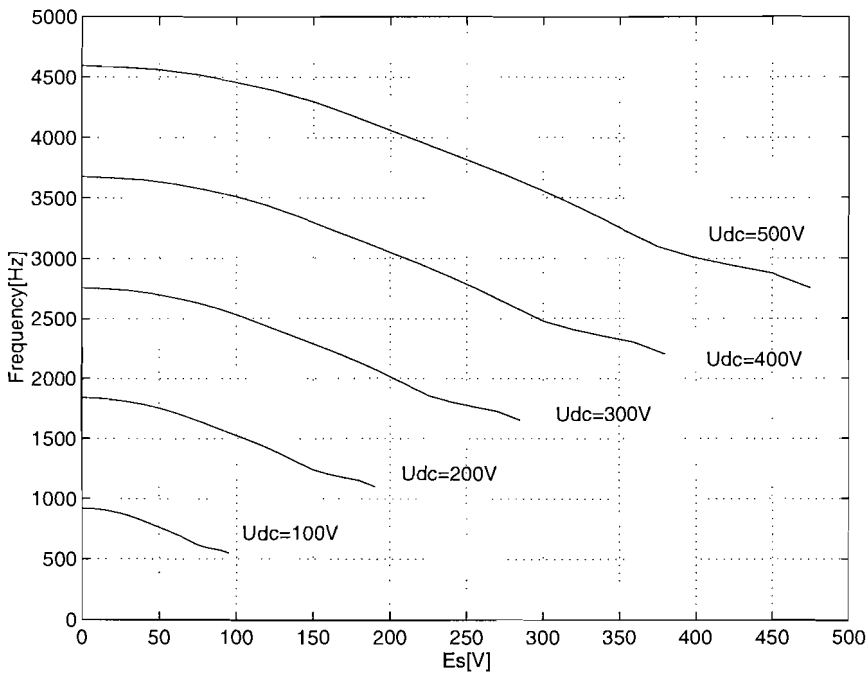


decreasing switching frequency. On the other hand, increase of the DC link voltage, gives an increase of switching frequency.

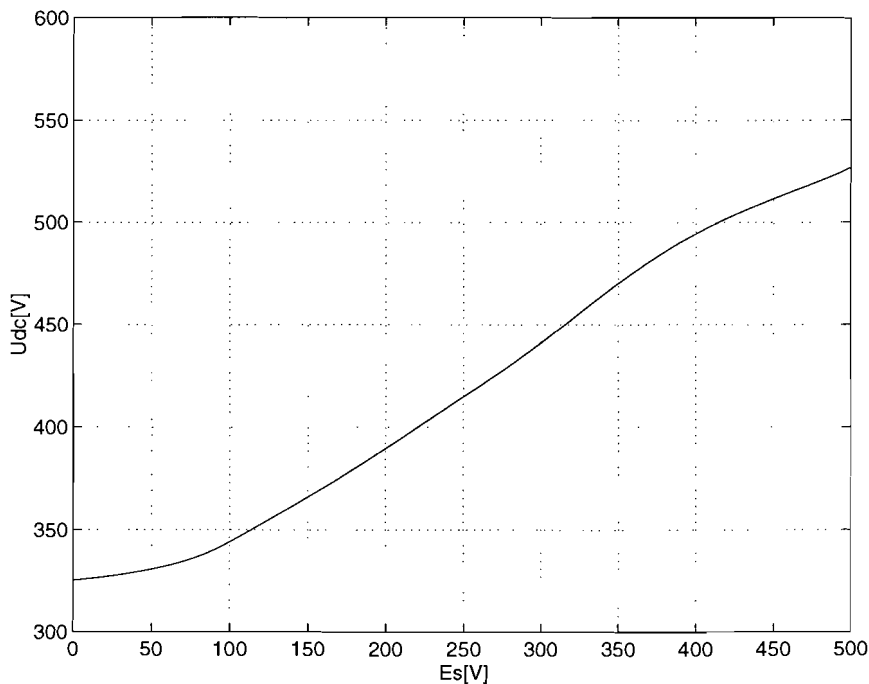
For normal operation it is desirable to keep the average switching frequency (the frequency during one period of the current) constant. This can be achieved by increasing the DC link voltage as the speed, i.e. the EMF voltage, increases.

Figure 3.8 shows the relationship between the coupled EMF voltage and the DC link voltage to keep the switching frequency constant. The DC link voltage is of course always larger than the coupled EMF voltage, otherwise it is impossible to get the current at the desired value. The switching frequency in this case is set by the hysteresis band width. The smaller the band width the larger the switching frequency will be. The switching frequency is kept constant by increasing the DC link voltage as the speed increases.

Of course it is also possible to change the hysteresis band width to keep the switching frequency constant. In this case it is possible to decrease the DC link voltage at lower speed, although the DC link voltage has to be larger than the coupled EMF voltage. This involves that the hysteresis band width has to be decreased as well, which gives a smaller ripple current. On the other hand it is also possible to keep the DC link voltage constant at 530V for example and control the switching frequency with the hysteresis band width. This involves that the hysteresis band width has to be increased at low speed, resulting in a higher ripple of the line currents.



**Figure 3.7: Switching frequency for different dc link voltages as a function of the coupled EMF voltage.**



**Figure 3.8: DC link voltage as a function of the coupled EMF voltage, to keep the switching frequency constant.**

In general it can be said that the switching frequency is proportional to the hysteresis band width. If the DC link voltage would be kept constant at 500V then the average switching frequency would be 2.8kHz at full speed. At speed zero the switching frequency would be 4.6kHz (Figure 3.7). To reduce the switching frequency to 2.8kHz, with  $U_{dc}=500V$ , the hysteresis band width has to be increased with 55%, as the switching frequency is proportional with the band width. This will give a larger ripple current at low speed. The ripple current can be influenced by the desired switching frequency. The larger the switching frequency is, the smaller the ripple current will be.

In conclusion there are two parameters which influence the switching frequency: The hysteresis band width and the DC link voltage. The hysteresis band width can be freely chosen, but the DC link voltage always has to be larger than the coupled EMF voltage. The switching frequency is limited by the switching losses, which increase as the frequency increases.

In fact there are three methods to control the switching frequency of the inverter:

1. Variation of the DC link voltage
2. Variation of the hysteresis band width
3. A combination of variation of the DC link voltage and the hysteresis band width.

### ***3.3. Influence of EMF on the momentary switching frequency.***

In the previous section the average switching frequency has been described. This section will describe the momentary switching frequency.

At low speed the momentary switching frequency is constant, but at higher speed the switching frequency is varying. This is caused by the changing trajectory the current error describes due to the influence of the EMF, as the desired current vector rotates (Figure 3.4).

The larger the trajectory's area is, the smaller the switching frequency. As the trajectory's area varies when the EMF voltage vector rotates, the switching frequency will vary too.

Figure 3.9 shows the result of a simulation and measurement at relatively low speed. The applied DC link voltage was 250V and the speed was 25% of rated speed. The measurements and simulations are carried out at rated flux level. The switching frequency varies slightly during one period of the stator current. Figure 3.10 shows the simulation and measurement results at 40% rated speed. The flux, DC link voltage and hysteresis band width are kept constant.

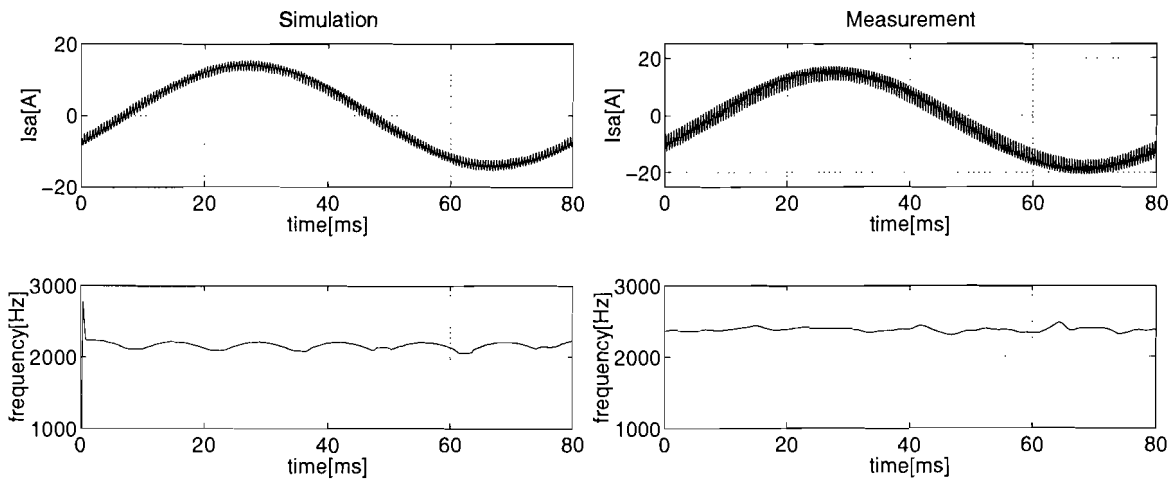


**Figure 3.9: Simulated and measured switching frequency at 25% of rated speed.**

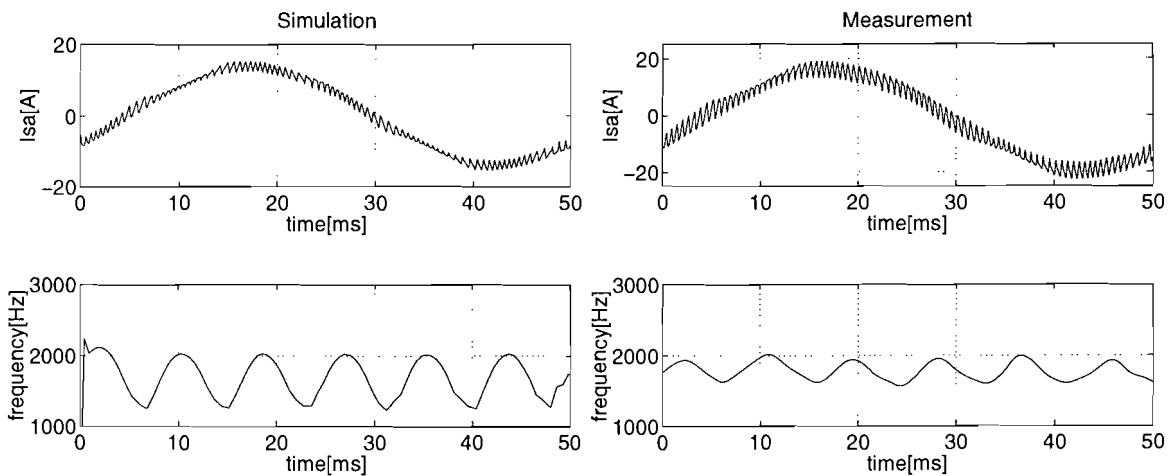


**Figure 3.10: Simulated and measured switching frequency at 40% of rated speed.**

The simulated switching frequency is lower and varies more than the measured switching frequency. This can be caused by a lower flux level in the machine. The flux level has been achieved by supplying the machine with an estimated reactive current  $I_s^b$ . If this current value is smaller than the rated value then the machine will operate with a flux level smaller than the rated level. This gives a lower EMF voltage, and thus less influence on the switching frequency and a higher average switching frequency. This meets the behaviour at lower speed.

### 3.4. Harmonic distortion.

Next the harmonic distortion has to be considered. The performance of the classic hysteresis current controller and of the novel hysteresis current controller have been compared. To accomplish this, measurements with both controllers have been carried out. The applied DC link voltage was 250V and the speed in both cases was 35% of rated speed. The average switching frequency of the inverter was 1600Hz. The measurements have been carried out at rated flux level.

Figure 3.11 shows the measured current for the classic hysteresis current controller. The speed was that high that the so called zero-voltage vector of the inverter was switched. The plot on the left shows the unfiltered measured stator current. For the plot on the right the stator current has been filtered with a low pass filter, the cut-off frequency being 300Hz. From both figures and especially the one with the filtered current, can be derived that the output current of the classic current controller is distorted at higher speed.

Figure 3.12 shows the measured stator current for the novel hysteresis current controller under the same conditions. The left plot shows the unfiltered and the right plot shows the filtered current. Comparing these results it can be concluded that the output current of the novel hysteresis current controller is less distorted than the output current of the classic current controller.

The difference in performance between both controllers is mainly caused by the fact that the classic controller shows random behaviour and the novel one does not. The moment a zero-voltage vector is switched, is random with the classic controller. After a zero-voltage vector has been switched it takes a certain time till the current error shows a stable behaviour again. But that doesn't last long as an other zero-voltage vector will be switched soon. In this case stable means stable for a certain time. As the desired current vector rotates slowly with regard to the switching frequency of the inverter, the shape of the current error can be called stable if it doesn't change fast with regard to the period time of the switching frequency. But of course the trajectory the current error describes will change during the period time of the desired current vector to make one cycle, as shown in Figure 3.5.

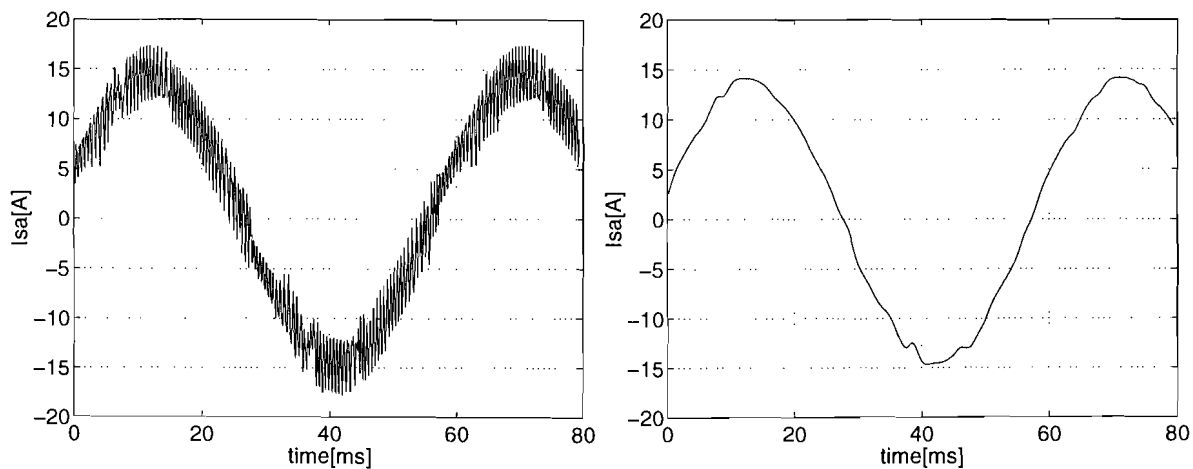
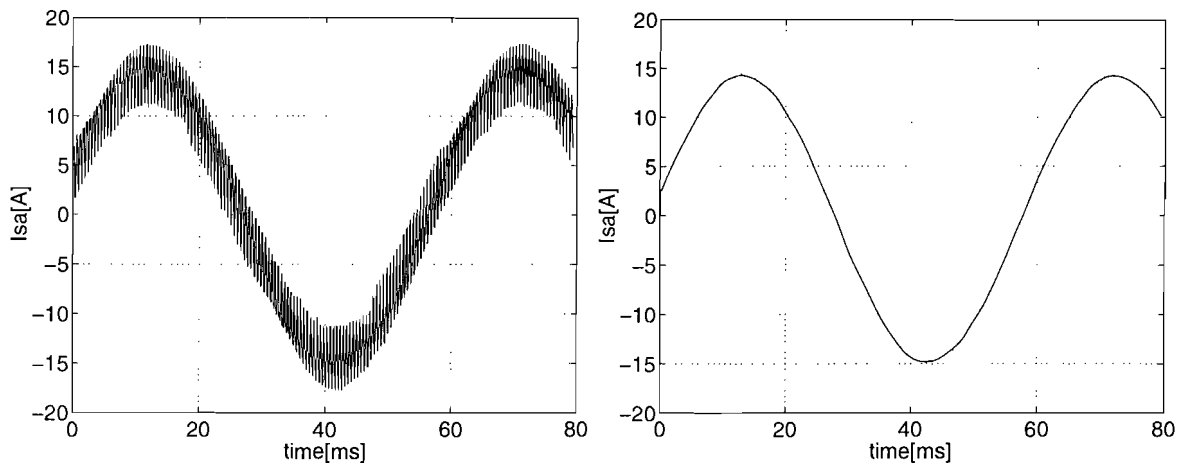


Figure 3.11: Measured current with classic hysteresis current controller.



**Figure 3.12: Measured current with novel hysteresis current controller.**

If the current error doesn't show a stable trajectory then the average current isn't constant, which gives the distortion, shown in the plot with the filtered current of Figure 3.11. The novel controller doesn't switch zero-voltage vectors. This means the momentary stable trajectory for the current error will not be disturbed, which yields a stable average current.

Next, the harmonic distortion of the novel current controller has been investigated for increasing speed. Figure 3.13 (a) to (f) show the measured line current spectrum of the machine for increasing speed and dc link voltage. The measurements are carried out with a rotating machine, without load, and a rated reactive current, which is assumed to be one third of the rated current. In that case the EMF voltage will have its rated value at full speed. The figures (a) to (c) show the measurements carried out with a dc link voltage of 250V. At 45% of rated speed the EMF voltage will be about 235V, which is near the applied dc link voltage.

From Figure 3.13(a) can be derived that there is hardly no harmonic distortion if the dc link voltage is much higher than the EMF voltage, except the distortion introduced by the switching of the inverter at 3kHz. If the EMF voltage is near the dc link voltage (figures b and c) then some harmonic distortion appears. In both cases the fifth harmonic is shown, which is about a few percents of the main current. The same behaviour is shown for higher speed and a dc link voltage of 400V (figures d to f). Figure d shows almost no distortion, as the difference between the EMF voltage and the DC link voltage is too large. Figure (e) shows again the fifth harmonic. At 70% of the rated speed (figure f), a third harmonic besides a fifth harmonic appears. If the machine is completely symmetric and the neutral of the machine is floating, then third harmonic distortion in the line current is not possible. But there is always some asymmetry, which involves that third harmonic distortion can appear.

From the spectrum analyses can be concluded that there is hardly harmonic distortion if the dc link voltage is much higher than the coupled EMF voltage. If the coupled EMF voltage is near the dc link voltage then a fifth harmonic line current appears. But the rms value of the fifth harmonic current is always less than five percent if the dc link voltage is 30V higher than the coupled EMF voltage.

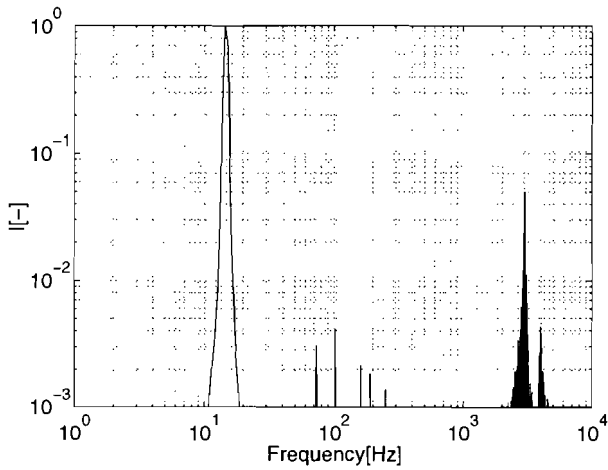


Figure 3.13(a):  $U_{dc}=250V$ ,  $n=30\%$

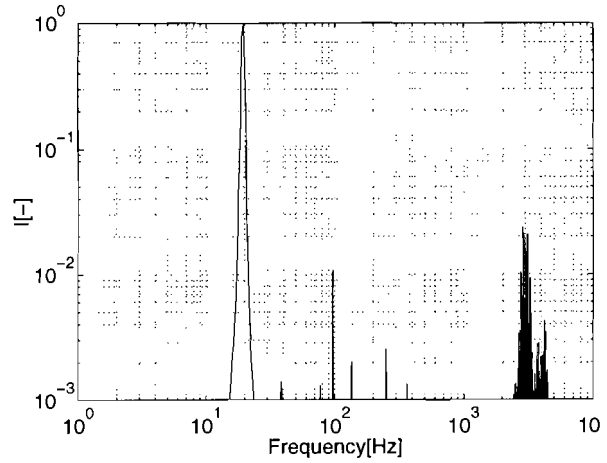


Figure 3.13(b):  $U_{dc}=250V$ ,  $n=40\%$

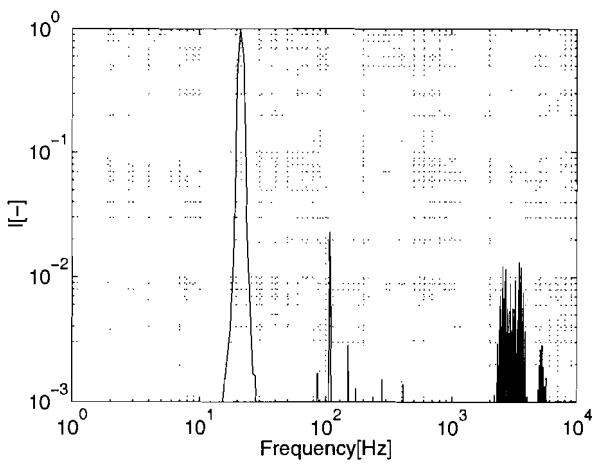


Figure 3.13(c):  $U_{dc}=250V$ ,  $n=45\%$

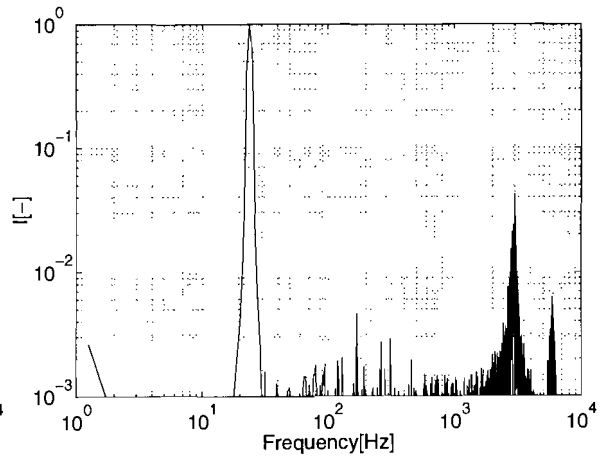


Figure 3.13(d):  $U_{dc}=400V$ ,  $n=50\%$

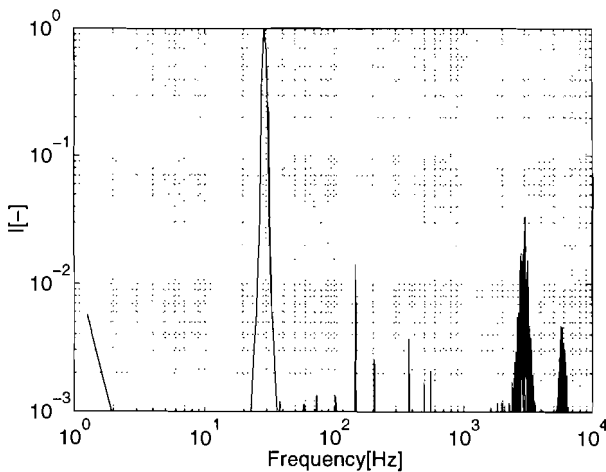


Figure 3.13(e):  $U_{dc}=400V$ ,  $n=60\%$

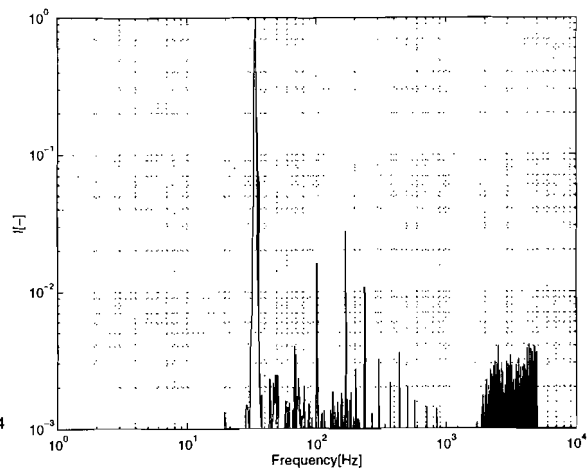


Figure 3.13(f):  $U_{dc}=400V$ ,  $n=70\%$

Figure 3.13: Measured line current spectrum for increasing speed.

### 3.5. Constant average switching frequency.

It is desirable to keep the average switching frequency of the inverter constant as the speed of the machine changes. This can be done by changing the dc link voltage according to the curve given in Figure 3.8 but it is hard to realise this automatically for two reasons, first the dc link voltage of the experimental set-up can only be changed by hand and secondly the dc link voltage has also to be larger than the EMF voltage. The last could be achieved by applying the curve given in Figure 3.8, but in that case no experimentation with a varying dc link voltage at a certain speed is afforded. So a frequency controller has been implemented to keep the switching frequency of the inverter constant, by means of varying the hysteresis band width. In that way the dc link voltage has not to be changed continuously when the speed of the machine changes a little bit conform the characteristic given in Figure 3.8. For the experimental application it is easier to change the band width automatically than changing the dc link voltage automatically. Figure 3.14 shows the working schematic of the frequency controller. The switching period time is measured by the vector driver in a digital way (chapter 5). This signal is converted from digital to analog by the D/A converter and subtracted from the desired period time. The error is integrated by an integrator which gives a hysteresis band width for the comparators. So actually, it is a period time controller instead of a frequency controller, but the result is the same.

The time constant of the integrator is rather high because the vector driver which measures the period time works discrete. The sampling time is  $330\mu\text{s}$  if the switching frequency of the inverter is  $3\text{kHz}$ . The inverter only works properly if the integrator's time constant is much higher than the sampling time. If the time constant is too low then oscillating of the hysteresis bandwidth could occur. On the other hand, a time constant which is too high makes the controller too slow. From practice is derived that a time constant of  $2.2\text{ms}$  for the integrator meets the requirements best.

Of course a better performing controller could be designed, but this one satisfies the demand for an automatic varying hysteresis band width, in order to keep the average switching frequency constant, in such a way that the dc link voltage doesn't have to be changed continuously.

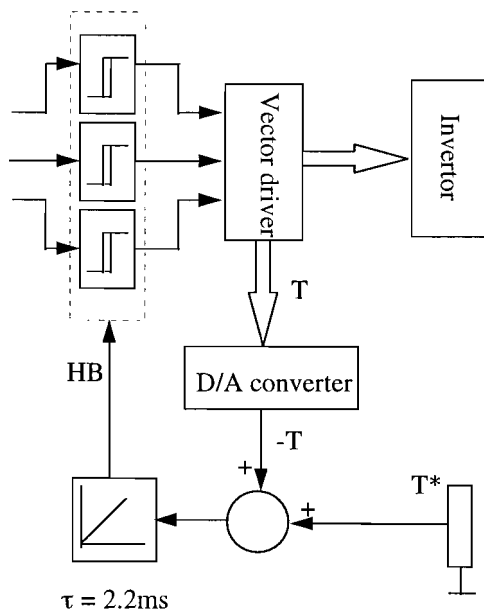


Figure 3.14: Switching frequency controller.

## 4. Drive control system

### 4.1. Slip control

For testing the hysteresis current controller it was desirable to have a drive system, where the flux of the machine could be kept at a rated level at different load situations. This is necessary, because the flux has influence on the EMF voltage and so on the working of the hysteresis controller at higher speeds.

Figure 4.1 shows the working diagram of the slip controller [3]. The desired active current  $I_s^{w*}$  is given by the speed controller and the desired reactive current  $I_s^{b*}$  is set at a certain value. This gives already the absolute value of the desired stator current vector  $I_s^*$ . Now only the angle of the stator current vector is still required. In a stationary operating condition one yields:

$$(4.1) \quad I_k^w = -I_s^w$$

With  $I_k^w$  representing the active current of the rotor.

For the rotor EMF voltage vector we can also write, just as for the stator EMF voltage vector (equation (3.1)):

$$(4.2) \quad E_r^r = \dot{\Psi}^r = R(\varphi^r) \cdot \dot{\Psi}^\Psi + R(\varphi^r) \cdot R\left(\frac{\pi}{2}\right) \cdot \Psi^\Psi \cdot \dot{\varphi}^r$$

If the flux is constant the rotor current only has an active component and no reactive component in steady-state operation. This involves that (4.2) can be written as:

$$(4.3) \quad E_r^r = \Psi \cdot \dot{\varphi}^r = -I_k^w \cdot R_k$$

$$(4.4) \quad \Psi = L \cdot I_s^b$$

From (4.3) and (4.4) follows:

$$(4.5) \quad \dot{\varphi}^r = \frac{R_k}{L} \cdot \frac{-I_k^w}{I_s^b} = \frac{R_k}{L} \cdot \frac{I_s^w}{I_s^b}$$



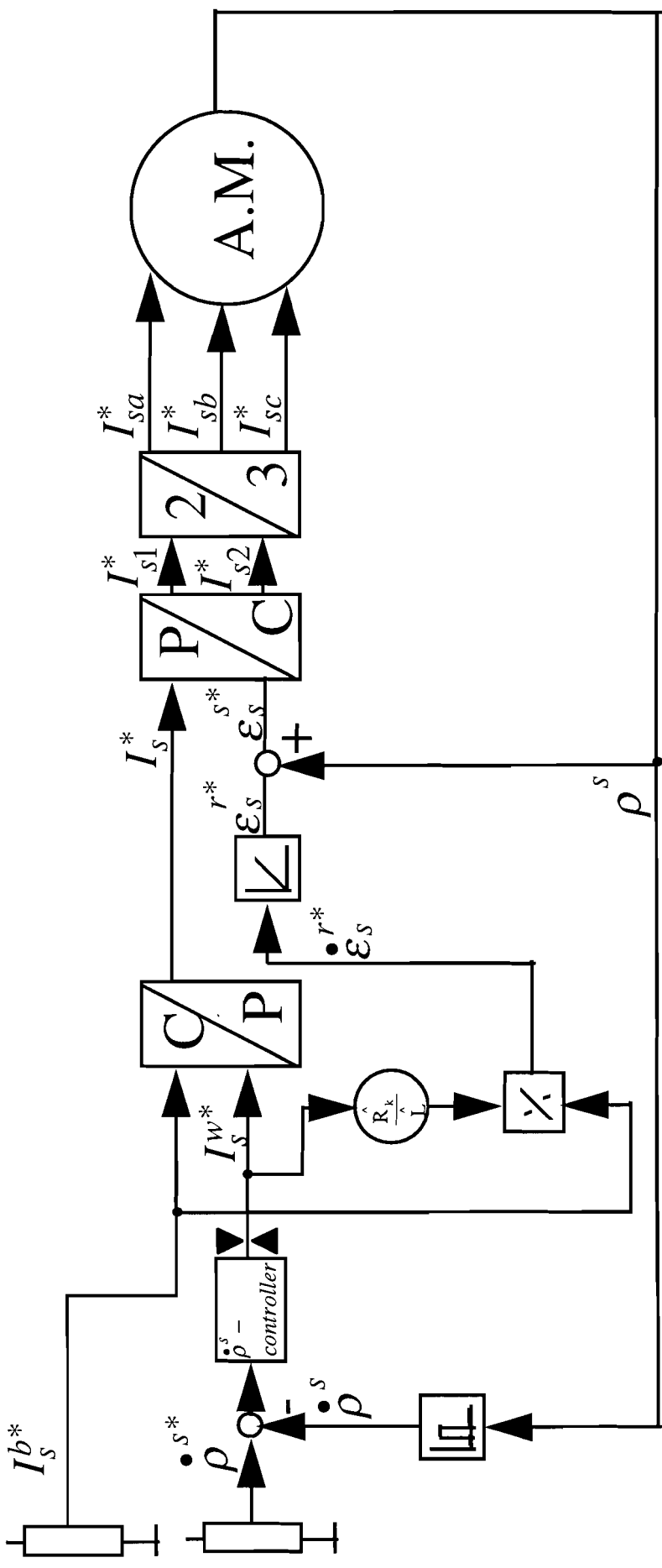


Figure 4.1: Simple slip control system.

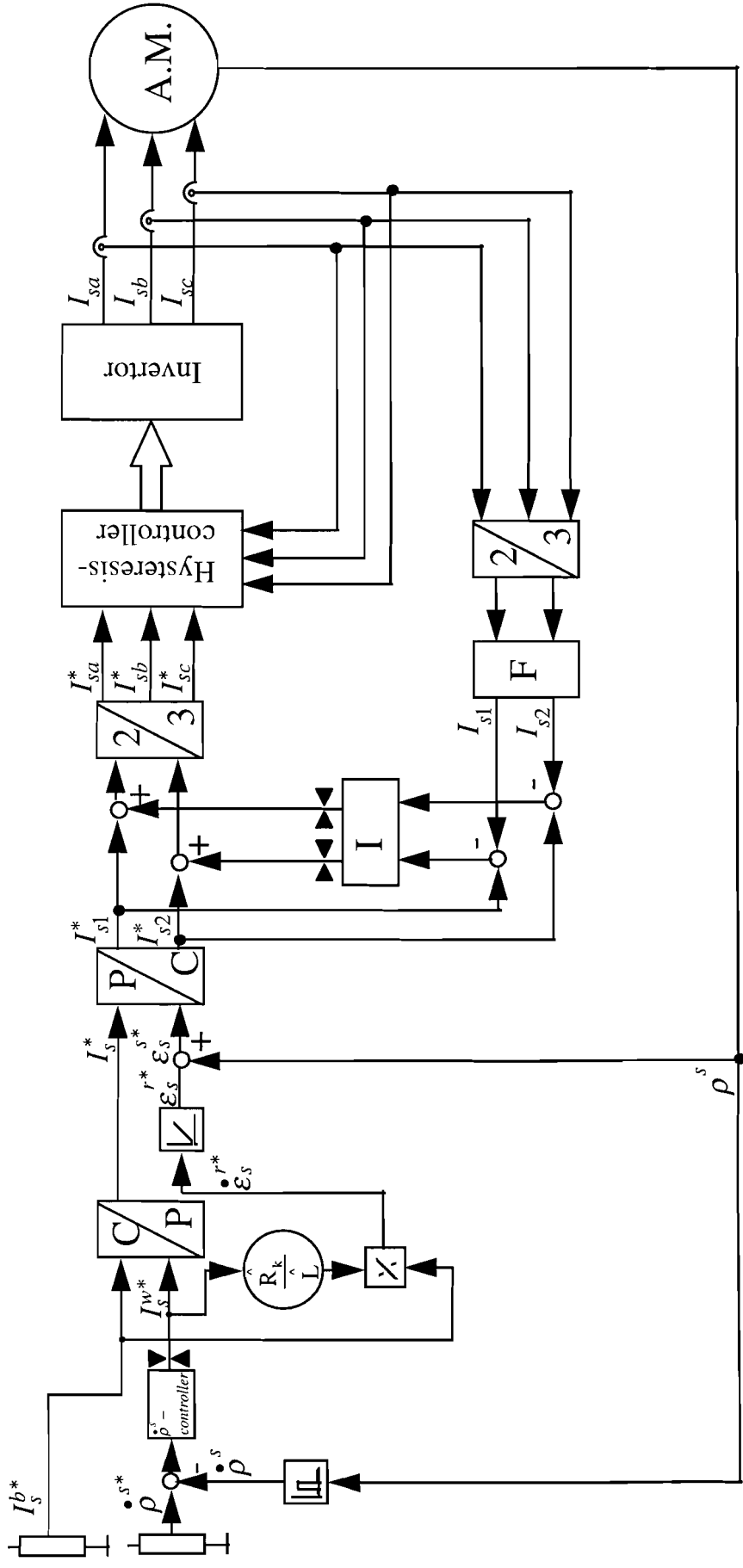


Figure 4.2: Slip control, with hysteresis controller

To keep the machine flux constant, the slip frequency  $\dot{\varepsilon}_s^r$ , the frequency of the stator current vector with regard to the rotor, has to be equal to  $\dot{\varphi}^r$ , the frequency of the flux vector with regard to the rotor. So from equation (4.5) can be derived that the desired slip frequency  $\dot{\varepsilon}_s^{r*}$  should be:

$$(4.6) \quad \dot{\varepsilon}_s^{r*} = \frac{\hat{R}_k}{\hat{L}} \cdot \frac{-I_k^w}{I_s^b} = \frac{\hat{R}_k}{\hat{L}} \cdot \frac{I_s^{w*}}{I_s^{b*}}$$

with  $\frac{\hat{R}_k}{\hat{L}}$  the quotient of the estimated main rotor resistance and inductance. After integrating this slip frequency and adding the rotor position  $\rho^s$ , the desired angle of the stator current in the stator reference frame  $\varepsilon_s^{s*}$  results (Figure 4.1). An encoder is connected with the machine to measure the rotor position  $\rho^s$ . This rotor position has also been differentiated to get the speed, used as feedback for the speed controller.

Figure 4.2 shows the complete slip control diagram, with hysteresis current controller and an additional I-current controller.

The hysteresis current controller gets its feedback immediately from the three measured stator currents  $I_{sa}$ ,  $I_{sb}$  and  $I_{sc}$ .

At higher speed the hysteresis controller introduces an error, i.e. the average stator current doesn't fit the desired value anymore (chapter 3). That's why an additional current controller is added to reduce this error. First of all, the measured 3 phase stator current system is transformed to a 2 phase system, because a 2 phase system is easier to handle. Second the current is filtered, because the additional controller is implemented in a DSP system and an anti-aliasing filter is needed. The current error, i.e. the difference between desired stator current and measured stator current, goes to an I-controller, with a time constant  $\tau = 4\text{ms}$  (value based on experiments). The output of the controller is added to the desired stator current and can be seen as a correction to the desired current. The output of the additional controller is limited at 10% of the rated current, to ensure the correction is not too high when the system is starting up. At low speed, when there is hardly no error introduced by the hysteresis current controller, the output of the additional current controller will be around zero.

## 4.2. Machine parameter identification

For a good working of the slip controller the machine's parameters  $R_k$  and  $L$  have to be well known (Figure 4.1). If the estimated quantities are wrong then the flux will not stay constant when the torque of the load is varying. Unfortunately this machine quotient  $\frac{R_k}{L}$  is changing, because  $R_k$  is dependent on the machine's temperature and  $L$  changes with saturation level. When the estimated coefficient is too high then the machine flux will decrease as the torque increases, because the slip will be too high. This means when the machine is warming up and thus  $R_k$  is enlarging, the flux will decrease. When the machine is cooling down,  $R_k$  will decrease and thus the flux increase.

So it is not easy to have a good slip controller as the rotor resistance of the machine is changing continuously. Second, it is difficult to measure the machine's parameters. As most of the measurements are done with a "cold" machine, the parameters are mostly related to a "cold" machine. Normally, a machine has to run for a few hours till the final stable temperature has been reached.

First of all the rotor resistance of the machine in the experimental application has been measured. The asynchronous machine has slip rings, which makes things much easier. Figure 4.3 shows a representation of the asynchronous machine [4]. A dc voltage source is connected to the rotor, to measure the rotor resistance. An additional resistance  $R$  is added to enlarge the total resistance, to make it easier to measure. The measured rotor resistance per phase is  $R_r = 0.073\Omega$

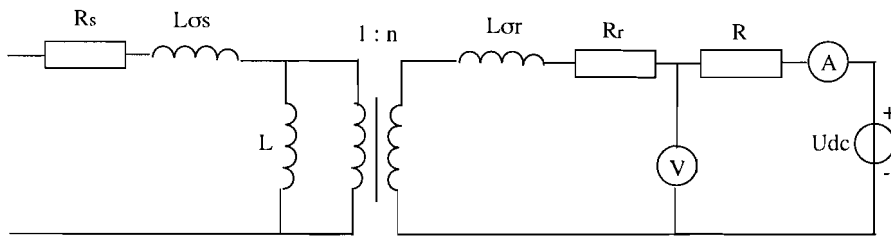


**Figure 4.3: Measurement of stator resistance.**

Next the main inductance  $L$  has been measured. This can be measured in two ways, as shown in Figure 4.4 and Figure 4.5. In the first figure an ac voltage source is connected to the stator side of the machine, with the rotor side open. From the stator side, now the total impedance of  $R_s$ ,  $L_{\sigma s}$  and  $L$  can be measured. The resistance's  $R_s$  and  $R_r$  can be neglected, so that only the inductances remain.

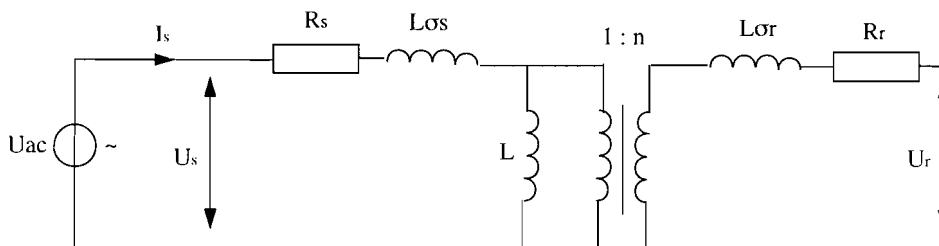


**Figure 4.4: Measuring inductance from stator side.**

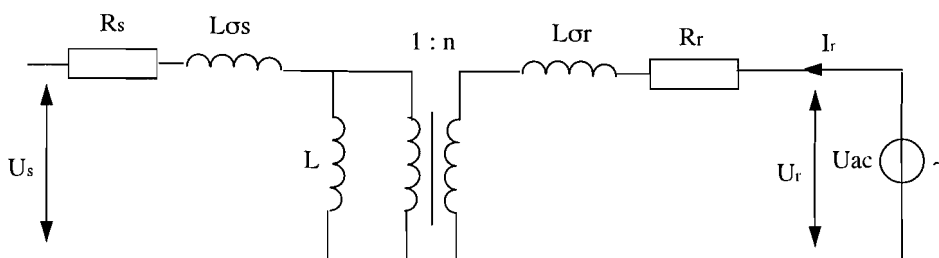


**Figure 4.5: Measuring inductance from rotor side.**

The stray inductances  $L_{\sigma s}$  and  $L_{\sigma r}$  are assumed to be equal when they are transformed to the stator side because for both inductances the same air gap in the machine is involved.

$$(4.7) \quad \begin{aligned} L_{os} &= L_{\sigma} \\ L_{or} &= n^2 \cdot L_{\sigma} \end{aligned}$$

For the measurements done with the test circuit given in Figure 4.4 we can write:

$$(4.8) \quad \frac{U_s}{I_s} = \omega \cdot (L_{\sigma} + L)$$

$$(4.9) \quad (L_{\sigma} + L) = \frac{U_s}{\omega \cdot I_s}$$

For the measurements done with the circuit from Figure 4.5 it can be written:

$$(4.10) \quad \frac{U_r}{I_r} = n^2 \cdot \omega \cdot (L_{\sigma} + L)$$

$$(4.11) \quad (L_{\sigma} + L) = \frac{U_r}{n^2 \cdot \omega \cdot I_r}$$

If two measurements are done, one with the test circuit from Figure 4.4, to measure  $\frac{I_s}{U_s}$  and one with the test circuit from Figure 4.5, to measure  $\frac{U_r}{I_r}$ , then with equation (4.9) and (4.11) can be calculated that:

$$(4.12) \quad n = \sqrt{\frac{U_r}{I_r} \cdot \frac{I_s}{U_s}}$$

The currents have to be kept small when the measurements are done, to ensure that the machine is not in saturation, which would make things complicated.

After n has been determined it is possible to calculate the main inductance L as follows. When the measurements are carried out with the test circuit from Figure 4.4:

$$(4.13) \quad L = \frac{U_r}{n \cdot \omega \cdot I_s}$$

First of all a measurement conform the circuit of Figure 4.5 has been carried out. The results are:

$U_r=42V$  and  $I_r=5A$ .

Next several measurements have been carried out with the circuit given in Figure 4.4. The transformer factor n has been calculated with equation (4.12) and the inductance L has been calculated with equation (4.13). The results are given in Table 4.1.

**Table 4.1: Measured results.**

n= 0,65			
$U_s$ [V <sub>rms</sub> ]	$I_s$ [A <sub>rms</sub> ]	$U_r$ [V <sub>rms</sub> ]	L [H]
58	3	36	0,059
115	5,9	73	0,061
144	7,4	91	0,060
173	9,3	109	0,057
202	11,6	126	0,053
231	16	144	0,044

From the results can be derived that till a stator current of  $10A_{rms}$  the inductance L stays practically constant, but if the stator current becomes higher than  $10A_{rms}$  the inductance L decreases. This means, the machine is in saturation when the current is higher than  $10A_{rms}$ . The estimated rated reactive current was one third of the rated machine current ( $30A_{rms}$ ) which also became  $10A_{rms}$ . Normally the reactive current is chosen at the point where the machine starts to go into saturation. This means the estimated rated reactive current is not bad.

At last the rotor resistance  $R_r$  has to be transformed to the stator side of the machine to use it in the slip controller:

$$(4.14) \quad \hat{R}_k = \frac{R_r}{n^2} = \frac{0.073}{0.65^2} = 0.173 \Omega$$

Now the coefficient used in the slip control, for a cold machine, can be calculated, when the machine is not in saturation. The inductance  $\hat{L}$  and resistance  $\hat{R}_k$  have to be transformed from a 3 phase reference frame to a 2 phase reference frame. Nevertheless this

transformation doesn't have any influence on the quotient  $\frac{\hat{R}_k}{\hat{L}}$ .

$$(4.15) \quad \frac{\hat{R}_k}{\hat{L}} = \frac{\frac{2}{3} \cdot 0.173}{\frac{2}{3} \cdot 0.060} = 2.88$$

### 4.3. Adjusting slip controller based on the load.

Although a good estimation of the machine parameters has been made, the slip control will still not work when the machine temperature changes. If for instance an asynchronous machine, with a cage rotor is used to the slip drive system, then it is even more difficult to identify the machine parameters. For this reason, an easy and fast way to adjust the slip controller at the machine's parameters would be useful, to perform good experiments.

There is a way to adjust the slip controller when using the load. However this is only possible if the torque of the machine can be measured, and the torque of the load can be adjusted.

When the flux stays constant, the torque will be proportional to the active stator current of the machine. When no load is connected to the machine the active current is theoretically zero. But due to some losses there will always be a small active current.

The speed of the machine with slip control is regulated by a speed controller, which drives the desired active stator current (Figure 4.1). If the torque of the load increases the speed controller will increase the desired active stator current till the machine torque equals the load torque and the machine runs with the desired speed. For instance when the machine parameters are estimated well, the desired active stator current  $I_s^{w*}$  will be doubled by the speed controller if the torque  $T$  of the load doubles. The machine flux stays constant. This has been proved by simulations, shown in Figure 4.6 and by applying the method in the experimental set-up.

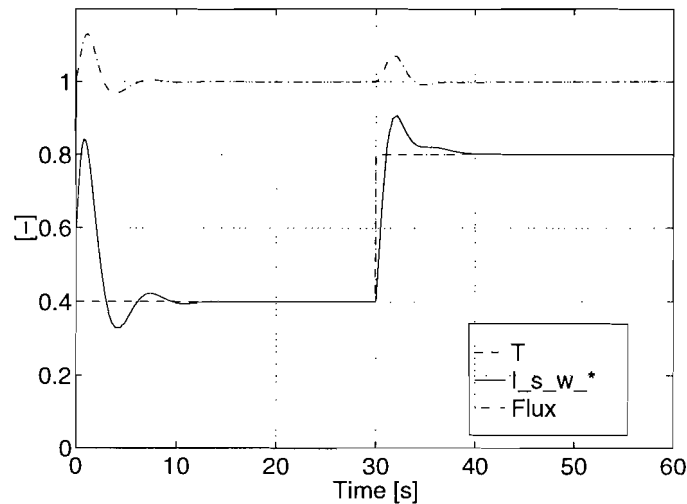


**Figure 4.6: Simulation of slip control with right estimated machine parameters.**

If the estimated coefficient  $\frac{\hat{R}_k}{\hat{L}}$  is too high then the slip of machine will be too large with regard to  $I_s^{w*}$  as  $\varepsilon_s = \frac{\hat{R}_k}{\hat{L}} \cdot I_s^{w*}$  (Figure 4.1). This involves that the machine flux will be too low as the real active stator current  $I_s^w$  is too high and the real reactive stator current  $I_s^b$  is too low. When the torque of the load has been doubled the flux will decrease and the

estimated active stator current will be more than doubled. Figure 4.7 gives the result of a simulation with  $\frac{\hat{R}_k}{\hat{L}}$  too high. In the figure can clearly be seen that the desired active stator current  $I_s^{w*}$  increases to a higher level than the double, when the torque is doubled, and the simulated machine flux decreases even more, when the torque is doubled.

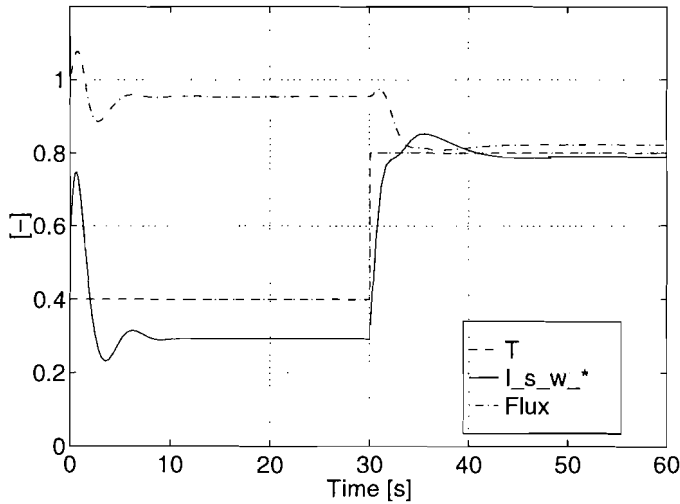


**Figure 4.7: Simulations of slip control with estimated  $\frac{\hat{R}_k}{\hat{L}}$  too large.**

When the estimated coefficient  $\frac{\hat{R}_k}{\hat{L}}$  is too small it will just be the other way around:

The slip of the machine will be too small, which involves that the flux of the machine will be too high. This will make that the desired active stator current  $I_s^{w*}$  will be less than doubled if the torque is doubled. Figure 4.8 shows the simulation results.

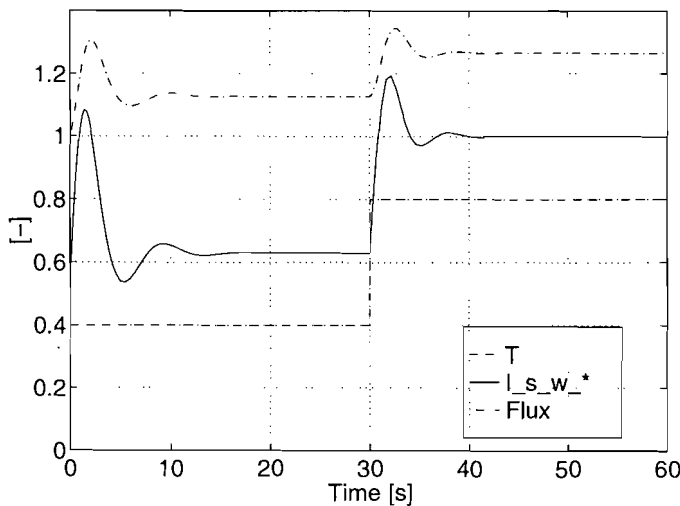


**Figure 4.8: Simulations of slip control with estimated  $\frac{\hat{R}_k}{\hat{L}}$  too small.**



When the estimated coefficient  $\frac{\hat{R}_k}{\hat{L}}$  fits the real machine parameters, then the desired active stator current will be doubled by the speed controller if the torque of the load is doubled. If this coefficient  $\frac{\hat{R}_k}{\hat{L}}$  is made adjustable in the controller, then it is possible to adjust the slip controller by doubling the load torque and checking whether the desired active stator current  $I_s^{w*}$  is doubled as well. If not, the coefficient  $\frac{\hat{R}_k}{\hat{L}}$  can be changed a little bit and the test can be done over again, till  $I_s^{w*}$  doubles when the torque doubles. This is a simple and fast manner to adjust the slip controller in the specific experimental set-up, because the load torque can be changed and measured easily.

## 5. Practical set-up

### 5.1. Entire set-up

The practical set-up has been divided into two parts. One part, which has been implemented in a DSP (digital signal processor) system and the second part which has been built on PCB's (printed circuit boards).

Figure 5.2 shows a scheme of the entire set-up. The slip controller (described in chapter 4) and the additional current controller (described in chapter 3) are implemented in a DSP system. The other parts, hysteresis current controller, 3 to 2 phase converter and the (anti aliasing) filter are implemented on PCB's.

The hysteresis current controller consists of 6 PCB's, as shown in figure 5.3. The connector pin numbers for the different PCB's are also given in the figure.

### 5.2. PCB 1, the hysteresis current controller.

From figure 5.3 it is clear that PCB 1 takes care of two functions: Comparing the desired and measured current values and protecting the whole system. Detailed schemes are given in the figures 5.4, 5.5 and 5.6.

From figure 5.3 can be derived that all the desired and measured current signals are buffered and subtracted from each other. The circuit shown in figure 5.4a takes care of this part. Next the current error signals  $\Delta I_{sa}$ ,  $\Delta I_{sb}$  and  $\Delta I_{sc}$  go to the vector rotation system, formed by the 3-2 converter, the vector rotator and the 2-3 converter. After rotation, they are compared with the current limits, set by 'vboven' and 'vonder' (figure 5.4b). If a current limit is crossed the output of the corresponding comparator will be low, otherwise it will be high. The outputs also set and reset a flip-flop, which can be used for a classic hysteresis current controller. The scheme of the generation part of the reference voltages 'vboven' and 'vonder' is shown in figure 5.6b.

PCB1 also takes care of protecting the system. There are several aspects, caused by short-circuits or other failures, which make that the vector driver has to switch off.

If one of the measured phase currents is higher than  $I_{max}$  then the inverter will be switched off by means of giving a driver reset (figure 5.3)

From the inverter two optic signals come back: one of them lights when the power is ok and another lights when a short circuit is detected. The enable signal is generated by the slip controller, and will enable the hysteresis controller if the slip controller is running. As a result, when an error occurs in the inverter (power not ok or short circuit detected) or if the slip controller doesn't work (no enable), the inverter will be switched off. The reset button has to be pushed, to start the system again.

The circuit lay-out of this part of PCB 1 is given in figure 5.5.

The measured currents are compared with the absolute maximal phase current by the comparators U6 and U7. The maximal phase current is set by the reference voltages 'vtrip+' and 'vtrip-', generated by the circuit given in figure 5.6b. If the maximal phase current is crossed, then flip-flop 4 will be reset by transistor T1. This flip-flop is also reset by transistor T2 if the power is not ok, or if an error is detected (U10). This flip-flop can only be set again by the reset switch if the power is ok and no short circuit is detected. The output of the concerning flip-flop goes to an 'and' port, formed by two 'nand' ports. If both the flip-flop is

set and the enable input is high (enabled) then the 'driver reset' signal will be deactivated (=high) and the inverter will be switched on.

Figure 5.6a provides the power supply of the PCB. The +15V and -15V come from an external power supply. The voltage regulator generates a +5V which is used for the TTL logic devices (Nand gates, Flip-flops) and for the power supply of PCB 5, the vector driver.

### 5.3. PCB 2, the 3-2 converter.

Three identical 3-2 converters are implemented on PCB 2. One has been used for converting the stator currents (figure 5.2), another one for the hysteresis current controller (figure 5.3) and the third one has been used to convert the measured stator voltages, which is not shown in the figures.

The 3-2 converter, used for the hysteresis current controller, is shown in figure 5.7 (sheet B).

The conversion from a 3 phase current reference frame to a 2 phase current reference frame is given by equation ( 5.1):

$$(5.1) \quad \begin{bmatrix} I_s^{s1} \\ I_s^{s2} \\ I_{s0} \end{bmatrix} = \begin{bmatrix} 1 & -\frac{1}{2} & -\frac{1}{2} \\ 0 & \frac{\sqrt{3}}{2} & -\frac{\sqrt{3}}{2} \\ 1 & 1 & 1 \end{bmatrix} \cdot \begin{bmatrix} I_{sa} \\ I_{sb} \\ I_{sc} \end{bmatrix}$$

$I_{s0}$  is the neutral current, which will be zero in the experimental set-up, because the neutral is floating (not connected to a reference voltage).

This calculation has been implemented in analog technique.

The three incoming signals are buffered, and also a negative equivalent is generated (U3 and U4). The potentiometers TRM7, TRM9 and TRM11 are implemented to correct the input signals for offset ( $\pm 60\text{mV}$ ). The potentiometers TRM8, TRM10 and TRM12 are implemented to adjust the units (volts/amp) by means of changing the amplification factor A of the op-amp circuit between  $A=0.83$  and  $A=1.17$ .

The output signals are formed by adding the three input signals, after being multiplied with a factor according to equation ( 5.1). The circuits to sum the signals are built around op-amps U2 and U5. The multiplication factors are set by the resistors R47, R48, R49, R60, R61, R72, R73 and R74. These resistors are named  $R_{mult}$ .

There are two configurations for the feedback resistors of the op-amps. One configuration is with only one resistor of  $20\text{k}\Omega$  and another configuration is with two resistors in parallel, one of  $20\text{k}\Omega$  and one of  $40\text{k}\Omega$ . Table 5.1 shows the multiplication factors of the input signals, for different configurations. The factors decrease with a factor  $2/3$  if the two feedback resistors of  $20\text{k}\Omega$  and  $40\text{k}\Omega$  are implemented instead of only one resistor of  $20\text{k}\Omega$ . This configuration is used for transformation of a three phase voltage reference frame to a two phase voltage reference frame.

**Table 5.1: Multiplication factor as function of the op-amp configuration.**

R <sub>mult</sub>	R <sub>feed</sub> =20k	R <sub>feed</sub> =20k with 40k parallel.
20k	1	2/3
23.09k	√3/2	√3/3
40k	1/2	1/3

The resistors R50, R62 and R75 have been removed from the circuit board which makes that the op-amps only have 20kΩ feed-back resistors. This gives the multiplication factors conform equation ( 5.1).

#### 5.4. PCB 3, the vector rotator.

The rotation of a vector, with a certain angle is given by equation ( 5.2).

$$(5.2) \quad \begin{bmatrix} \Delta I_{s\text{rot}}^{s1} \\ \Delta I_{s\text{rot}}^{s2} \end{bmatrix} = \begin{bmatrix} \text{Cos}(\gamma) & -\text{Sin}(\gamma) \\ \text{Sin}(\gamma) & \text{Cos}(\gamma) \end{bmatrix} \cdot \begin{bmatrix} \Delta I_s^{s1} \\ \Delta I_s^{s2} \end{bmatrix}$$

This equation has also been implemented in analog technique. The circuit is given in figure 5.8.

The multiplication of the signals, with the different factors, is carried out by the op-amps of U1. The coefficients given by Cos(γ) and Sin(γ) are set by adjusting the amplification factor of the op-amps by adjusting the potentiometers R9 to R12:

Op-amp U1D generates  $-\Delta I_s^{s1} \cdot \text{Cos}(\gamma)$ ,

op-amp U1C generates  $\Delta I_s^{s2} \cdot \text{Sin}(\gamma)$ ,

op-amp U1B generates  $-\Delta I_s^{s1} \cdot \text{Sin}(\gamma)$  and

op-amp U1A generates  $-\Delta I_s^{s2} \cdot \text{Cos}(\gamma)$

The angle γ is negative.

Next the signals are added to get the rotation according to equation ( 5.2).

Op-amp U2B gives  $\Delta I_{s\text{rot}}^{s1} = -[-\Delta I_s^{s1} \cdot \text{Cos}(\gamma) + \Delta I_s^{s2} \cdot \text{Sin}(\gamma)]$  with γ negative.

Op-amp U2A gives  $\Delta I_{s\text{rot}}^{s2} = -[-\Delta I_s^{s1} \cdot \text{Sin}(\gamma) - \Delta I_s^{s2} \cdot \text{Cos}(\gamma)]$ .

To make adjusting of the amplification factors easier, also a 10V reference voltage has been implemented, built around op-amp U2C. The inputs can be connected either to the 10V reference or to the input signals by switch S1.

### 5.5. PCB 4, the 2-3 converter.

The equation which has to be solved, to transform the two phase system back into a three phase system is given in equation ( 5.3).

$$(5.3) \quad \begin{bmatrix} I_{sa\ rot} \\ I_{sb\ rot} \\ I_{sc\ rot} \end{bmatrix} = \begin{bmatrix} \frac{2}{3} & 0 & \frac{1}{3} \\ -\frac{1}{3} & \frac{1}{\sqrt{3}} & \frac{1}{3} \\ -\frac{1}{3} & \frac{1}{\sqrt{3}} & \frac{1}{3} \end{bmatrix} \cdot \begin{bmatrix} I_{s\ rot}^{s1} \\ I_{s\ rot}^{s2} \\ I_{s0} \end{bmatrix}$$

The 2 to 3 coordinate converter has been built on a modified PCB of a 3 to 2 converter.

First of all the resistors to adjust offset and unit have been removed, because these features are only necessary to compensate the errors introduced by the measuring sensors. The part to transform the neutral current has not been implemented as well, because no neutral current is involved.

Figure 5.9 shows the scheme of the remaining circuit. The input signals are buffered, and also negative equivalents are generated by U1. Next the input signals are added with each other according to equation ( 5.3) (built around the op-amps U2). The multiplication factors are set by the resistors R9, R22, R23, R34 and R35. The resistors R12, R24 and R37 are also implemented, to introduce a multiplication factor of 2/3. The multiplication factors are derived in the same way as the factors of the 3-2 converter, given in Table 5.1.

### 5.6. PCB 5, the vector driver.

The vector driver is implemented on an existing PCB 5, which contains some buffer IC's and a PLD (Programmable Logic Device). The scheme of this PCB is given in figure 5.10.

The IC's U1, U2, U18 and U19 are the input buffers. IC U3 is the PLD and U4 is an output buffer. U5, U6, U7 and U8 are the drivers, to drive the 6 optic fibre outputs, which lead to the inverter, to switch the 6 IGBT's. The buffers U2 and U18 have been removed and the corresponding input and output pins of the IC socket have been short-circuited. In this way these inputs can be used as output, for the switching time T.

The driver algorithm, which is given in figure 5.1, has been programmed in the PLD. The programmed schematic is given in figure 5.11. Every state has been represented by a flip-flop. When the vector driver is in a certain state, then the output of the corresponding flip-flop will be high and all the other flip-flop outputs will be low.

A flip-flop can only be set if the corresponding current limit is crossed (input is low), if the flip-flop isn't set already and if the vector driver is not in the next two states. The latter means that switching one or two states back has been excluded.

A certain flip-flop can be reset when the driver is switched into an other state. If for example state 1 is switched on and the B- current limit is crossed, then first the driver will switch into state 2 while state 1 is still active. Immediately when state 2 is switched on, the flip-flop of state 1 will be reset, and state 1 will be switched off.

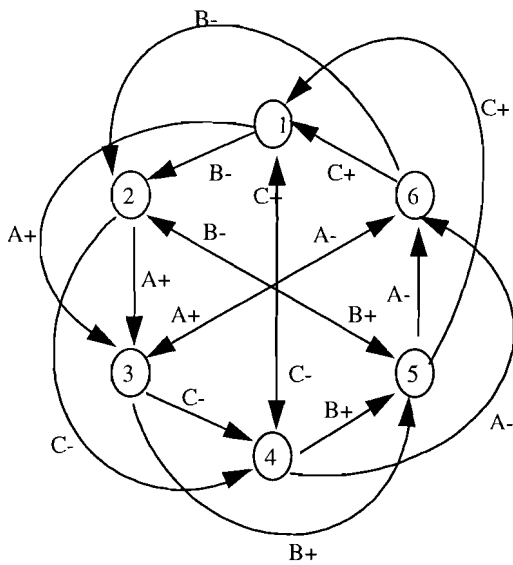


**Figure 5.1: Switching algorithm of the vector driver.**

The table (table 2.1) with six possible inverter states, which tells us which IGBT's have to be switched on when the driver is in a certain state, has been represented by three 'or gates'. If the output of an 'or gate' is high, then the corresponding machine phase will be connected to the positive rail. If the output signal is low, then the corresponding phase will be connected to the negative rail.

The 'Timing Ok' blocks are implemented to take care of the delay time. This implies that there is a certain delay between switching an IGBT off and switching the other IGBT on, in a certain phase. This delay time is necessary to give the IGBT's enough time to switch off, before switching another one on, to avoid a short-circuit. The delay time has been set at  $10\mu\text{s}$ .

At the output of each 'Timing Ok' block a protection circuit has been connected, which makes sure that the two IGBT's of a certain phase never will be switched on at the same time, which would cause a short-circuit.

The circuit, which measures the switching period of the IGBT's, is also implemented in the PLD. This period time has been used for the switching frequency controller (see PCB 6 in figure 5.3). Figure 5.12 shows the circuit lay-out of the PLD circuit which takes care of this. The clock frequency of 8MHz is divided by four to 2MHz by a counter. This divided clock signal goes to a second counter (used as a 12 bit counter). The number of the counter will be clocked into the edge triggered latches, every time when the output signal Q4, the drive signal of IGBT C-, goes up. After the number is stored in the latches, the counter will be reset by the reset circuit, and the counter will start from zero. The comparators are implemented, to stop the counter when there is an overflow detected, i.e. if the period time T is larger than 4096 (12 bits) clock cycles (clock cycles after frequency divider), then the counter will stop at its maximum.

The number, stored in the latch has to be divided by  $2 \cdot 10^6$  MHz, to get the period time:

$$T = 5 \cdot 10^{-7} \cdot \text{stored number} [\text{sec}].$$

The binary period time, given in clock cycles, goes to the outputs, to be used by the frequency controller.

### 5.7. PCB 6, the switching frequency controller.

PCB 6 contains the switching frequency controller (figure 5.13). The digital period time is converted from digital to analog, resulting in a negative analog period time T. The unit is:

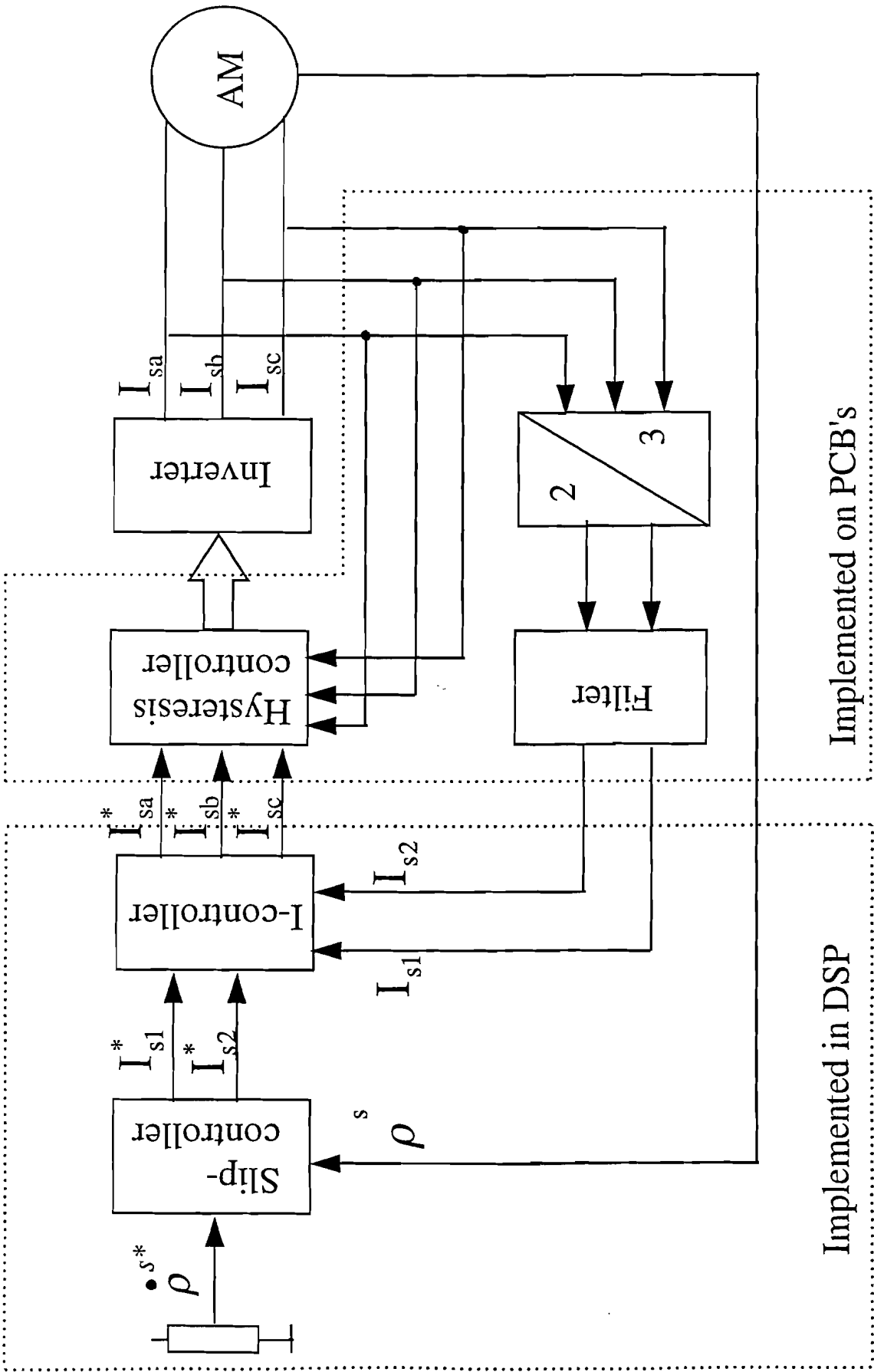
$\frac{4096 \cdot 5 \cdot 10^{-7}}{10} [\text{s} / \text{V}] = 205 \mu\text{s} / \text{V}$ , with an accuracy of 500ns (=2,4mV) which is one bit. Full scale is 10V, which is 2.05ms, and this corresponds with 489Hz. The 10V reference voltage for the DA converter is generated by op-amp U2A. The data sheet of the DA-converter AD7541A of Analog Devices is given in appendix 3.

The measured period time is subtracted from the desired time to get the difference between the desired and measured value,  $\Delta T$  (op-amp U1A).

The time difference is integrated by an integrator with a time constant of 2.2ms, built around op-amp U1B. The time constant has been derived from experiments. The output of the controller has to be limited, in such a way that a hysteresis band width, which is too small or even negative, has been excluded. This has been done by rectifying the output voltage of the integrator and adding a voltage of 0.53V. In this way the minimal hysteresis band voltage has been set at 0.53V. The difference between the desired current and the measured current is multiplied by 12 before it is compared with the hysteresis band width. The unit of the measured current is 11A/V. This means a minimal hysteresis band voltage of 0.53V is equal to a hysteresis band width of:

$$2 * \frac{0.53[\text{V}] * 11[\text{A} / \text{V}]}{12} = 1A_{pp}.$$

When the switch S1 is open, the hysteresis band voltage will be 3V, given by the reference voltage of op-amp U1D. This can be useful when a fixed hysteresis band width is desired. If the switch S1 is closed, then the switching frequency controller will be operational.



Implemented on PCB's

Implemented in DSP

Figure 5.2: Entire experimental set-up.



Figure 5.3: Overview of the hysteresis current controller.

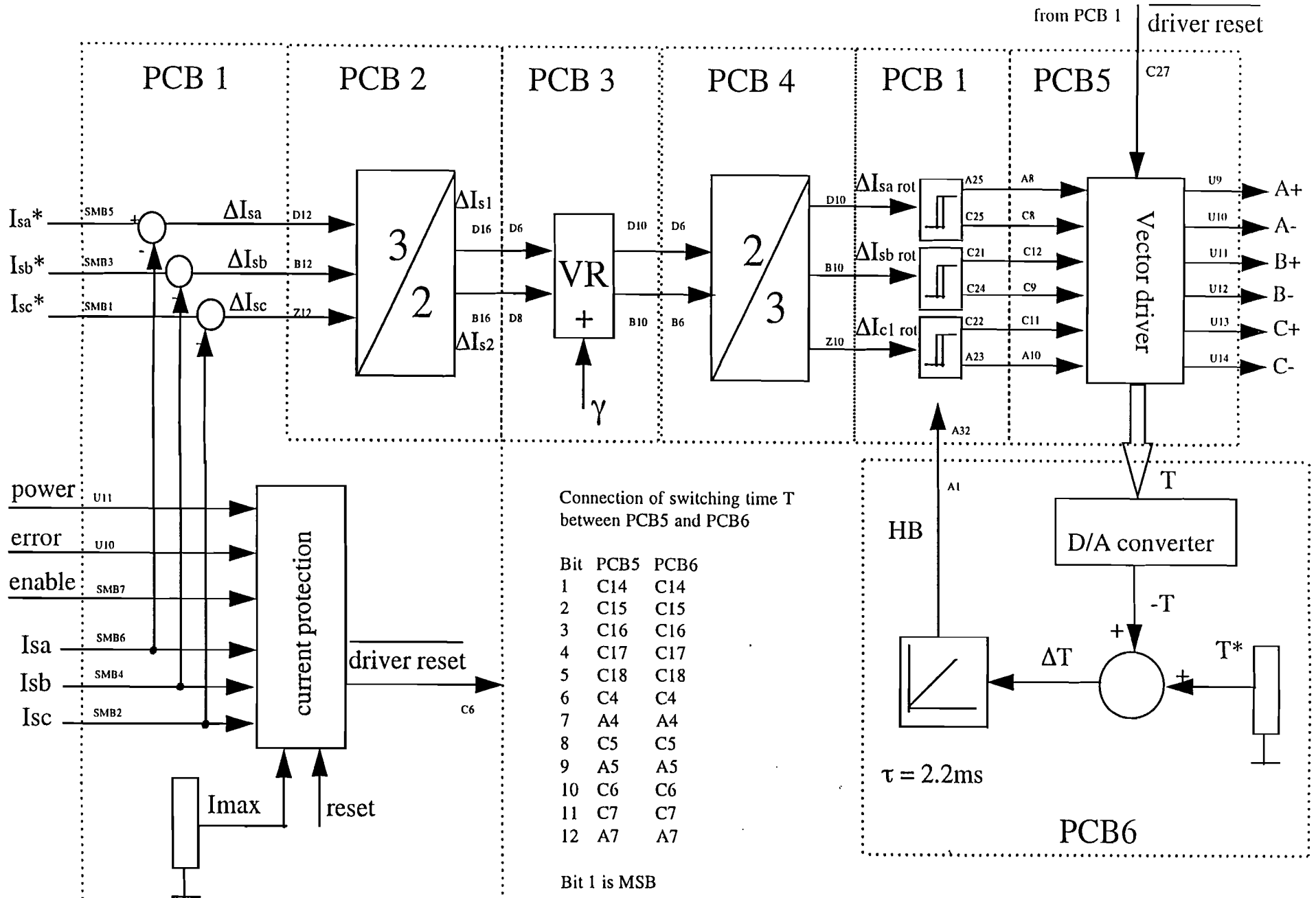




Figure 5.5: Hysteresis current controller, protection part (PCB 1).

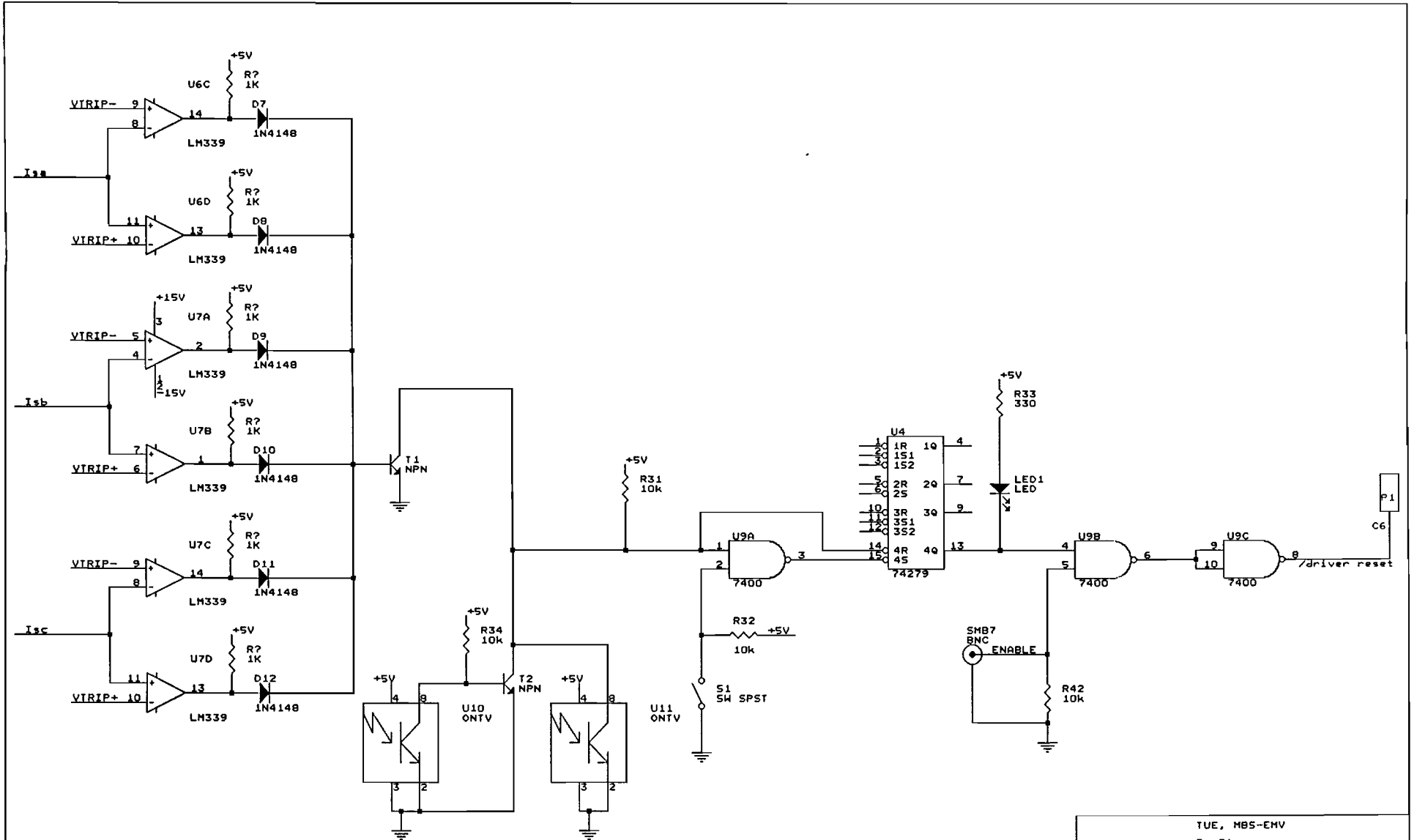
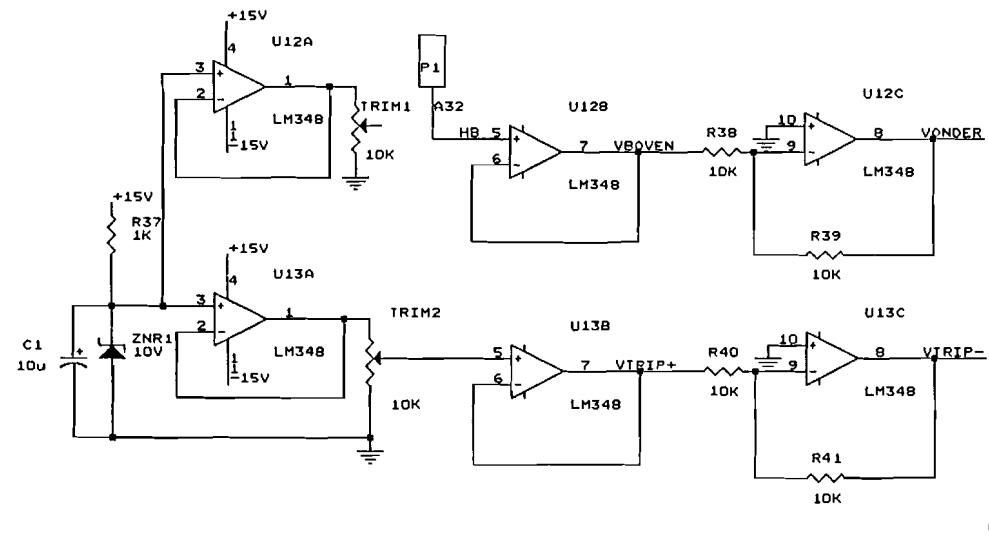
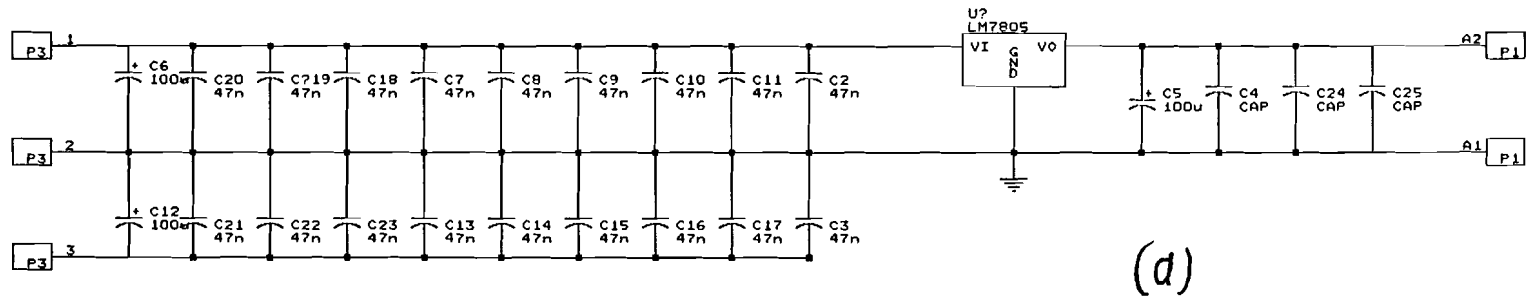


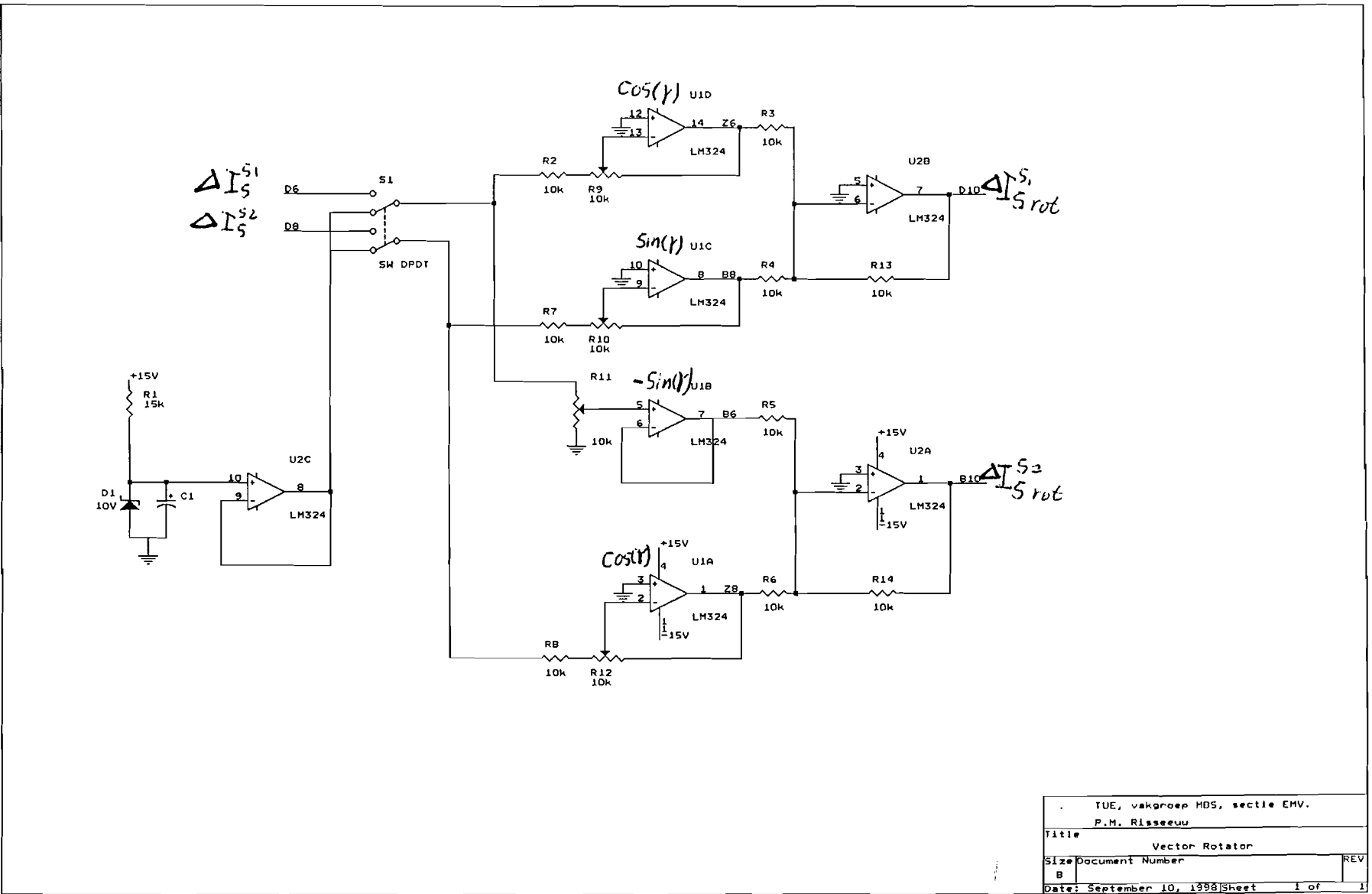
Figure 5.6: Hysteresis current controller, power supply (PCB 1).



TUE, M85-EMV	
P. Risseuw.	
Title Hysteresis current controller	
Size B	Document Number
Date: September 11, 1998	Sheet 3 of 3

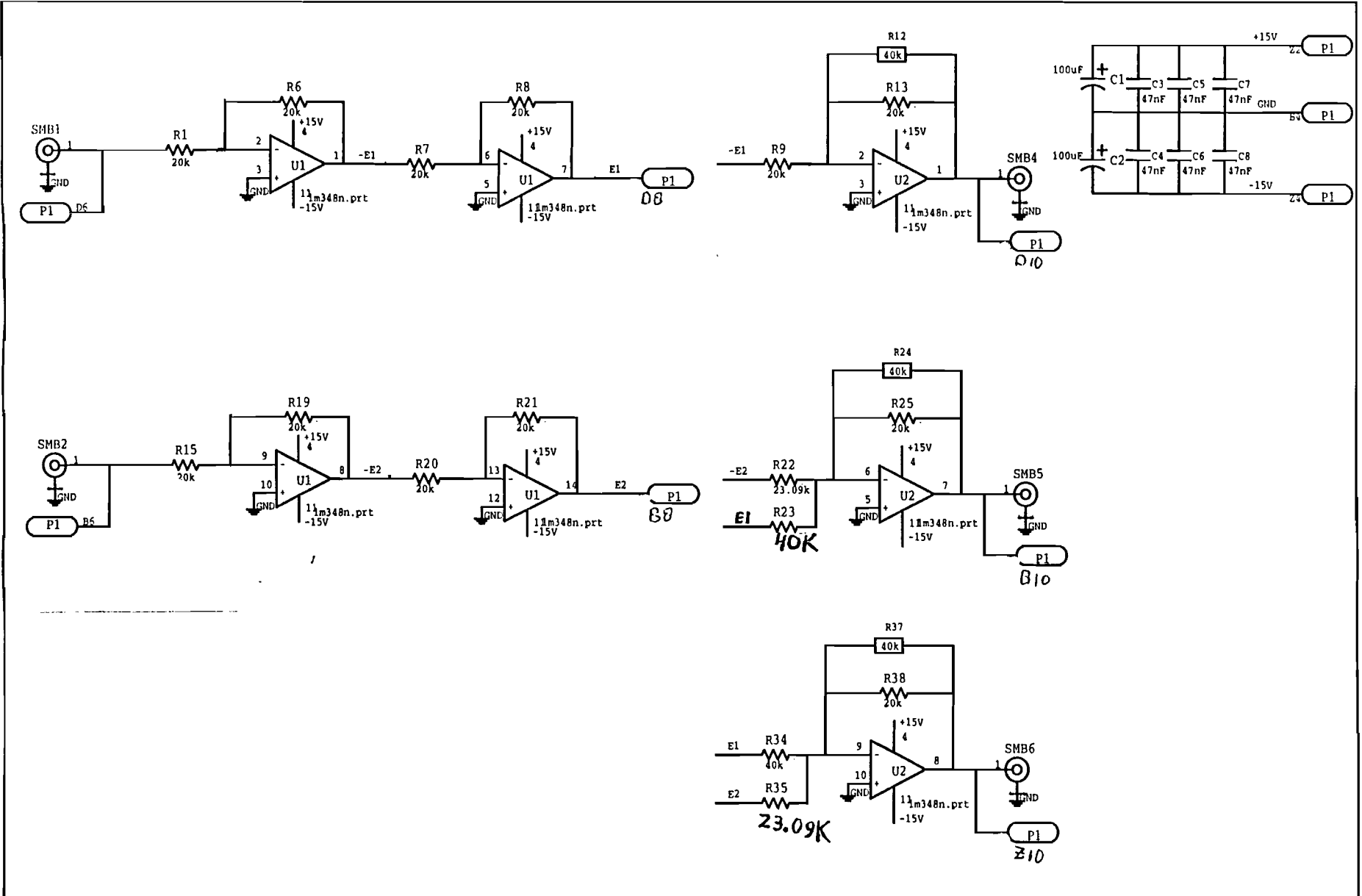


Figure 5.8: Vector rotator (PCB 3).



TUE, vakgroep MBS, sectie EMV.	
P.M. Risseuu	
Title Vector Rotator	
Size B	Document Number REV
Date: September 10, 1998	Sheet 1 of 1

Figure 5.9: 2-3 converter (PCB 4).

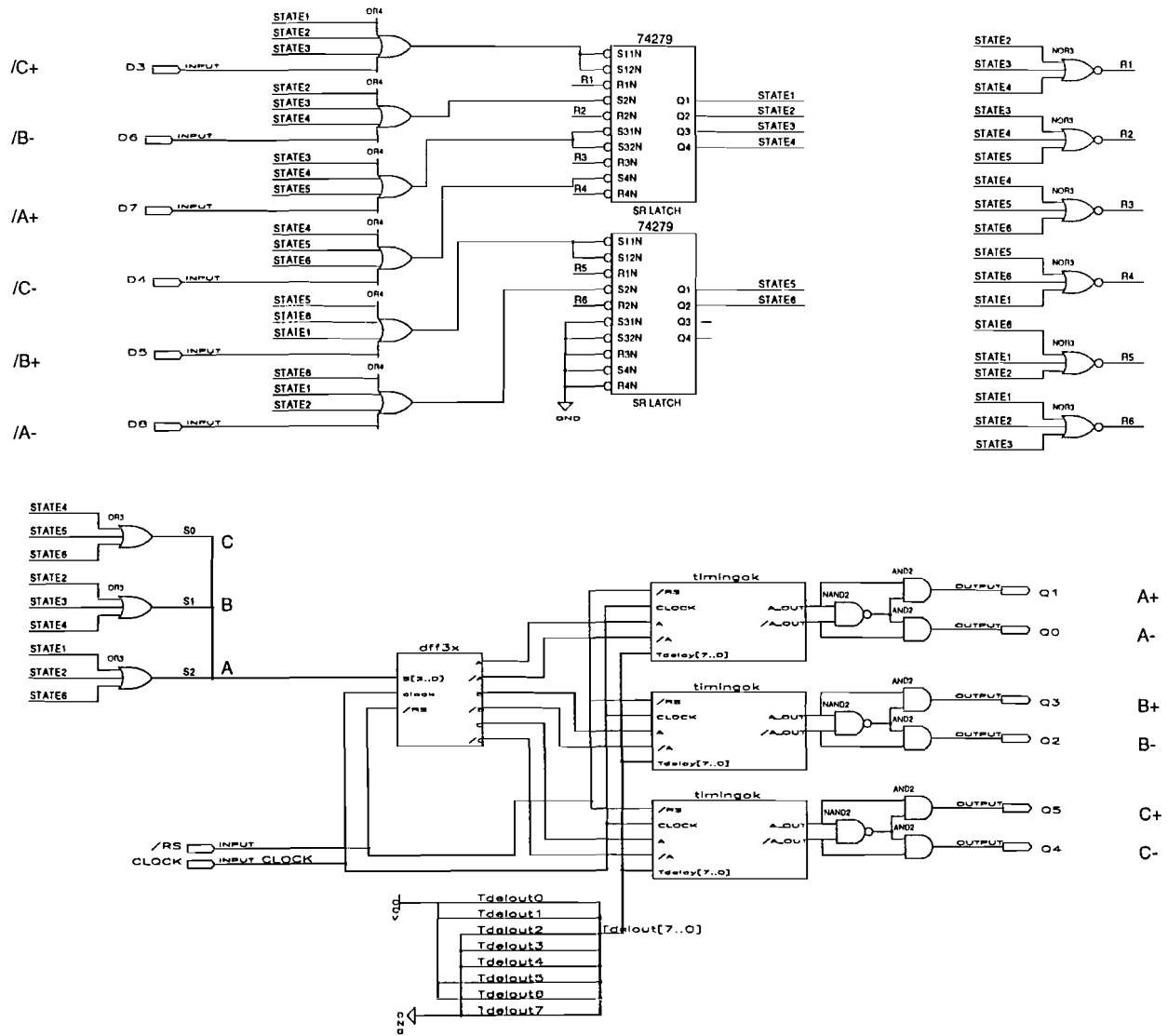


TUOE	TITEL	2-3 WANDLER	
VAKGROEP ENV	OMSCHRIJVING		
REVISIE			
Datum	Door		
	DATUM21-02-1	TEKENAARM	Uyt de Williger
	sheetA	Number of sheets	from 66





Figure 5.11: Vector driver PLD, switching algorithm (PCB 5).



TITLE			
Vector driver			
COMPANY			
IUF -- VAKGROEP FMV			
DESIGNER			
P.M. Rissouw			
ISS D	NUMBER	1.00	REV A
DATE	10-12-90	0-18-1993	SHEET 1 OF 2





## 6. Conclusion

A good working hysteresis current controller which doesn't use the zero-voltage vectors has been developed. It is a controller which can be used for every asynchronous machine.

Tuning of any parameter is not necessary.

At low speed the hysteresis current controller shows stable operation which involves that all the six possible inverter voltage vectors (the zero-voltage vectors are excluded) are equally used, resulting in a stable average output current.

Stable operation can be disturbed by the influence of the stator resistances and asymmetry of the machine parameters. The conditions for stable operation have been derived: Besides a right switching algorithm for the inverter, the error current vector (difference between the measured and desired current values) has to be rotated over a negative angle. Experiments confirm these stability conditions.

At higher speed the inverter shows also stable operation. The stator current trajectory in the stator reference frame is regular and predictable. Only the average output current of the inverter doesn't fit the desired value anymore. The latter introduces some harmonic distortion.

At zero speed the hysteresis current controller gives no harmonic distortion, except the switching frequency component. This is due to the equal current slope values of the three phase currents, when the six possible voltage vectors are switched on. At higher speed some harmonic distortion appears, because the average inverter output current values doesn't meet the desired current values. Fact is, the lower the difference between the DC-link voltage and the EMF voltage, the higher the harmonic distortion at higher speed, due to the increasing influence of the EMF voltage on the stator current trajectory with regard to the influence of the inverter voltage. This means there are two factors, that cause an increase of harmonic distortion: Increase of the EMF voltage (speed), and decrease of the DC-link voltage. Nevertheless, the maximal measured harmonic distortion under different circumstances was less than 3%.

At low speed the classic hysteresis current controller can meet the same specifications as the novel hysteresis current controller. But at higher speed, above 5% of the rated speed, the classic hysteresis current controller shows random behaviour, due to the zero-voltage vectors, which are switched on now and then. The switching algorithm of the novel hysteresis controller gives a predictive and stable operation of the inverter over the whole speed range.

A disadvantage of avoiding the use of zero-voltage vectors is that the switching frequency of the inverter increases at low speed. An increase of the switching frequency involves that the switching losses of the inverter increase. There are several ways to decrease the switching frequency to an acceptable value: Increase of the hysteresis band width or decrease of the DC-link voltage. The first method can easily be implemented. But increase of the hysteresis band width gives a larger ripple current, resulting in higher machine losses. Nevertheless, a larger hysteresis band width doesn't influence the harmonic current distortion at low speed. With a variable DC-link voltage, the switching frequency can also be limited. But the DC-link voltage can't be freely chosen at every value, because the DC-link voltage has always to be larger than the EMF voltage. The combination of a variable hysteresis band width and DC-link voltage, to handle the switching frequency at low speed, gives a good solution: The hysteresis band width can be limited, resulting in a smaller ripple current and on the other hand, the minimal difference between the DC-link voltage and the EMF voltage can be guaranteed.

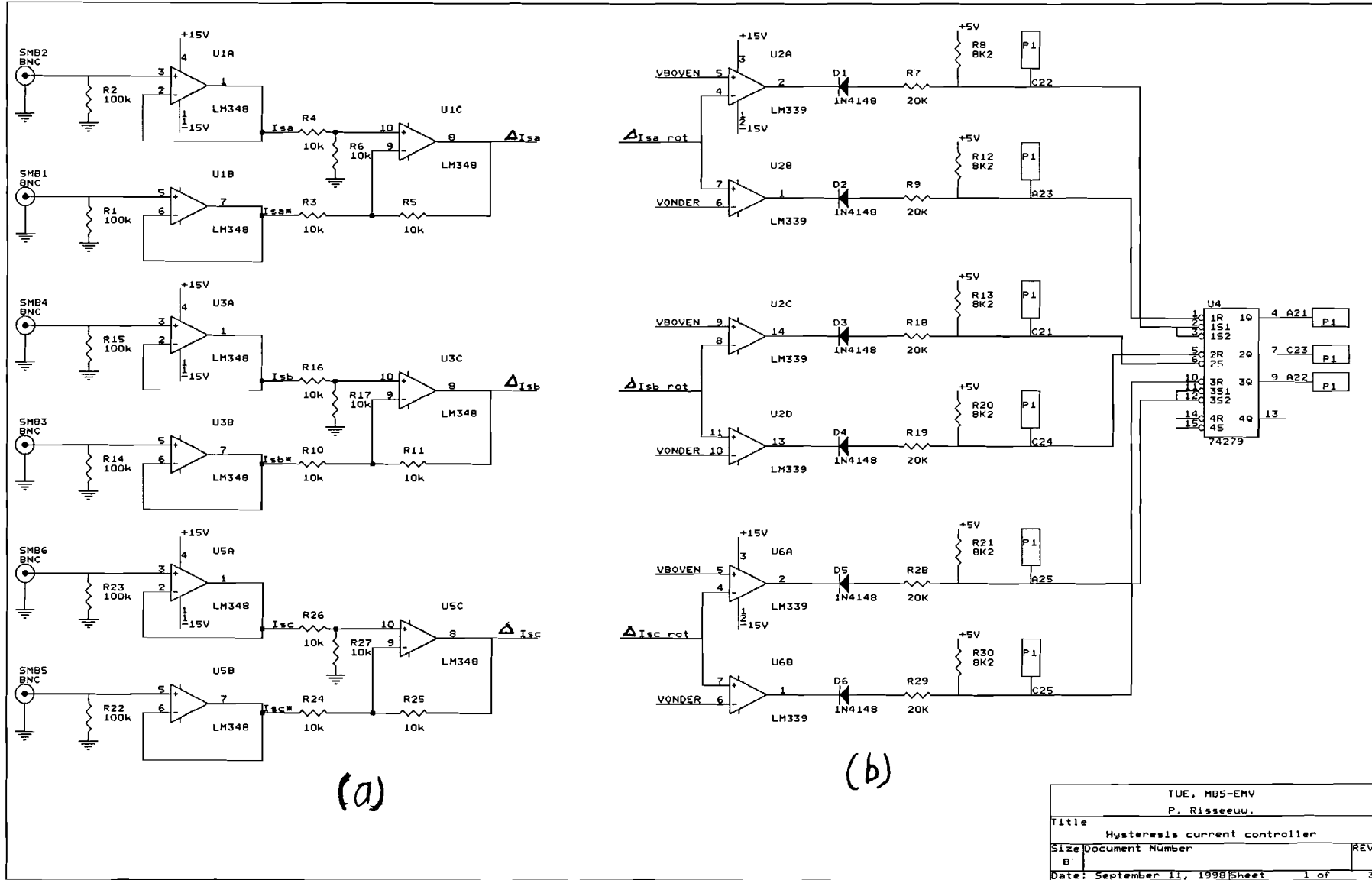
Another way to reduce the switching frequency, which hasn't been examined in this report, could be inserting inductors between the inverter and machine in combination with a variable hysteresis band width. In high power inverters output inductors are implemented anyway. In this way the stray inductances are artificially increased which gives smaller current slope values, resulting in a larger switching period time. When the values of the inductances are chosen well, it should be possible to limit the switching frequency at low speed, with an acceptable hysteresis band width. At high speed the hysteresis band width will be decreased to keep the switching frequency at the desired value. Decrease of the hysteresis band width at high speed can also result in a decrease of harmonic distortion. A problem could be that the rated flux value of the machine can't be reached anymore at full speed, if the voltage drop over the output inductors of the inverter is too high. Investigation has to be done, to learn whether this phenomenon can be neglected or not.

## References

- [1] Blaschke, F., J. van der Burgt and A. Vandenput  
*Sensorless Direct Field Orientation at Zero Flux Frequency.*  
In: IEEE Industry Applications Conference Thirty-First, San Diego, USA, 6-10 Oct. 1996.  
New York: IEEE, 1996. Vol. 1, p. 189-196.
- [2] Brod, D. and D. Novotny  
*Current Control of VSI-PWM inverters.*  
IEEE Transactions on Industrial Applications, Vol. IA-21 (1985), p. 562-570.
- [3] Blaschke, F. and A. Vandenput  
*Control of ac machines, Vol. 1 Text, Vol.2 Figures (in Dutch).*  
Eindhoven University of Technology Report 96-E-296, 1996.
- [4] Schot, J.A.  
*Elektrische machines 1.*  
Eindhoven University of Technology. Dictation 5509.

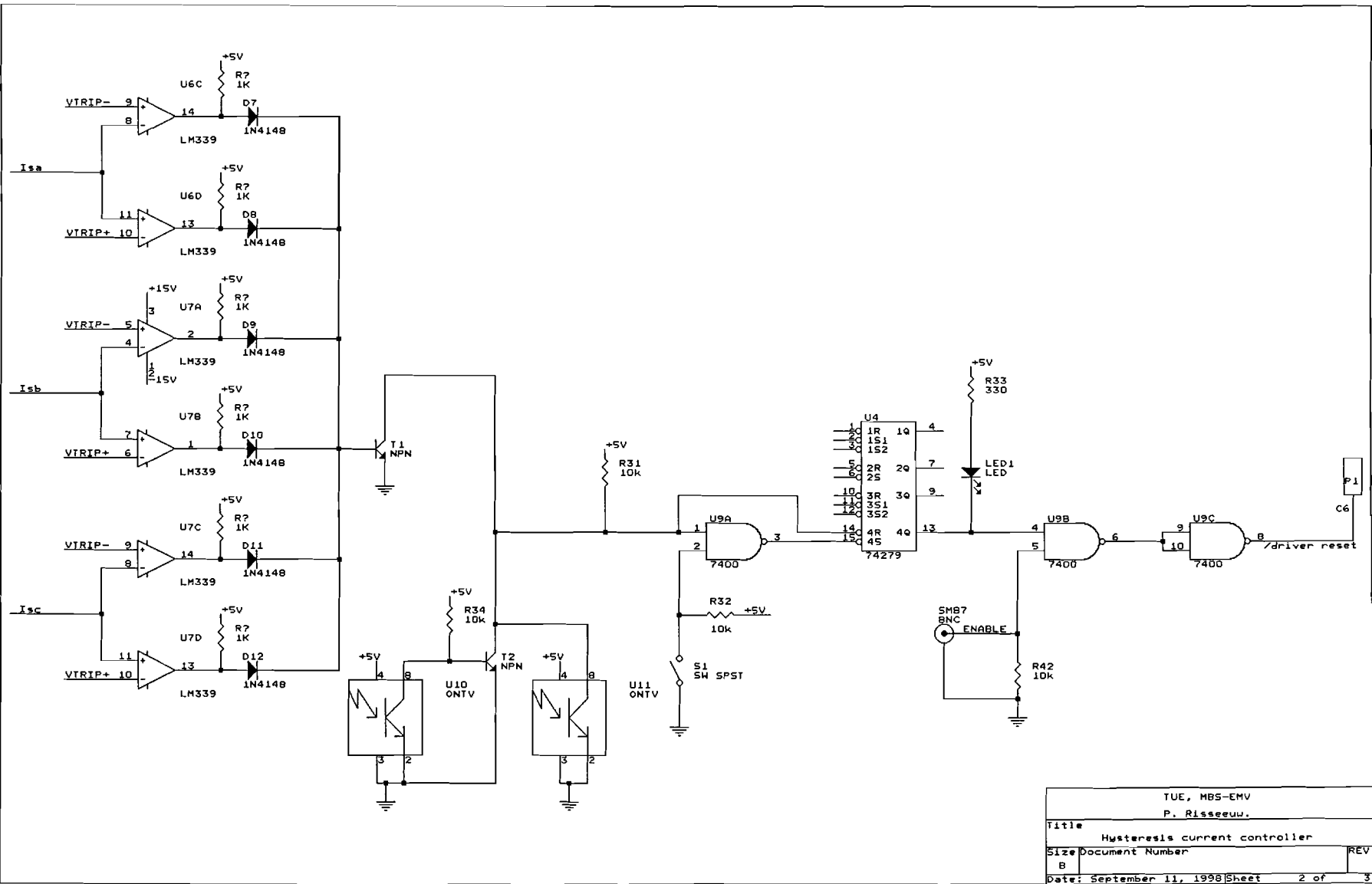
## **Appendix A**

**Circuit lay-out of PCB 1: Hysteresis current controller.**

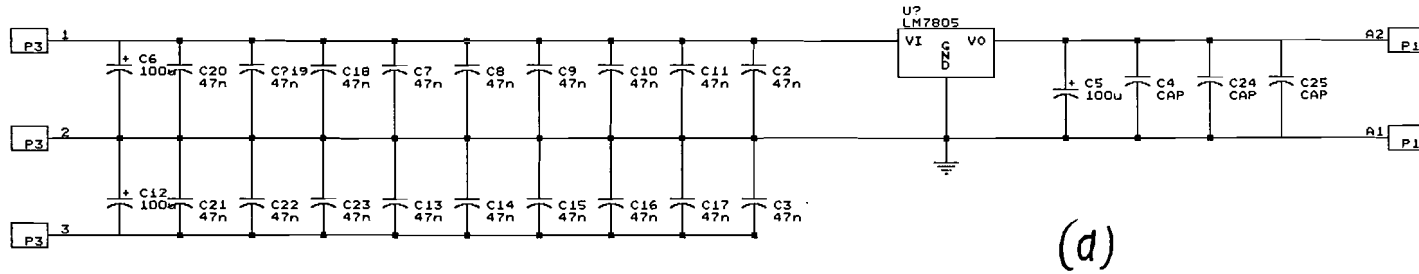


TUE, HB5-EMV	
P. Risseuu.	
Title Hysteresis current controller	
Size Document Number	REV
B'	
Date: September 11, 1998	Sheet 1 of 3

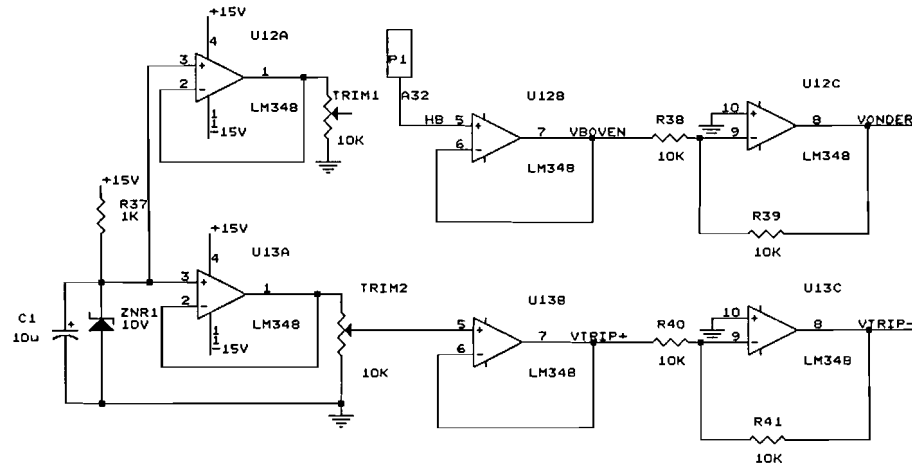




TUE, MBS-EMV	
P. Risseuw,	
Title Hysteresis current controller	
Size B	Document Number REV
Date: September 11, 1998	Sheet 2 of 3

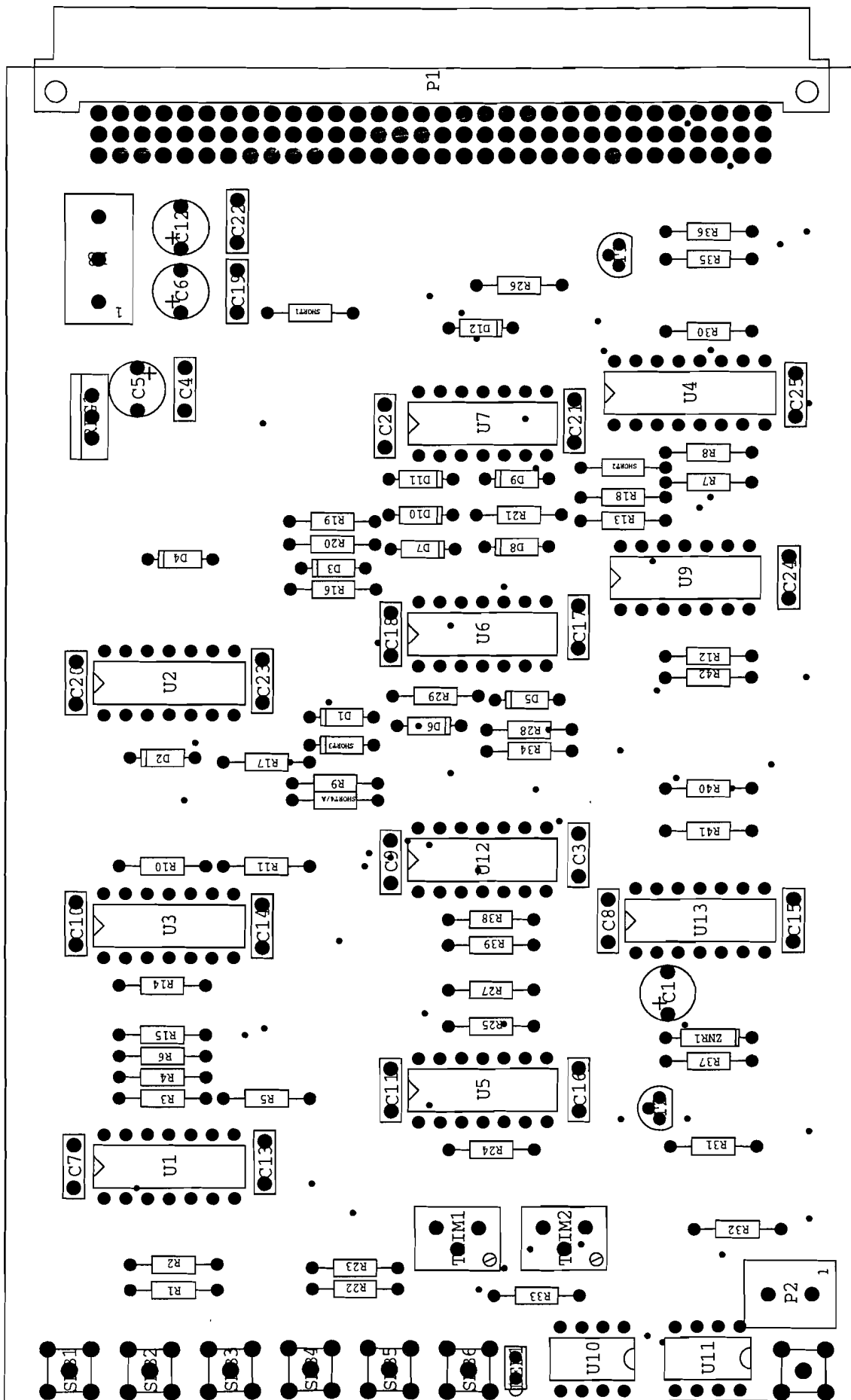


(a)



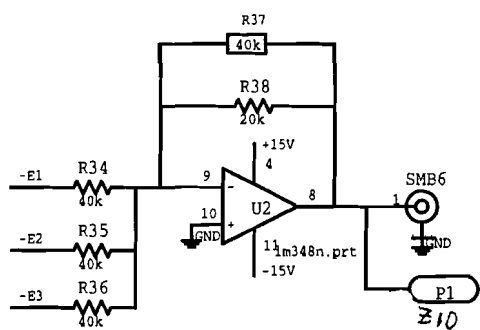
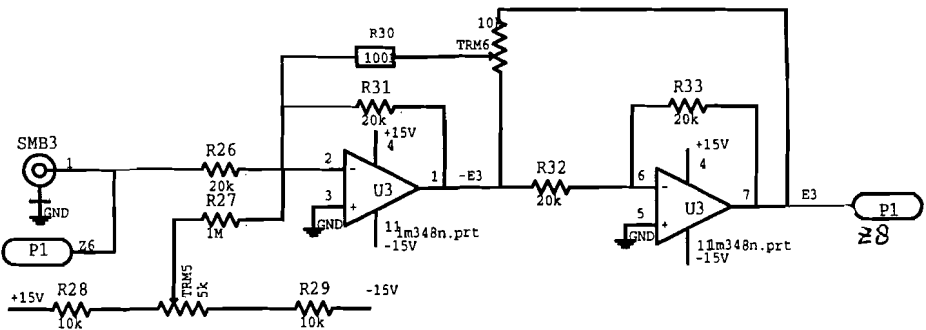
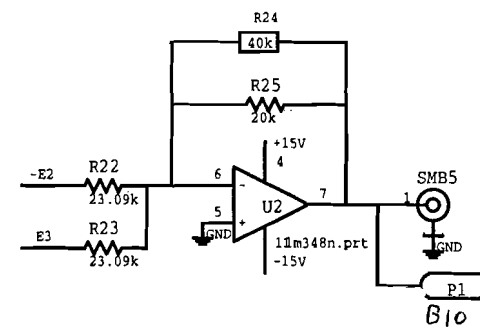
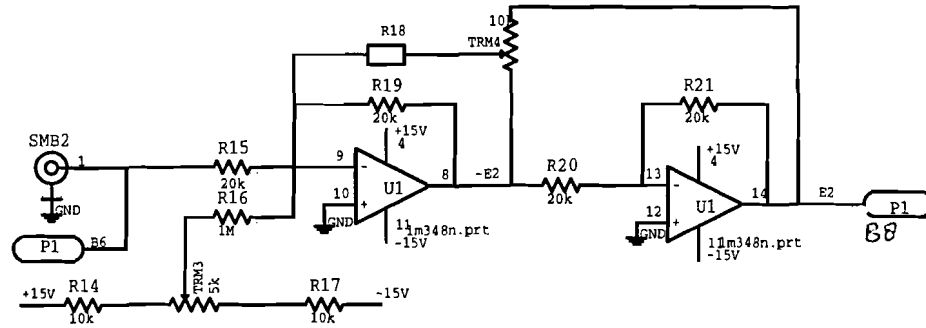
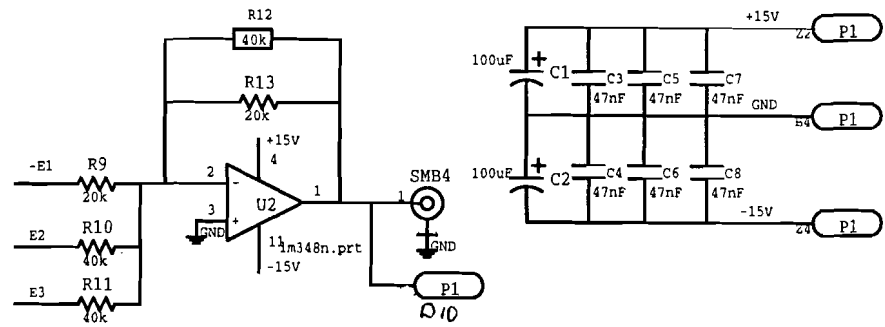
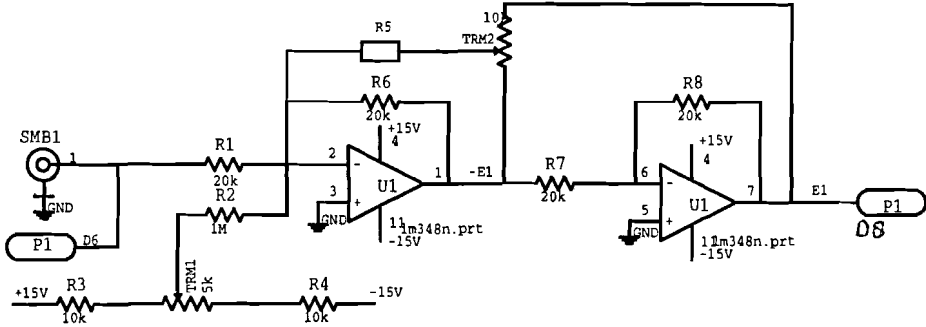
(b)

TUE, MBS-EMV		
P. Risseuw.		
Title Hysteresis current controller		
Size	Document Number	REV
B		
Date: September 11, 1998	Sheet	3 of 3

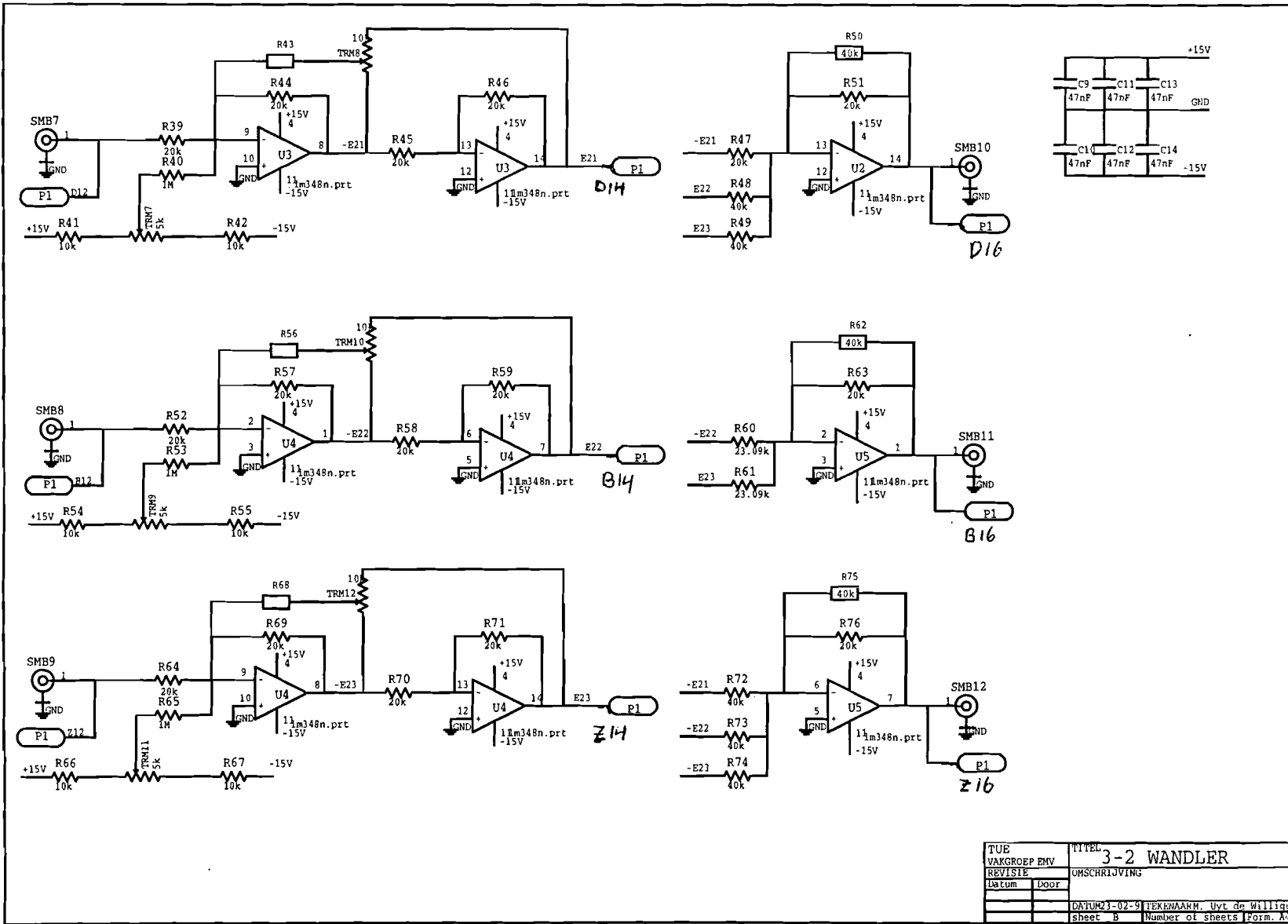


**Appendix B**

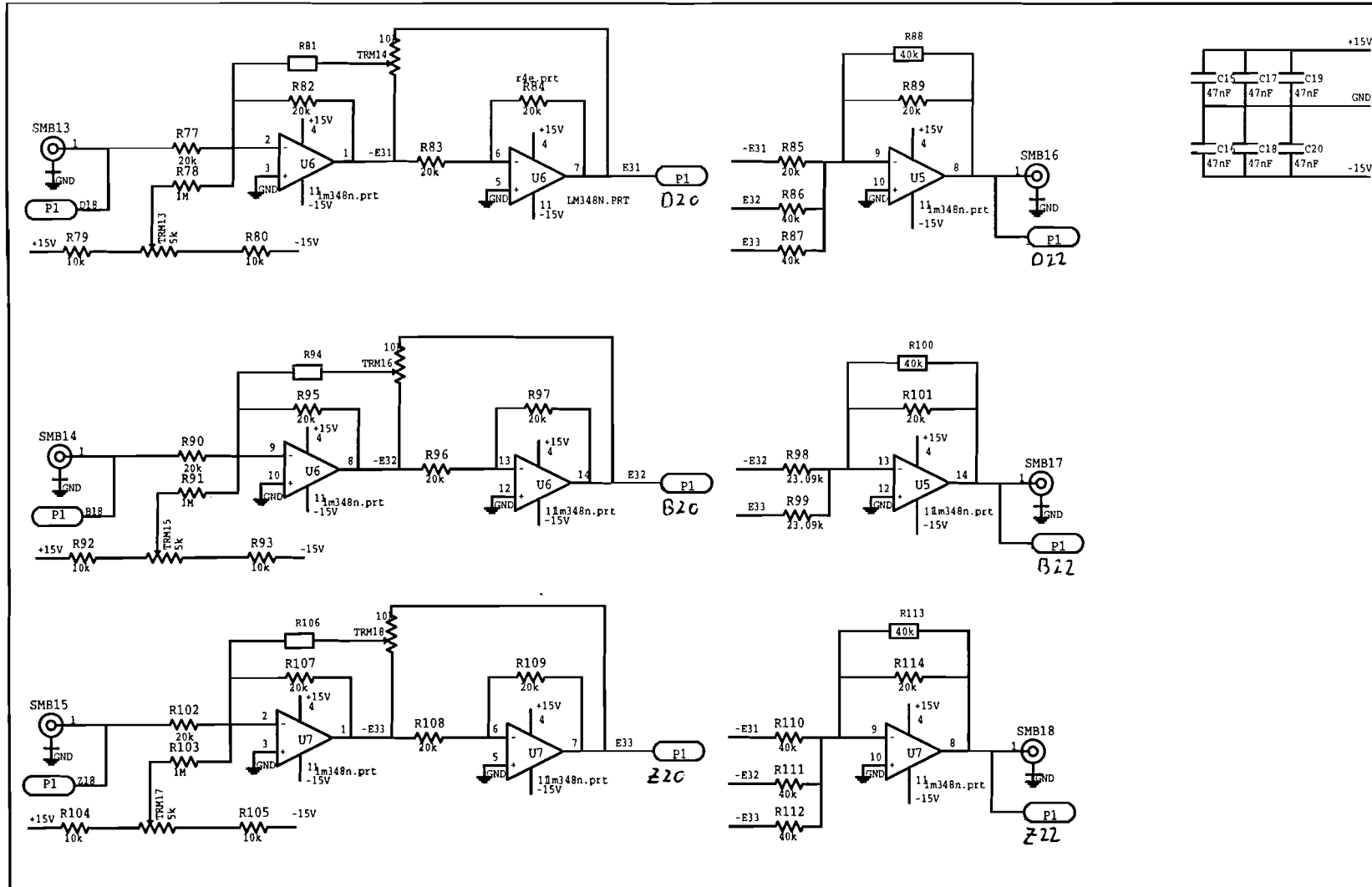
**Circuit lay-out of PCB 2: 3-2 converters.**



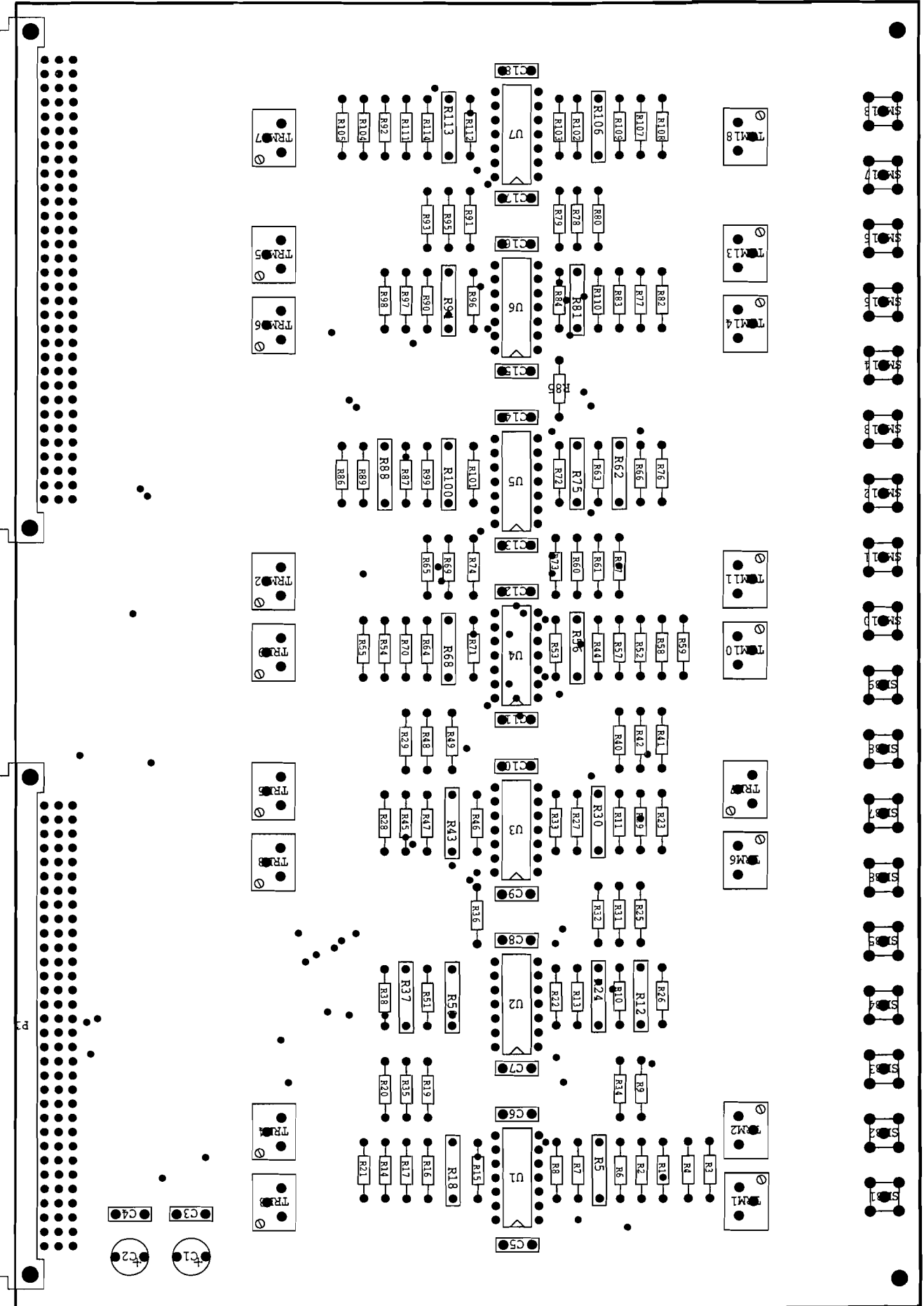
TUE	TITEL 3-2 WANDLER
VAKGROEP EMV	OMSCHRIJVING
REVISIE	
Datum	Door
	DATUM23-02-4 BEKENAARM.Uyt de Williger
	sheetA Number of sheets Form. A4



TUE	TITEL	3-2 WANDLER
VAKGROEP EMV	REVISIE	OMSCHRIJVING
Datum	Door	
	DATUM23-02-91	TEKHNIAARM, Vyt de Willigen
	sheet B	Number of sheets Form. A



TUUE	TITEL	3-2 WANDLER
VAKGROEP EMV	REVISIE	OMSCHRIJVING
Datum	Door	
	DATUM: 23-02-97	TEKENAAR: Jvt de williger
	sheet C	Number of sheets Form. A4





## **Appendix C**

### **Data sheet of the D/A converter AD7541A**

### FEATURES

- Improved Version of AD7541
- Full Four-Quadrant Multiplication
- 12-Bit Linearity (Endpoint)
- All Parts Guaranteed Monotonic
- TTL/CMOS Compatible
- Low Cost
- Protection Schottky Diodes Not Required
- Low Logic Input Leakage

### GENERAL DESCRIPTION

The Analog Devices AD7541A is a low cost, high performance 12-bit monolithic multiplying digital-to-analog converter. It is fabricated using advanced, low noise, thin film on CMOS technology and is available in a standard 18-lead DIP and in 20-terminal surface mount packages.

The AD7541A is functionally and pin compatible with the industry standard AD7541 device and offers improved specifications and performance. The improved design ensures that the device is latch-up free so no output protection Schottky diodes are required.

This new device uses laser wafer trimming to provide full 12-bit endpoint linearity with several new high performance grades.

### ORDERING GUIDE<sup>1</sup>

Model <sup>2</sup>	Temperature Range	Relative Accuracy T <sub>MIN</sub> to T <sub>MAX</sub>	Gain Error T <sub>A</sub> = +25°C	Package Options <sup>3</sup>
AD7541AJN	0°C to +70°C	±1 LSB	±6 LSB	N-18
AD7541AKN	0°C to +70°C	±1/2 LSB	±1 LSB	N-18
AD7541AJP	0°C to +70°C	±1 LSB	±6	P-20A
AD7541AKP	0°C to +70°C	±1/2 LSB	±1	P-20A
AD7541AKR	0°C to +70°C	±1/2 LSB	±1	R-18
AD7541AAQ	-25°C to +85°C	±1 LSB	±6 LSB	Q-18
AD7541ABQ	-25°C to +85°C	±1/2 LSB	±1 LSB	Q-18
AD7541ASQ	-55°C to +125°C	±1 LSB	±6 LSB	Q-18
AD7541ATQ	-55°C to +125°C	±1/2 LSB	±1 LSB	Q-18
AD7541ASE	-55°C to +125°C	±1 LSB	±6 LSB	E-20A
AD7541ATE	-55°C to +125°C	±1/2 LSB	±1 LSB	E-20A

### NOTES

<sup>1</sup>Analog Devices reserves the right to ship either ceramic (D-18) or cerdip (Q-18) hermetic packages.

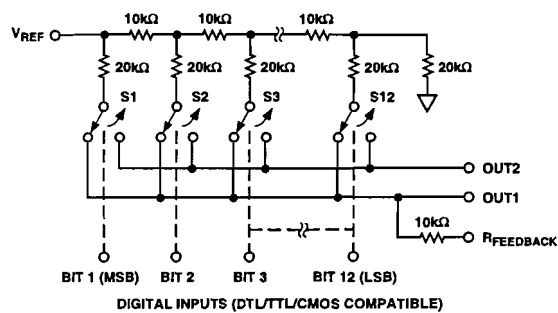
<sup>2</sup>To order MIL-STD-883, Class B process parts, add /883B to part number. Contact local sales office for military data sheet.

<sup>3</sup>E = Leadless Ceramic Chip Carrier; N = Plastic DIP; P = Plastic Leaded Chip Carrier; Q = Cerdip; R = Small Outline IC.

### REV. B

Information furnished by Analog Devices is believed to be accurate and reliable. However, no responsibility is assumed by Analog Devices for its use, nor for any infringements of patents or other rights of third parties which may result from its use. No license is granted by implication or otherwise under any patent or patent rights of Analog Devices.

### FUNCTIONAL BLOCK DIAGRAM



LOGIC: A SWITCH IS CLOSED TO I<sub>OUT1</sub> FOR ITS DIGITAL INPUT IN A "HIGH" STATE.

### PRODUCT HIGHLIGHTS

**Compatibility:** The AD7541A can be used as a direct replacement for any AD7541-type device. As with the Analog Devices AD7541, the digital inputs are TTL/CMOS compatible and have been designed to have a ±1 μA maximum input current requirement so as not to load the driving circuitry.

**Improvements:** The AD7541A offers the following improved specifications over the AD7541:

1. Gain Error for all grades has been reduced with premium grade versions having a maximum gain error of ±3 LSB.
2. Gain Error temperature coefficient has been reduced to 2 ppm/°C typical and 5 ppm/°C maximum.
3. Digital-to-analog charge injection energy for this new device is typically 20% less than the standard AD7541 part.
4. Latch-up proof.
5. Improvements in laser wafer trimming provides 1/2 LSB max differential nonlinearity for top grade devices over the operating temperature range (vs. 1 LSB on older 7541 types).
6. All grades are guaranteed monotonic to 12 bits over the operating temperature range.

# AD7541A—SPECIFICATIONS (V<sub>DD</sub> = +15 V, V<sub>REF</sub> = +10 V; OUT 1 = OUT 2 = GND = 0 V unless otherwise noted)

Parameter	Version	T <sub>A</sub> = +25°C	T <sub>A</sub> = T <sub>MIN</sub> , T <sub>MAX</sub> <sup>1</sup>	Units	Test Conditions/Comments
<b>ACCURACY</b>					
Resolution	All	12	12	Bits	
Relative Accuracy	J, A, S K, B, T	±1 ±1/2	±1 ±1/2	LSB max LSB max	±1 LSB = ±0.024% of Full Scale ±1/2 LSB = ±0.012% of Full Scale
Differential Nonlinearity	J, A, S K, B, T	±1 ±1/2	±1 ±1/2	LSB max LSB max	All Grades Guaranteed Monotonic to 12 Bits, T <sub>MIN</sub> to T <sub>MAX</sub> .
Gain Error	J, A, S K, B, T	±6 ±3	±8 ±5	LSB max LSB max	Measured Using Internal R <sub>FB</sub> and Includes Effect of Leakage Current and Gain TC. Gain Error Can Be Trimmed to Zero.
Gain Temperature Coefficient <sup>2</sup> ΔGain/ΔTemperature	All	5	5	ppm/°C max	Typical Value Is 2 ppm/°C.
Output Leakage Current OUT1 (Pin 1)	J, K A, B S, T	±5 ±5 ±5	±10 ±10 ±200	nA max nA max nA max	All Digital Inputs = 0 V.
OUT2 (Pin 2)	J, K A, B S, T	±5 ±5 ±5	±10 ±10 ±200	nA max nA max nA max	All Digital Inputs = V <sub>DD</sub> .
<b>REFERENCE INPUT</b>					
Input Resistance (Pin 17 to GND)	All	7–18	7–18	kΩ min/max	Typical Input Resistance = 11 kΩ. Typical Input Resistance Temperature Coefficient = -300 ppm/°C.
<b>DIGITAL INPUTS</b>					
V <sub>IH</sub> (Input HIGH Voltage)	All	2.4	2.4	V min	
V <sub>IL</sub> (Input LOW Voltage)	All	0.8	0.8	V max	
I <sub>IN</sub> (Input Current)	All	±1	±1	μA max	Logic Inputs Are MOS Gates. I <sub>IN</sub> typ (25°C) = 1 nA.
C <sub>IN</sub> (Input Capacitance) <sup>2</sup>	All	8	8	pF max	V <sub>IN</sub> = 0 V
<b>POWER SUPPLY REJECTION</b>					
ΔGain/ΔV <sub>DD</sub>	All	±0.01	±0.02	% per % max	ΔV <sub>DD</sub> = ±5%
<b>POWER SUPPLY</b>					
V <sub>DD</sub> Range	All	+5 to +16	+5 to +16	V min/V max	Accuracy Is Not Guaranteed Over This Range.
I <sub>DD</sub>	All	2 100	2 500	mA max μA max	All Digital Inputs V <sub>IL</sub> or V <sub>IH</sub> . All Digital Inputs 0 V or V <sub>DD</sub> .

## AC PERFORMANCE CHARACTERISTICS

These Characteristics are included for Design Guidance only and are not subject to test. V<sub>DD</sub> = +15 V, V<sub>IH</sub> = +10 V except where noted, OUT1 = OUT2 = GND = 0 V, Output Amp is AD544 except where noted.

Parameter	Version <sup>1</sup>	T <sub>A</sub> = +25°C	T <sub>A</sub> = T <sub>MIN</sub> , T <sub>MAX</sub> <sup>1</sup>	Units	Test Conditions/Comments
PROPAGATION DELAY (From Digital Input Change to 90% of Final Analog Output)	All	100	—	ns typ	OUT 1 Load = 100 Ω, C <sub>EXT</sub> = 13 pF. Digital Inputs = 0 V to V <sub>DD</sub> or V <sub>DD</sub> to 0 V.
DIGITAL TO ANALOG GLITCH IMPULSE	All	1000	—	nV-sec typ	V <sub>REF</sub> = 0 V. All digital inputs 0 V to V <sub>DD</sub> or V <sub>DD</sub> to 0 V. Measured using Model 50K as output amplifier.
MULTIPLYING FEEDTHROUGH ERROR <sup>3</sup> (V <sub>REF</sub> to OUT1)	All	1.0	—	mV p-p typ	V <sub>REF</sub> = ±10 V, 10 kHz sine wave.
OUTPUT CURRENT SETTLING TIME	All	0.6	—	μs typ	To 0.01% of full-scale range. OUT 1 Load = 100 Ω, C <sub>EXT</sub> = 13 pF. Digital Inputs = 0 V to V <sub>DD</sub> or V <sub>DD</sub> to 0 V.
<b>OUTPUT CAPACITANCE</b>					
C <sub>OUT1</sub> (Pin 1)	All	200	200	pF max	Digital Inputs = V <sub>IH</sub>
C <sub>OUT2</sub> (Pin 2)	All	70	70	pF max	Digital Inputs = V <sub>IL</sub>
C <sub>OUT1</sub> (Pin 1)	All	70	70	pF max	
C <sub>OUT2</sub> (Pin 2)	All	200	200	pF max	

**NOTES**  
 Temperature range as follows: J, K versions, 0°C to +70°C; A, B versions, -25°C to +85°C; S, T versions, -55°C to +125°C.  
 Guaranteed by design but not production tested.  
 To minimize feedthrough in the ceramic package (Suffix D) the user must ground the metal lid.  
 Specifications subject to change without notice.

## ABSOLUTE MAXIMUM RATINGS\*

(T<sub>A</sub> = +25°C unless otherwise noted)

V <sub>DD</sub> to GND	.....	+17 V
V <sub>REF</sub> to GND	.....	±25 V
V <sub>RFB</sub> to GND	.....	±25 V
Digital Input Voltage to GND	.....	-0.3 V, V <sub>DD</sub> + 0.3 V
OUT 1, OUT 2 to GND	.....	-0.3 V, V <sub>DD</sub> + 0.3 V
Power Dissipation (Any Package)		
To +75°C	.....	450 mW
Derates above +75°C	.....	6 mW/°C

## Operating Temperature Range

Commercial (J, K Versions)	.....	0°C to +70°C
Industrial (A, B Versions)	.....	-25°C to +85°C
Extended (S, T Versions)	.....	-55°C to +125°C
Storage Temperature	.....	-65°C to +150°C
Lead Temperature (Soldering, 10 secs)	.....	+300°C

\*Stresses above those listed under Absolute Maximum Ratings may cause permanent damage to the device. This is a stress rating only; functional operation of the device at these or any other conditions above those indicated in the operational sections of this specification is not implied. Exposure to absolute maximum rating conditions for extended periods may affect device reliability.

## CAUTION

ESD (electrostatic discharge) sensitive device. Electrostatic charges as high as 4000 V readily accumulate on the human body and test equipment and can discharge without detection. Although the AD7541A features proprietary ESD protection circuitry, permanent damage may occur on devices subjected to high energy electrostatic discharges. Therefore, proper ESD precautions are recommended to avoid performance degradation or loss of functionality.



## TERMINOLOGY

### RELATIVE ACCURACY

Relative accuracy or endpoint nonlinearity is a measure of the maximum deviation from a straight line passing through the endpoints of the DAC transfer function. It is measured after adjusting for zero and full scale and is expressed in % of full-scale range or (sub)multiples of 1 LSB.

### DIFFERENTIAL NONLINEARITY

Differential nonlinearity is the difference between the *measured* change and the *ideal* 1 LSB change between any two adjacent codes. A specified differential nonlinearity of ±1 LSB max over the operating temperature range insures monotonicity.

### GAIN ERROR

Gain error is a measure of the output error between an ideal DAC and the actual device output. For the AD7541A, ideal maximum output is

$$-\left(\frac{4095}{4096}\right)(V_{REF})$$

Gain error is adjustable to zero using external trims as shown in Figures 4, 5 and 6.

### OUTPUT LEAKAGE CURRENT

Current which appears at OUT1 with the DAC loaded to all 0s or at OUT2 with the DAC loaded to all 1s.

### MULTIPLYING FEEDTHROUGH ERROR

AC error due to capacitive feedthrough from V<sub>REF</sub> terminal to OUT1 with DAC loaded to all 0s.

### OUTPUT CURRENT SETTLING TIME

Time required for the output function of the DAC to settle to within 1/2 LSB for a given digital input stimulus, i.e., 0 to full scale.

### PROPAGATION DELAY

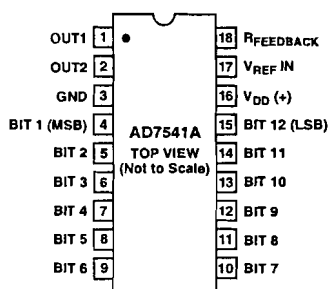
This is a measure of the internal delay of the circuit and is measured from the time a digital input changes to the point at which the analog output at OUT1 reaches 90% of its final value.

### DIGITAL-TO-ANALOG CHARGE INJECTION (QDA)

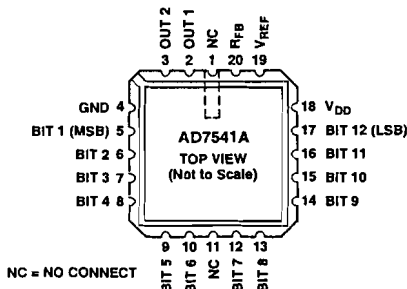
This is a measure of the amount of charge injected from the digital inputs to the analog outputs when the inputs change state. It is usually specified as the area of the glitch in nV secs and is measured with V<sub>REF</sub> = GND and a Model 50K as the output op amp, C1 (phase compensation) = 0 pF.

## PIN CONFIGURATIONS

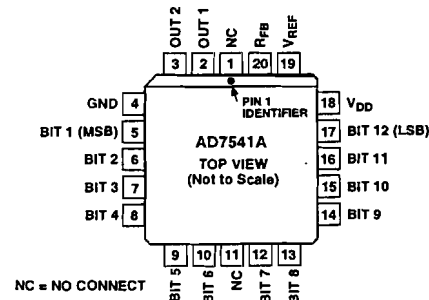
### DIP/SOIC



### LCSS



### PLCC



# AD7541A

## GENERAL CIRCUIT INFORMATION

The simplified D/A circuit is shown in Figure 1. An inverted R-2R ladder structure is used—that is, the binarily weighted currents are switched between the OUT1 and OUT2 bus lines, thus maintaining a constant current in each ladder leg independent of the switch state.

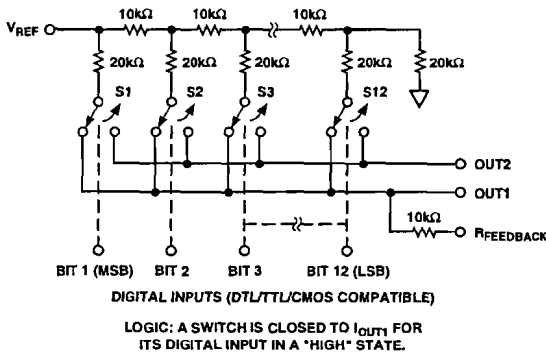


Figure 1. Functional Diagram (Inputs HIGH)

The input resistance at  $V_{REF}$  (Figure 1) is always equal to  $R_{LDR}$  ( $R_{LDR}$  is the R/2R ladder characteristic resistance and is equal to value "R"). Since  $R_{IN}$  at the  $V_{REF}$  pin is constant, the reference terminal can be driven by a reference voltage or a reference current, ac or dc, of positive or negative polarity. (If a current source is used, a low temperature coefficient external  $R_{FB}$  is recommended to define scale factor.)

## EQUIVALENT CIRCUIT ANALYSIS

The equivalent circuits for all digital inputs LOW and all digital inputs HIGH are shown in Figures 2 and 3. In Figure 2 with all digital inputs LOW, the reference current is switched to OUT2. The current source  $I_{LEAKAGE}$  is composed of surface and junction leakages to the substrate, while the  $I_{4096}$  current source represents a constant 1-bit current drain through the termination resistor on the R-2R ladder. The ON capacitance of the output N-channel switch is 200 pF, as shown on the OUT2 terminal. The OFF switch capacitance is 70 pF, as shown on the OUT1 terminal. Analysis of the circuit for all digital inputs HIGH, as shown in Figure 3 is similar to Figure 2; however, the ON switches are now on terminal OUT1, hence the 200 pF at that terminal.

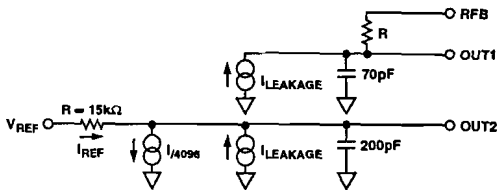


Figure 2. DAC Equivalent Circuit All Digital Inputs LOW

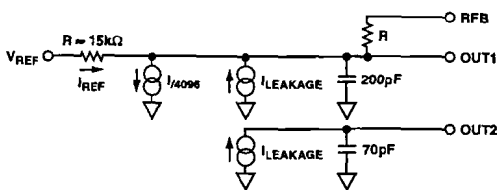


Figure 3. DAC Equivalent Circuit All Digital Inputs HIGH

## APPLICATIONS

### UNIPOLAR BINARY OPERATION (2-QUADRANT MULTIPLICATION)

Figure 4 shows the analog circuit connections required for unipolar binary (2-quadrant multiplication) operation. With a dc reference voltage or current (positive or negative polarity) applied at Pin 17, the circuit is a unipolar D/A converter. With an ac reference voltage or current, the circuit provides 2-quadrant multiplication (digitally controlled attenuation). The input/output relationship is shown in Table II.

$R1$  provides full-scale trim capability [i.e., load the DAC register to 1111 1111 1111, adjust  $R1$  for  $V_{OUT} = -V_{REF}$  (4095/4096)]. Alternatively, Full Scale can be adjusted by omitting  $R1$  and  $R2$  and trimming the reference voltage magnitude.

$C1$  phase compensation (10 pF to 25 pF) may be required for stability when using high speed amplifiers. ( $C1$  is used to cancel the pole formed by the DAC internal feedback resistance and output capacitance at OUT1).

Amplifier A1 should be selected or trimmed to provide  $V_{OS} \leq 10\%$  of the voltage resolution at  $V_{OUT}$ . Additionally, the amplifier should exhibit a bias current which is low over the temperature range of interest (bias current causes output offset at  $V_{OUT}$  equal to  $I_B$  times the DAC feedback resistance, nominally 11 kΩ). The AD544L is a high speed implanted FET input op amp with low factory-trimmed  $V_{OS}$ .

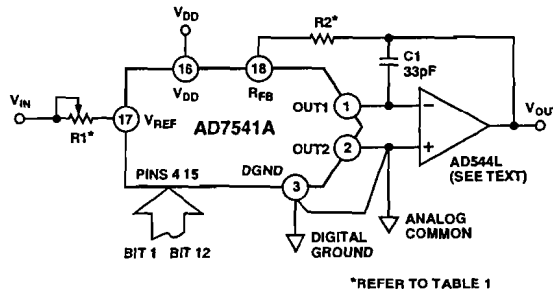


Figure 4. Unipolar Binary Operation

Table I. Recommended Trim Resistor Values vs. Grades

Trim Resistor	JN/AQ/SD	KN/BQ/TD
R1	100 Ω	100 Ω
R2	47 Ω	33 Ω

Table II. Unipolar Binary Code Table for Circuit of Figure 4

Binary Number in DAC	MSB	LSB	Analog Output, $V_{OUT}$
1111 1111 1111			$-V_{IN} \left( \frac{4095}{4096} \right)$
1000 0000 0000			$-V_{IN} \left( \frac{2048}{4096} \right) = -1/2 V_{IN}$
0000 0000 0001			$-V_{IN} \left( \frac{1}{4096} \right)$
0000 0000 0000			0 Volts

## BIPOLAR OPERATION (4-QUADRANT MULTIPLICATION)

Figure 5 and Table III illustrate the circuitry and code relationship for bipolar operation. With a dc reference (positive or negative polarity) the circuit provides offset binary operation. With an ac reference the circuit provides full 4-quadrant multiplication.

With the DAC loaded to 1000 0000 0000, adjust R1 for  $V_{OUT} = 0$  V (alternatively, one can omit R1 and R2 and adjust the ratio of R3 to R4 for  $V_{OUT} = 0$  V). Full-scale trimming can be accomplished by adjusting the amplitude of  $V_{REF}$  or by varying the value of R5.

As in unipolar operation, A1 must be chosen for low  $V_{OS}$  and low  $I_B$ . R3, R4 and R5 must be selected for matching and tracking. Mismatch of  $2R3$  to R4 causes both offset and full-scale error. Mismatch of R5 to R4 or  $2R3$  causes full-scale error. C1 phase compensation (10 pF to 50 pF) may be required for stability, depending on amplifier used.

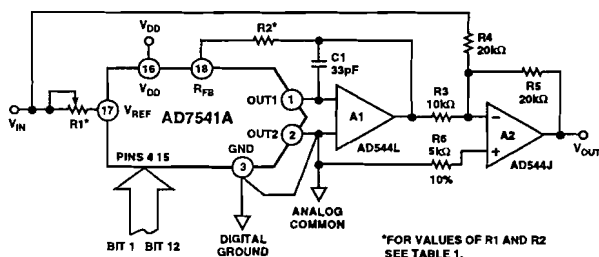


Figure 5. Bipolar Operation (4-Quadrant Multiplication)

Table III. Bipolar Code Table for Offset Binary Circuit of Figure 5

Binary Number in DAC			Analog Output, $V_{OUT}$
MSB	LSB		
1 1 1 1	1 1 1 1	1 1 1 1	$+V_{IN} \left( \frac{2047}{2048} \right)$
1 0 0 0	0 0 0 0	0 0 0 1	$+V_{IN} \left( \frac{1}{2048} \right)$
1 0 0 0	0 0 0 0	0 0 0 0	0 Volts
0 1 1 1	1 1 1 1	1 1 1 1	$-V_{IN} \left( \frac{1}{2048} \right)$
0 0 0 0	0 0 0 0	0 0 0 0	$-V_{IN} \left( \frac{2048}{2048} \right)$

Figure 6 and Table IV show an alternative method of achieving bipolar output. The circuit operates with sign plus magnitude code and has the advantage of giving 12-bit resolution in each quadrant, compared with 11-bit resolution per quadrant for the circuit of Figure 5. The AD7592 is a fully protected CMOS changeover switch with data latches. R4 and R5 should match each other to 0.01% to maintain the accuracy of the D/A converter. Mismatch between R4 and R5 introduces a gain error.

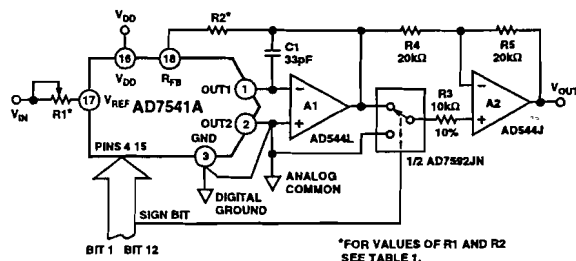


Figure 6. 12-Bit Plus Sign Magnitude Operation

Table IV. 12-Bit Plus Sign Magnitude Code Table for Circuit of Figure 6

Sign Bit	Binary Number in DAC			Analog Output, $V_{OUT}$
	MSB	LSB		
0	1 1 1 1	1 1 1 1	1 1 1 1	$+V_{IN} \times \left( \frac{4095}{4096} \right)$
0	0 0 0 0	0 0 0 0	0 0 0 0	0 Volts
1	0 0 0 0	0 0 0 0	0 0 0 0	0 Volts
1	1 1 1 1	1 1 1 1	1 1 1 1	$-V_{IN} \times \left( \frac{4095}{4096} \right)$

Note: Sign bit of "0" connects R3 to GND.

# AD7541A

## APPLICATIONS HINTS

**Output Offset:** CMOS D/A converters exhibit a code-dependent output resistance which in turn can cause a code-dependent error voltage at the output of the amplifier. The maximum amplitude of this offset, which adds to the D/A converter nonlinearity, is  $0.67 V_{OS}$  where  $V_{OS}$  is the amplifier input offset voltage. To maintain monotonic operation it is recommended that  $V_{OS}$  be no greater than  $(25 \times 10^{-6}) (V_{REF})$  over the temperature range of operation. Suitable op amps are AD517L and AD544L. The AD517L is best suited for fixed reference applications with low bandwidth requirements: it has extremely low offset ( $50 \mu\text{V}$ ) and in most applications will not require an offset trim. The AD544L has a much wider bandwidth and higher slew rate and is recommended for multiplying and other applications requiring fast settling. An offset trim on the AD544L may be necessary in some circuits.

**Digital Glitches:** One cause of digital glitches is capacitive coupling from the digital lines to the OUT1 and OUT2 terminals. This should be minimized by screening the analog pins of the AD7541A (Pins 1, 2, 17, 18) from the digital pins by a ground track run between Pins 2 and 3 and between Pins 16 and 17 of the AD7541A. Note how the analog pins are at one end of the package and separated from the digital pins by  $V_{DD}$  and GND to aid screening at the board level. On-chip capacitive coupling can also give rise to crosstalk from the digital-to-analog sections of the AD7541A, particularly in circuits with high currents and fast rise and fall times.

**Temperature Coefficients:** The gain temperature coefficient of the AD7541A has a maximum value of  $5 \text{ ppm}/^\circ\text{C}$  and a typical value of  $2 \text{ ppm}/^\circ\text{C}$ . This corresponds to worst case gain shifts of 2 LSBs and 0.8 LSBs, respectively, over a  $100^\circ\text{C}$  temperature range. When trim resistors R1 and R2 are used to adjust full-scale range, the temperature coefficient of R1 and R2 should also be taken into account. The reader is referred to Analog Devices Application Note "Gain Error and Gain Temperature Coefficient of CMOS Multiplying DACs," Publication Number E630c-5-3/86.

## SINGLE SUPPLY OPERATION

Figure 7 shows the AD7541A connected in a voltage switching mode. OUT1 is connected to the reference voltage and OUT2 is connected to GND. The D/A converter output voltage is available at the  $V_{REF}$  pin (Pin 17) and has a constant output impedance equal to  $R_{LDR}$ . The feedback resistor  $R_{FB}$  is not used in this circuit.

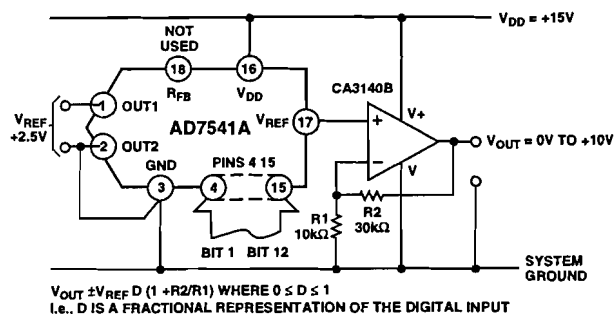


Figure 7. Single Supply Operation Using Voltage Switching Mode

The reference voltage must always be positive. If OUT1 goes more than 0.3 V less than GND, an internal diode will be turned on and a heavy current may flow causing device damage (the AD7541A is, however, protected from the SCR latch-up phenomenon prevalent in many CMOS devices). Suitable references include the AD580 and AD584.

The loading on the reference voltage source is code-dependent and the response time of the circuit is often determined by the behavior of the reference voltage with changing load conditions. To maintain linearity, the voltage at OUT1 should remain within 2.5 V of GND, for a  $V_{DD}$  of 15 V. If  $V_{DD}$  is reduced from 15 V or the reference voltage at OUT1 increased to more than 2.5 V, the differential nonlinearity of the DAC will increase and the linearity of the DAC will be degraded.

## SUPPLEMENTAL APPLICATION MATERIAL

For further information on CMOS multiplying D/A converters, the reader is referred to the following texts:

CMOS DAC Application Guide, Publication Number G872b-8-1/89 available from Analog Devices.

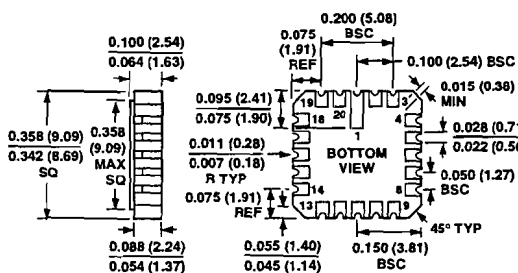
Gain Error and Gain Temperature Coefficient of CMOS Multiplying DACs Application Note, Publication Number E630c-5-3/86 available from Analog Devices.

Analog-Digital Conversion Handbook—available from Analog Devices.

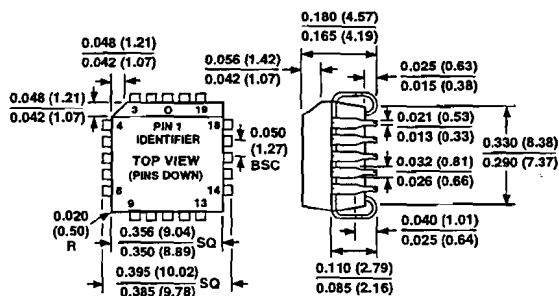
OUTLINE DIMENSIONS

Dimensions shown in inches and (mm).

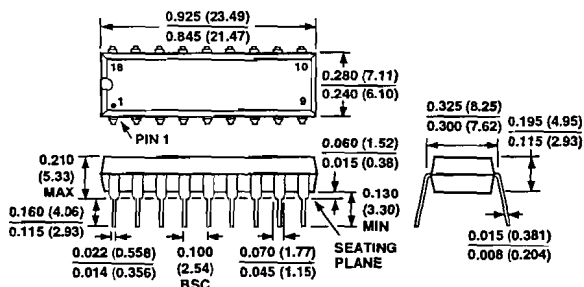
20-Terminal Ceramic Leadless Chip Carrier  
(E-20A)



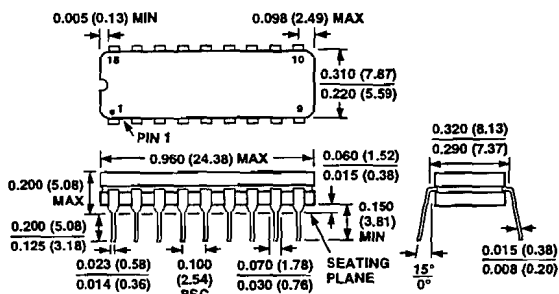
20-Lead Plastic Leadless Chip Carrier  
(P-20A)



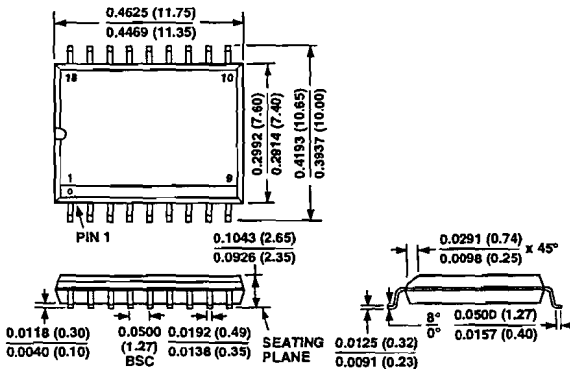
18-Lead Plastic DIP  
(N-18)



18-Lead Cerdip  
(Q-18)



18-Lead SOIC  
(R-18)





## **Appendix D**

### **Digital Signal Processor routines of the Slip-Controller.**

```

; *****
; * STROOMR *
; *
; * Bestand: STROOMR.asm *
; * Auteur: Pieter Risseuw *
; * Creatiedatum: 6 maart 1998 *
; * Wijzigingen: 3 maart 1997 *
; * Processor: B *
; *
; *****
;
;
; * Listing setup *
; *-----*
; .title "Stroomregeling KA motor, met slip regeling"
; .length 6000 ; paginalengte
; .width 115 ; paginabreedte
; .asg 7, macrolist ; macro's wel/niet uitschrijven
; .mncolist
; .fcncolist ; if/endif wel/niet uitschrijven
; *
; *****
;
; * Toepassingsonafhakelijke initialisatie *
; *-----*
; .include "../sjoerd/c40/p08cinit.asm" ; reset en interrupt vectors
; .include "../sjoerd/c40/globdef.asm" ; macro's voor het definifren
; ; van globale variabelen
; .include "../sjoerd/c40/mathlib.asm" ; bibliotheek met wisk. macro's
; .include "../sjoerd/c40/p06io.asm" ; macro's en analoge I/O kaart
; .include "../sjoerd/c40/p09io.asm" ; macro's voor digitale I/O
; .include "../sjoerd/c40/blocklib.asm" ; machinemacro's
; .include "../sjoerd/c40/uilib.asm" ; u/i-model macro's
; .include "../sjoerd/c40/matlab.asm" ; voor aanmaak van matlab bestand
; .include "../sjoerd/c40/commport.asm" ; definities voor comm. poorten
; .include "../sjoerd/c40/teksten.asm" ; bibliotheek voor bitmap teksten
; .include "../sat_lib.asm" ; bibliotheek voor verzadiging
; *
; *****
;
; * Toepassingsafhakelijke initialisatie *
; *-----*
; .include "../sjoerd/c40/config.asm" ; config. van DP, timers en
; ; wait-states
; *
; *****
;
; * Definiëren sampletijd en rekestijdstap *
; *-----*
; .data
; definei sample, 1000 ; timer period, 1 == 100ns
; definei sample_pu, 3.1415927e-2 ; (timer period)*100pi
; definei _sample_pu, 31.830989 ; lpu time == 1/(2pi*50) sec
; definei dt, 3.1415927e-2 ; == 100 us tijdstap
; definei HALFdt, 1.570796327e-2 ; gebruikt in integrator, dt/2
; definei _dt, 31.830989
;
; definei detijd, 0 ; telt het aantal tijdstappen
;
; definei teller, -1 ; voor matlab opslag
; definei eerder, 0 ; voor matlab opslag
;
; definei fout, 0 ; voor opslag van foutcode
;
; definei debits, 64 ; geheugen voor de outputbits
; *
; *****
;
; * Interrupt routines *
; *-----*
; .include "../sjoerd/c40/isr0leeg.asm" ; lege interrupt routine
; *
; *****
;
; .page ; vervolg op nieuwe bladzijde
; *****
; * Variabelen *
; *-----*
; .data
; scimp_0$70 .float 3.418e-4
;
; rho_pos .set 1
;
; define rho__s, 0
; define rho_off_s, 0
; define cosrho__s, 1
; define sinrho__s, 0
; definei dir, 0

```

```

;
define v_voeding, 0
define i_dc, 0
define i_dc_des, 0
define i_dc_des_real, 0
define i_regdc, 6.64e-2
define p_regdc, 3.72
define v_voed_begr, 0.5
;
define cosgamma, 1
define singamma, 0
;
define gammaP_s, 0
define i_speed, 1000
define p_speed, 1
define pi_in, 0
;
define e_s_s1, 0
define e_s_s2, 0
define e_s, 0
define e_s_meas, 0
define e_s_meas1, 0
define k_est, 1
define v_meter, 0
;
define flux_s_s1, 0
define flux_s_s2, 0
define flux_s, 0
define flux_s_meas, 0
define flux_s_meas_prev, 0
define flux_meter, 0
;
define phiP_s_s, 0 ; variabelen U/I-model
define s2, 0.4
define x_offset, -4.08205e-4
define y_offset, -3.1656204e-5
;
define mlast, 0 ; stroomsturing simoreg
define rhoP_s_des, 0 ; wenstoerental
define rhoP_s, 0 ; toerental
define i_rhoP_s, 0.02 ; i-aktie toerentalregeling gelijkstroommachine
define p_rhoP_s, 6.2 ; p-aktie toerentalregeling gelijkstroommachine
define i_rhoP_s_ka, 0.55e-2 ; i-aktie toerentalregeling KA-machine
define p_rhoP_s_ka, 2.1 ; p-aktie toerentalregeling KA machine
;
define mlast_begr, 0 ; begrenzing van de ankerstroom DC-machine
;
defineI schakel, 0 ; stand van drie schakelaars
defineI stand, 0 ; stand van de 8-standenschakelaar
;
define betaP, 0 ; hoeksnelheid statorstroom
define cosbeta, 1
define sinbeta, 0
define eps_s_s_d, 0
define epsP_s_r_d, 0
define coseps, 1
define sineps, 0
;
define i_s_b1_d, 0 ; wenswaarde statorstroom in flux coördinaten
define i_s_b2_d, 0
define i_s_s1_dd, 0 ; wenswaarde statorstroom in stator coördinaten
define i_s_s2_dd, 0
define i_s_d, 0 ; wenswaarde statorstroom in carthesische coördinaten.
define i_s_w_d, 0 ; wenswaarde werkstroom.
define i_s_b_d, 0.154 ; wenswaarde blindstroom
define i_s_s1_d, 0 ; wenswaarde statorstroom in stator coördinaten
define i_s_s2_d, 0
define i_s_s1, 0 ; statorstroom in stator coördinaten
define i_s_s2, 0
define i_s_b1, 0 ; statorstroom in flux coördinaten
define i_s_b2, 0
define i_sa_d, 0 ; wenswaarde statorstroom in 3 fase systeem
define i_sb_d, 0
define i_sc_d, 0
;
define rkl, 0.01026 ; rk/l*I_s_b (factor voor slipregeling)
;
define schakfr, 0 ; Schakelfrequentie
define schakfr_d, -0.24 ; gewenste schakelfrequentie
define i_schakfr, 0 ; Integratieconstante hysteresebandregelaar.
define hb, 0.3 ; hystereseband
;
define i_stroomr, 0.722 ; Integratieconstante
;
define scimp_ip, 3.663e-4 ; scalering voor stator stroom,
define scexp_ip, 2730 ; 110A is 10V
; en 1 unit(in dsp)=(2730/4096)*10V=6,66V=73A
; *-----States-----*
states
define SpigammaP, 0 ; begin van de states
define Spi_rhoP_s, 0
define Spi_idc, 0
define Sflux_s_fil, 0
define Sflux_s, 0
define Sbeta, 0
define Si_s_s1, 0 ; states voor PI regelaar statorstroom

```

```

define Si_s_s2,0
define Shb,4 ; Hysteresebandbreedte

anglst ; begin van de hoek-states
define Sgamma, 0
define Sphi_s_s, 0
define Seps_s_r_d,0 ; wenswaarde hoek statorstroom

newst ; begin van de nieuwe states
.asg (newst - states), NUMBER_STATES
.space NUMBER_STATES

bakst ; begin van Bak(State)
define BpgammaP, 0
define Bpi_rhoP_s, 0
define Bpi_idc, 0
define Bflux_s_fil, 0
define Bflux_s, 0
define Bi_s_sl,0 ; states voor PI regelaar statorstroom
define Bi_s_s2,0
define Bbeta,0
define Bi_s_b1,0 ; states voor PI regelaar statorstroom
define Bi_s_b2,0
define Bgamma, 0
define Bphi_s_s, 0
define Beps_s_r_d,0 ; wenswaarde hoek statorstroom
define Bhb,0 ; hystereseband

;
astates .word states ; 32 bits adressen van states
anewst .word newst ; en van newst. Nodig voor
; ; upd_sta.
; *
; *****
;
; *****
; *
; *****
; * Macro's - voor zover niet in blocklib.asm *
; *-----*
; *
; *****
; # Macro dimprho "Het inlezen van rotorpositie" #
; # In: Rho_off #
; # Uit: Rho, Dir, Cosrho, Sinrho # #
; # Integ.: #
; # Reg's: R5, R7 #
; # Macros: #
; # MN, 3 maart 1997 #
; # n.b. #
; #-----#
dimprho .macro Rho_off,Rho, Dir, Cosrho, Sinrho
listmac 2
LDI *+AR7(rho_pos), R7
LDI R7, R5
AND 08000h, R5
LSH -15, R5
STI R5, Dir ;Dir = richtingsbit
AND 07FFFh, R7
SUBI 40, R7
LSH -2, R7
FLOAT R7
MPYF @sc_ax_pos, R7 ; Tweepolige machine, 3000 omw/min =50Hz
ADDF R7,R7 ; Omzetten naar vierpolige machine, 1500 omw/min = 50Hz
ADDF Rho_off,R7
STF R7, Rho
cossin R7, Cosrho, Sinrho

.endm ; dimprho
;
; *****
; *
; *****
; # Macro filt2o "2e orde filter" #
; # In: In,A1,A2,B1,B2 #
; # Uit: Uit #
; # Integ.: SState1, SState2 (adres) #
; # Reg's: R2, R3 #
; # Macros: intscal #
; # PR, 10 maart 1998 #
; # n.b. #
; # Uit=(1+A1*s+A2*s^2)/(s^2+B1*s+B2) #
; #-----#
filt2o .macro In, A1,A2,B1,B2,Uit,SState1,SState2

LDF In,R2 ;x0=In-B1*State1-B2*State2
LDF @SState1,R4
MPYF B1,R4
SUBF R4,R2
LDF @SState2,R4
MPYF B2,R4
SUBF R4,R2

LDF @SState2,R3 ;Uit=State2+B1*state1+B2*x0
LDF R2,R4

```

```

MPYF    A2,R4
ADDF    R4,R3
LDF     @STate1,R4
MPYF    B1,R4
ADDF    R4,R3

STF     R3,Uit

intscal @STate1,x,-2,2,STate2
intscal R2,x,-2,2,STate1

.endm    ; filt2o
;
; #####
; #####
; # Macro n_reg "PI-regelaar voor toerental" #
; # In: RhoP__s_des, RhoP__s, Mlast_begr, P_rhoP__s, #
; # I_rhoP__s #
; # Uit: Mlast #
; # Integ.: SPi_rhoP__s #
; # Reg's: R7, R8, R5, R0, R1, R2 #
; # Macros: pi_regel (int_scal) #
; # MN, 24 maart 1997 #
; # n.b. #
; # P_versterking = 10 #
; # I_versterking = 0.07 #
; # bij een bekrachtingsstroom van 0.9 A #
; # mlast begrenzing = maximaal 0.4 PU!!!! #
; #-----#
n_reg .macro RhoP__s_des, RhoP__s, Mlast_begr, P_rhoP__s, I_rhoP__s, SPi_rhoP__s, Mlast
LDF Mlast_begr, R7
NEGF R7, R8
LDF RhoP__s_des, R5
SUBF RhoP__s, R5
piregel R5, P_rhoP__s, I_rhoP__s, R8, R7, SPi_rhoP__s, Mlast
LDF Mlast, R0
CMPF Mlast_begr, R0
BLE max_ok? ; mlast > begrenzing dan
LDF Mlast_begr, R1
STF R1, Mlast ; mlast := begrenzing
EU min_ok?
max_ok?:
LDF Mlast_begr, R1
NEGF R1, R2
CMPF R2, R0
BGE min_ok? ; mlast < begrenzing dan
LDF R2, R1
STF R1, Mlast ; mlast := -begrenzing
min_ok?:
.endm ; n_reg
;
; #####
; #####
; # Macro i_reg "PI-regelaar voor DC stroom" #
; # In: I_dc_des, I_dc, V_voed_begr, P_regdc, #
; # I_regdc #
; # Uit: V_voeding #
; # Integ.: SPi_idc #
; # Reg's: R7, R8, R5, R0, R1, R2 #
; # Macros: pi_regel (int_scal) #
; # MN, 3 april 1997 #
; # n.b. #
; # P_versterking = 10 #
; # I_versterking = 0.07 #
; # bij een bekrachtingsstroom van 0.9 A #
; # V_voeding begrenzing = maximaal 0.5 PU!!!! #
; #-----#
i_reg .macro I_dc_des, I_dc, V_voed_begr, P_regdc, I_regdc, SPi_idc, V_voeding
LDF I_dc_des, R5
SUBF I_dc, R5
piregel R5, P_regdc, I_regdc, 0, V_voed_begr, SPi_idc, V_voeding
LDF V_voeding, R0
CMPF V_voed_begr, R0
BLE max_ok? ; v_voeding > begrenzing dan
LDF V_voed_begr, R1
STF R1, V_voeding ; v_voeding := begrenzing
EU min_ok?
max_ok?:
LDF 0, R2
CMPF R2, R0
BGE min_ok? ; v_voeding < 0 dan
LDF R2, R1
STF R1, V_voeding ; v_voeding := 0
min_ok?:
.endm ; i_reg
;
; #####
;
; .page ; vervolg op nieuwe bladzijde
; *****
; * Programma *
; *****
; .text
PROGRAM:
; :::::::::::::::::::: ; Instellen sampletijd
LDI @T0_PERIOD_REG,AR0 ; address timer 0 period register

```

```

LDI @sample,R0 ; desired period
STI R0,*ARO ; AD and DA conv start at +flank
; ..... ; Initialisatie van de COMM-poort
crempty @CPCR4
; ..... ; Initialisatie van de "tijd"
STIK 0, @detijd
; ..... ; Initialisatie van matlab file
matinit @dt,1,1024,"""e_s_s1""","""e_s_s2""","""flux_s_s1""","""flux_s_s2""";
; STIK 0, @teller ; begin meteen met opslaan
; ..... ; Initialisatie van variabelen

;
; ..... ; Wachten op interrupt
WACHT: LDI @EN_INT0,IIF ; enable INT0 from pAIO
OR @GIE,ST ; allow interrupt action
IDLE ; waiting for INT0

;
; ..... ; Inlezen van analoge inputs
;
point_to DIO_b6 ; gebruik digitale kaart op pos. 6
sww_to WAIT_STATE_3 ; naar 3 wait-states
d8impotw @debits,@stand,@schakel ; lees stand schakelaars in
dimrho @rho_off_s, @rho_s, @dir, @cosrho_s, @sinrho_s ; lees meteen
rotorpositie in

point_to AIO_b1 ; gebruik analoge kaart 1

impo @rho_off_s, ch1, @scimp_1$00 ; inlezen hoekoffset van pot1
impo @rhoP_s_des, ch5, @scimp_1$00 ; inlezen wenstoerental van pot 2
; impo @p_rhoP_s_ka, ch7, @scimp_10$0 ; inlezen versterking toerentalregeling
; impo @i_rhoP_s_ka, ch6, @scimp_0$05 ; inlezen integratieconstante toerentalregeling
impo @rk1, ch6, @scimp_0$02 ; inlezen rk/1*I_s_b
; impo @i_schakfr, ch6, @scimp_10$0 ; inlezen integratieconstante schakelfrequentieregeling
; impo @schakfr_d, ch7, @scimp_1$00 ; inlezen wens schakelfrequentie
; impo @i_stroomr, ch7, @scimp_1$00 ; inlezen integratieconstante stroomregeling
; impo @i_s_w_d, ch4, @scimp_1$00 ; inlezen wenswaarde werkstroom van pot 4
impo @mlast, ch4, @scimp_1$00 ; inlezen wenswaarde werkstroom van pot 4
; impo @i_s_b_dd, ch5, @scimp_1$00 ; inlezen stroom wenswaarde van pot 5

impo @i_s_b_d, ch7, @scimp_0$20 ; inlezen blind stroom wenswaarde van pot 7

point_to AIO_b3 ; gebruik analoge kaart 3
impo @i_s_s1, ch1, @scimp_ip ; inlezen statorstroom s1-as
impo @i_s_s2, ch2, @scimp_ip ; inlezen statotstroom s2-as
impo @schakfr, ch3, @scimp_1$00 ; inlezen inverter schakelfrequentie

sww_to WAIT_STATE_0 ; naar 0 wait-states

; *****
; * Hystereseband regeling *
; *****
LDF @schakfr_d, R5
SUBF @schakfr, R5
STF R5, @schakfr
intscal @schakfr, @i_schakfr, 0.1, 1, Shb
LDF @Shb, R1
STF R1, @hb
LDI @schakel, R1

TSTB 1, R1

BEQ verder? ; if schakelaar1 then hysteresebreedte=0.3
LDF 0.3, R1 ; en schakelfrequentieregeling uitgeschakeld.
STF R1, @hb
verder?:

; ***** ; toerentalregeling gelijkstroommachine
syregel @cosrho_s, @sinrho_s, 0.67, 0.1185, @rhoP_s, @cosgamma, @singamma, SpigammaP, Sgamma
; n_reg @rhoP_s_des, @rhoP_s, 0.9, @p_rhoP_s, @i_rhoP_s, Spi_rhoP_s, @mlast ; Toerentalregeling
;

; ***** ; toerentalregeling KA machine
n_reg @rhoP_s_des, @rhoP_s, 0.55, @p_rhoP_s_ka, @i_rhoP_s_ka, Spi_rhoP_s, @i_s_w_d
; Toerentalregeling
; P=2,9 en
I=0.00239
;

; ***** ; slipregeling met machinemodel
c_l @i_s_w_d, @i_s_b_d, @i_s_d ; i_s_d=(i_s_w^2+i_s_b^2)^0.5, blindstroom is 14A(=10Aeff)
LDF @i_s_w_d, R1
MPYF @rk1, R1
LDF @i_s_b_d, R2
invf R2, R3
MPYF R3, R1
STF R1, @epsP_s_r_d ; epsP_s_r_d=(Rk/L/I_s_b_d)I_s_w_d
intangl @epsP_s_r_d, x, Seps_s_r_d ; Integratie epsP_s_r_d

```

```

LDF    @Seps_s_r_d, R2
ADDF   @rho_s, R2
STF    R2, @eps_s_s_d      ; eps_s_s_d=eps_s_r_d+rho_s
cossin @eps_s_s_d,@coseps, @sineps

;***** ; polair carthesisch transf.

p_c    @i_s_d, @coseps,@sineps, @i_s_sl_dd, @i_s_s2_dd

;***** ; Stroomregeling

;      intangl @betaP,x,Sbeta
;      cossin @Sbeta, @cosbeta, @sinbeta

;      vecrotn @i_s_s1, @i_s_s2, @cosbeta, @sinbeta, @i_s_b1, @i_s_b2

LDF    @i_s_sl_dd,R4
;***** ; tussenvoeging filter
SUBF   @i_s_sl,R4
intscal R4,@i_stroomr,-0.1,0.1,Si_s_s1    ; tau=4.4ms
LDF    @Si_s_sl,R4
ADDF   @i_s_sl_dd,R4
STF    R4,@i_s_sl_d

LDF    @i_s_s2_dd,R4
;***** ; tussenvoeging filter
SUBF   @i_s_s2,R4
intscal R4,@i_stroomr,-0.1,0.1,Si_s_s2    ; tau=4.4ms
LDF    @Si_s_s2,R4
ADDF   @i_s_s2_dd,R4
STF    R4,@i_s_s2_d

;      vecrot  @i_s_sl_d, @i_s_s2_d, @cosbeta, @sinbeta, @i_s_sl_d, @i_s_s2_d
ti_2_3 @i_s_sl_d, @i_s_s2_d,x, @i_sa_d, @i_sb_d, @i_sc_d

;***** ; Uitvoer analoge outputs

sww_to WAIT_STATE_3      ; naar 3 wait-states

point_to AIO_b1          ; gebruik analoge kaart 1

LDI    @stand,R0
expv   @cosrho_s,@sccexp_1$00,R1 ; afbeelden rotorpositie op scope
expv   @sinrho_s,@sccexp_1$00,R2 ; afbeelden rotorpositie op scope
;      expv   @mlast, @sccexp_1$00, R7 ; uitvoer naar simoreg voor n reg
expv   @mlast, @sccexp_1$00, R4,1 ; uitvoer mlast naar scope2 y, schak=1 of 2
expv   @i_s_w_d, @sccexp_1$00, R4,1 ; uitvoer i_s_w_d naar scope2 y, schak=1 of 2
expv   @mlast, @sccexp_1$00, R4,2
expv   @epsP_s_r_d, @sccexp_1$00,R3,1 ; uitvoer toerental naar scope 2 x-as, schak=1
expv   @rhoP_s_des, @sccexp_1$00,R3,2 ; uitvoer wenstoerental naar scope 2 x-as, schak=2
expv   @rhoP_s, @sccexp_1$00,R8 ; uitvoer toerental op multimeter
expv   @i_s_sl_d, @sccexp_1$00,R3,3 ; Uitvoer wens stroomvector naar scope 2, schak=3
expv   @i_s_s2_d, @sccexp_1$00,R4,3 ; Uitvoer wens stroomvector naar scope 2, schak=3
expv   @eps_s_s_d, @sccexp_2$00,R3,4 ; Uitvoer wens stroom stator hoek
expv   @Shb, @sccexp_1$00,R4,4 ; Uitvoer hysterese breedte
expv   @i_s_w_d,@sccexp_1$00,R5,5 ; Uitvoer werkstroom
expv   @i_s_sl_d,@sccexp_1$00,R4,5

expa   AIO_b1, WAIT_STATE_3

point_to AIO_b3          ; gebruik analoge kaart 3
expv   @i_sa_d, @sccexp_ip, R1 ; uitvoer wenswaarde stroom naar hysterese regeling
expv   @i_sb_d, @sccexp_ip, R2
expv   @i_sc_d, @sccexp_ip, R3
expv   @betaP, @sccexp_1$00,R4 ; uitvoer frequentie naar kanaal 4 t.b.v. filter.
;      expv   @hb,@sccexp_1$00,R5 ; uitvoer hysteresebandbreedte
negf   R4,R4
expa   AIO_b3, WAIT_STATE_3

sww_to WAIT_STATE_0      ; naar 0 wait-states

upd_sta          ;update integrator toestanden

sww_to WAIT_STATE_3      ; schrijf met 3 wait-states
point_to DIO_b4          ; gebruik digitale kaart op pos. 4

;      LDI    1, R3 ; deel freq. beveiligingssignaal door 2
;      AND   @detijd, R3 ; i.v.m. hoge sample-frequentie (f = 20 kHz)
;      d8expo R3,bit7,ch3,@debits ; selectie/beveiligingsbit

;      d8expo @teller, bit8, ch3, @debits ; matlab schrijfindicator

;      sww_to WAIT_STATE_0 ; terug naar 0 wait-states

; ***** ; Wacht tot volgende tijdstap
LDI    @detijd, R0
ADDI   1, R0
STI    R0, @detijd
BR     WACHT

einde
;
; *****
; * STROOMRB.asm *
; *****
.end

```

## **Appendix E**

**Simulation software for simulation of the hysteresis current controller.**



```

file$ = "simfreq1.dat"
OPEN "test.dat" FOR OUTPUT AS #1: fileopen = 2

Rr = .228
Rs = .228
Rt = .228

Lr = .015
Ls = .015
Lt = .015

hi = 0
AI = 14

udc = 250

SCREEN 9
win = 2
WINDOW (-win, .9 * win)-(win, -.9 * win)
oldstate = 10
filenum$ = "3"
ix = COS(hi / 57.3) * AI
iy = SIN(hi / 57.3) * AI

irs = 2 / 3 * COS(hi / 57.3) * AI
iss = -1 / 3 * COS(hi / 57.3) * AI + 1 / SQR(3) * SIN(hi / 57.3) * AI
its = -1 / 3 * COS(hi / 57.3) * AI - 1 / SQR(3) * SIN(hi / 57.3) * AI

f = .25: REM toerental [%]
a = (f * 530) / udc: REM tegenspanning
hoek = 0
hoekstap = 20
dh = -15: REM verdraaing van de vectoren
fdel = 3
r = 0: s = 1: t = 0
ix = -ix
iy = -iy
ix = 0: iy = 0

o = 1

schoon:
CLS
IF hoek >= 360 THEN hoek = hoek - 360
IF hi >= 360 THEN hi = hi - 360

vx = a * COS((hoek + dh) * 3.14 / 180)
vy = a * SIN((hoek + dh) * 3.14 / 180)

ut = 1: us = 1: ur = 1
GOSUB bervect
GOSUB omzetten
GOSUB grenzen
GOSUB tekenv
REM GOSUB optimise
PSET (ix, iy)
start:
tijd = tijd + stap
hi = (f * 18000 * tijd)
vx = a * COS((hoek + dh) * 3.14 / 180)
vy = a * SIN((hoek + dh) * 3.14 / 180)
COLOR 15
LOCATE 3, 1: PRINT "Sp.hoek="; hoek
LOCATE 2, 1: PRINT "tegensp.="; : PRINT USING "###.##"; a
LOCATE 4, 1: PRINT "Verdr.hoek="; : PRINT USING "###.##"; dh
LOCATE 5, 1: PRINT "freq="; : PRINT USING "#####"; freq
LOCATE 6, 1: PRINT "Uster="; Uster
LOCATE 7, 1: PRINT "di/dt="; : PRINT USING "#.##^ ^ ^ ^"; didt
IF deltaxhoek < 10 AND deltaxhoek > -10 THEN LOCATE 8, 1: PRINT "Delta hoek"; : PRINT USING "###.##"; deltaxhoek
LOCATE 9, 1: PRINT "Hi="; : PRINT USING "###"; hi

REM IF (r = 0 AND s = 0 AND t = 0) OR (r = 1 AND s = 1 AND t = 1) THEN COLOR 12

REM LOCATE 4, 1: PRINT r; s; t
REM LOCATE 4, 1: PRINT "Vertr="; vertr

hoek = hi + 90
irs = 2 / 3 * COS(hi / 57.3) * AI
iss = -1 / 3 * COS(hi / 57.3) * AI + 1 / SQR(3) * SIN(hi / 57.3) * AI
its = -1 / 3 * COS(hi / 57.3) * AI - 1 / SQR(3) * SIN(hi / 57.3) * AI

GOSUB omzetten
GOSUB progl: '!!!!!!!!!!!!!!!!!!!!!!!!!!!!!!!!!!!!!!!!!!!!!!!!!!!!!!!!!!!!!!!!!!!!!!!!!!!!!!
GOSUB frequentie
GOSUB deltax

LOCATE 1, 1: PRINT o

GOSUB bervect
stap = 10 / (150 * (dirdt ^ 2 + disdt ^ 2 + ditdt ^ 2) ^ .5)
IF (ir > .9 AND ir < 1.1) OR (ir < -.9 AND ir > -1.1) OR (iss > .9 AND iss < 1.1) OR (iss < -.9 AND iss > -1.1) OR (it > .9 AND it < 1.1) OR (it < -.9 AND it > -1.1) THEN stap = stap / 10

```

```

'stap = .000001

diadt = (dirdt - .5 * disdt - .5 * ditdt): dibdt = (3 ^ .5 / 2 * disdt - 3 ^ .5 / 2 * ditdt)
didt = (diadt ^ 2 + dibdt ^ 2) ^ .5
diadt = stap * diadt: dibdt = stap * dibdt

ix = ix + COS(dh * 3.14 / 180) * diadt - SIN(dh * 3.14 / 180) * dibdt
iy = iy + SIN(dh * 3.14 / 180) * diadt + COS(dh * 3.14 / 180) * dibdt

LINE -(ix, iy)
ixold = ix: iyold = iy

k$ = INKEY$
IF k$ = " " THEN hi = hi + 10: GOTO schoon
IF k$ = "=" OR k$ = "+" THEN a = a + .05: GOTO schoon
IF k$ = "-" THEN a = a - .05: GOTO schoon
IF k$ = "c" THEN GOSUB wis
IF k$ = "p" THEN dh = dh + 1: GOTO schoon
IF k$ = "m" THEN dh = dh - 1: GOTO schoon
IF k$ = "s" THEN vertr = vertr - 10
IF k$ = "t" THEN vertr = vertr + 10
IF k$ = "d" THEN ix = 2: iy = 0: o = 1
IF k$ = CHR$(16) THEN SHELL "copy ff lpt1": BEEP
IF k$ = CHR$(19) AND OPSLAAN = 1 THEN BEEP: GOSUB klaar
IF k$ = CHR$(19) AND OPSLAAN = 0 THEN OPSLAAN = 1: BEEP
IF k$ = CHR$(13) THEN ix = 1: iy = -.2: o = 1
IF vertr < 0 THEN vertr = 0

REM ***** opslaan van serie*****
IF OPSLAAN = 1 AND oldstate <> o THEN GOSUB OPSLAAN
REM ***** opslaan van een keer rond*****

tijdstap = tijdstap + stap
IF tijdstap > .00005 THEN PRINT #1, tijd, irs + ir, isss + iss, its + it, freq: tijdstap = 0
IF hi > 360 THEN CLOSE : SHELL "copy test+test " + file$: END
REM *****
'IF hi > 120 THEN PRINT #1, a, aantals / (tijdss - tijds), tijd: a = a + .05: aantals = 0: tijd = 0
'IF a >= 1 THEN END

GOTO start

REM *****Stroom begrenzing*****
prog0:
IF ir > 1 THEN ur = 0
IF ir < -1 THEN ur = udc
IF iss > 1 THEN us = 0
IF iss < -1 THEN us = udc
IF it > 1 THEN ut = 0
IF it < -1 THEN ut = udc
n = 0
p = udc
IF ur = p AND us = n AND ut = n THEN o = 1
IF ur = p AND us = p AND ut = n THEN o = 2
IF ur = n AND us = p AND ut = n THEN o = 3
IF ur = n AND us = p AND ut = p THEN o = 4
IF ur = n AND us = n AND ut = p THEN o = 5
IF ur = p AND us = n AND ut = p THEN o = 6
IF ur = p AND us = p AND ut = p THEN o = 7
IF ur = n AND us = n AND ut = n THEN o = 8

REM filter
'dh = -didt * 15 / 30000!
dh = -15

RETURN

REM *****definitive algorithm*****
prog1:
IF vertr > 200 THEN vertr = 200

teller = teller + 1

IF ir >= 1 AND o <> 2 AND o <> 3 THEN teller1 = teller1 + 1 ELSE teller1 = 0
IF teller1 > vertr THEN o = 1: schakel = 1
IF it <= -1 AND o <> 3 AND o <> 4 THEN teller2 = teller2 + 1 ELSE teller2 = 0
IF teller2 > vertr THEN o = 2: schakel = 1
IF iss >= 1 AND o <> 4 AND o <> 5 THEN teller3 = teller3 + 1 ELSE teller3 = 0
IF teller3 > vertr THEN o = 3: schakel = 1
IF ir <= -1 AND o <> 5 AND o <> 6 THEN teller4 = teller4 + 1 ELSE teller4 = 0
IF teller4 > vertr THEN o = 4: schakel = 1
IF it >= 1 AND o <> 6 AND o <> 1 THEN teller5 = teller5 + 1 ELSE teller5 = 0
IF teller5 > vertr THEN o = 5: schakel = 1
IF iss <= -1 AND o <> 1 AND o <> 2 THEN teller6 = teller6 + 1 ELSE teller6 = 0
IF teller6 > vertr THEN o = 6: schakel = 1

REM IF schakel = 1 AND vertr < teller / 2 THEN vertr = vertr + 10 ELSE IF schakel = 1 THEN vertr = vertr - 5
REM IF schakel = 1 THEN teller = 0: schakel = 0

IF o = 6 THEN ut = 0: us = udc: ur = udc
IF o = 5 THEN ur = udc: us = 0: ut = 0
IF o = 1 THEN us = udc: ur = 0: ut = 0
IF o = 2 THEN ur = 0: us = udc: ut = udc
IF o = 3 THEN ut = udc: ur = 0: us = 0

```

```

IF o = 4 THEN us = 0: ut = udc: ur = udc

RETURN

REM *****"grenzen 30 graden verdraaid"*****
prog2:
IF ir > 1 THEN r = 1
IF ir < -1 THEN r = -1
IF ir < 1 AND ir > -1 THEN r = 0
IF iss > 1 THEN s = 1
IF iss < -1 THEN s = -1
IF iss < 1 AND iss > -1 THEN s = 0
IF it > 1 THEN t = 1
IF it < -1 THEN t = -1
IF it < 1 AND it > -1 THEN t = 0

IF r = 1 AND o <> 1 AND o <> 2 AND o <> 3 THEN o = 6
IF t = -1 AND o <> 2 AND o <> 3 AND o <> 4 THEN o = 1
IF s = 1 AND o <> 3 AND o <> 4 AND o <> 5 THEN o = 2
IF r = -1 AND o <> 4 AND o <> 5 AND o <> 6 THEN o = 3
IF t = 1 AND o <> 5 AND o <> 6 AND o <> 1 THEN o = 4
IF s = -1 AND o <> 6 AND o <> 1 AND o <> 2 THEN o = 5

IF r = 1 AND t = 1 THEN o = 1
IF t = -1 AND s = -1 THEN o = 2
IF r = 1 AND s = 1 THEN o = 3
IF r = -1 AND t = -1 THEN o = 4
IF s = 1 AND t = 1 THEN o = 5
IF r = -1 AND s = -1 THEN o = 6

RETURN

prog3:
IF ir > 1 THEN s = 1: t = 0
IF ir < -1 THEN s = 0: t = 1
IF iss > 1 THEN r = 0: t = 1
IF iss < -1 THEN r = 1: t = 0
IF it > 1 THEN r = 1: s = 0
IF it < -1 THEN r = 0: s = 1
IF r = 1 AND s = 0 AND t = 0 THEN o = 6
IF r = 1 AND s = 1 AND t = 0 THEN o = 1
IF r = 0 AND s = 1 AND t = 0 THEN o = 2
IF r = 0 AND s = 1 AND t = 1 THEN o = 3
IF r = 0 AND s = 0 AND t = 1 THEN o = 4
IF r = 1 AND s = 0 AND t = 1 THEN o = 5
IF (r = 0 AND s = 0 AND t = 0) OR (r = 1 AND s = 1 AND t = 1) THEN REM
RETURN

prog4:
IF ir >= 1 AND o <> 2 THEN o = 1
IF it <= -1 AND o <> 3 THEN o = 2
IF iss >= 1 AND o <> 4 THEN o = 3
IF ir <= -1 AND o <> 5 THEN o = 4
IF it >= 1 AND o <> 6 THEN o = 5
IF iss <= -1 AND o <> 1 THEN o = 6
RETURN

REM *****constante schakelfrequentie*****
prog5:
IF vertr < 100 THEN vertr = 300
teller = teller + 1
IF teller < vertr THEN RETURN

IF ir >= 1 AND o <> 2 THEN o = 1
IF it <= -1 AND o <> 3 THEN o = 2
IF iss >= 1 AND o <> 4 THEN o = 3
IF ir <= -1 AND o <> 5 THEN o = 4
IF it >= 1 AND o <> 6 THEN o = 5
IF iss <= -1 AND o <> 1 THEN o = 6
teller = 0
RETURN

REM *****omzetten coördinaten xy->rst*****
omzetten:
c60 = COS(60 * 3.14 / 180)
c30 = COS(30 * 3.14 / 180)
ir = ix / (1)
iss = (-c60 * ix + c30 * iy) / (1)
it = -ir - iss
REM LOCATE 2, 1: PRINT ir + iss + it
RETURN

REM *****teken vectoren*****
tekenv:
LINE (0, 0)-(-vrxm + vx, -vrym + vy), 11
LINE (0, 0)-(-vsxm + vx, -vsym + vy), 11
LINE (0, 0)-(-vtxm + vx, -vtym + vy), 11
LINE (0, 0)-(vrxm + vx, vrym + vy), 11
LINE (0, 0)-(vsxm + vx, vsym + vy), 11
LINE (0, 0)-(vtxm + vx, vtym + vy), 11
LINE (0, 0)-(vx, vy), 10
RETURN

```

```

REM *****Bereken vectoren*****
bervect:
ex = udc * vx / 3 ^ .5
ey = udc * vy / 3 ^ .5
er = ex
es = -1 / 2 * ex + 3 ^ .5 * ey / 2
et = -1 / 2 * ex - 3 ^ .5 * ey / 2
Uster = ((ur - (ir + irs) * Rr - er) * Ls * Lt + (us - (iss + isss) * Rs - es) * Lr * Lt + (ut - (it + its)
* Rt - et) * Lr * Ls) / (Lr * Ls + Lt * Ls + Lr * Lt)

dirdt = (ur - (ir + irs) * Rr - er - Uster) / Lr
disdt = (us - (iss + isss) * Rs - es - Uster) / Ls
ditdt = (ut - (it + its) * Rt - et - Uster) / Lt

vrxm = -COS((0 + dh) * 3.14 / 180)
vrym = -SIN((0 + dh) * 3.14 / 180)
vsxm = COS((300 + dh) * 3.14 / 180)
vsym = SIN((300 + dh) * 3.14 / 180)
vtxm = COS((60 + dh) * 3.14 / 180)
vtyl = SIN((60 + dh) * 3.14 / 180)

RETURN

REM***** optimaliseer vectoren*****
optimise:
RETURN
e = (vrxp ^ 2 + vryp ^ 2) ^ .5
srp = 1 / e
vrxp = vrxp / e
vryp = vryp / e

e = (vsxp ^ 2 + vsyp ^ 2) ^ .5
ssp = 1 / e
vsxp = vsxp / e
vsyp = vsyp / e

e = (vtxp ^ 2 + vtyp ^ 2) ^ .5
stp = 1 / e
vtxp = vtxp / e
vtyp = vtyp / e

e = (vrxm ^ 2 + vrym ^ 2) ^ .5
srm = 1 / e
vrxm = vrxm / e
vrym = vrym / e

e = (vsxm ^ 2 + vsym ^ 2) ^ .5
ssm = 1 / e
vsxm = vsxm / e
vsym = vsym / e

e = (vtxm ^ 2 + vtyl ^ 2) ^ .5
stm = 1 / e
vtxm = vtxm / e
vtyl = vtyl / e

e = (vx ^ 2 + vy ^ 2) ^ .5
IF e = 0 THEN RETURN
vx = vx / e
vy = vy / e

RETURN

REM *****teken grenzen*****
grenzen:
grens = 4
hoek30 = 1 / SIN(30 * 3.14 / 180)
hoek60 = 1 / TAN(30 * 3.14 / 180)
yp = -( -grens - hoek30) * hoek60 / (hoek30 + 1)
yn = -( -grens - hoek30) * hoek60 / (hoek30 + 1)
LINE (1, -grens)-(1, grens), 12
LINE (-1, -grens)-(-1, grens), 12

LINE (-grens, yp)-(-grens, yn), 12
LINE (grens, yp)-(-grens, yn), 12

LINE (-grens, -yp)-(-grens, -yn), 12
LINE (grens, -yp)-(-grens, -yn), 12

RETURN

wis:
CLS
'vx = a * COS((hoek + dh) * 3.14 / 180)
'vy = a * SIN((hoek + dh) * 3.14 / 180)
'Ut = 1: Ur = 1: Us = 1

```

```

GOSUB bervect
GOSUB omzetten
GOSUB grenzen
GOSUB tekenv
'GOSUB optimise
PSET (ix, iy)

RETURN

REM *****bereken schakelfrequentie*****

frequentie:
IF k$ = "f" THEN fdel = 1
snelh = snelh + stap
IF aantals = 0 THEN tijds = tijd

REM IF o < richt AND fdel > 0 THEN fdeler = snelh: fdel = fdel - 1
IF o < richt THEN LOCATE 5, 1: freq = 1 / (snelh): aantals = aantals + 1: PRINT "freq="; : PRINT USING
"#####"; freq: snelh = 0: hijmag = 1: tijdss = tijd
richt = o
RETURN

REM *****loop om meerder simulaties te doorlopen en op te slaan

OPSLAAN:

IF fileopen = 0 THEN GOSUB openfiles

x = COS(hi * .01745) * AI + ix
y = SIN(hi * .01745) * AI + iy
PRINT #1, x, y
oldstate = o
RETURN

REM ***** openfiles*****
openfiles:
oldstate = 10
LOCATE 22, 1: INPUT "Filenaam:"; file$
LOCATE 22, 1: PRINT SPACE$(11 + LEN(file$));
LOCATE 22, 1: PRINT "OPSLAAN"
OPEN file$ + ".m" FOR OUTPUT AS #1
fileopen = 1
PRINT #1, "%Sp.hoek="; hoek
PRINT #1, "%tegensp.="; : PRINT #1, USING "##.##"; a
PRINT #1, "%Verdr.hoek="; dh
PRINT #1, "%freq="; : PRINT #1, USING "#####"; freq

PRINT #1, "m=["
RETURN

REM *****klaar met schrijven file*****
klaar:
GOSUB OPSLAAN
k$ = ""
OPSLAAN = 0
PRINT #1, "];"
PRINT #1, "Ix=m(:,1);"
PRINT #1, "Iy=m(:,2);"
PRINT #1, "plot(Ix,Iy);"
PRINT #1, "hold on;"
x = COS(hi / 57.3) * AI
y = SIN(hi / 57.3) * AI
grens = 2.5
yp = -(-grens - hoek30) * hoek60 / (hoek30 + 1)
yn = -(grens - hoek30) * hoek60 / (hoek30 + 1)

PRINT #1, "plot(["; x + 1, x + 1; "],["; y - grens, y + grens; "],':r');"
PRINT #1, "plot(["; x - 1, x - 1; "],["; y - grens, y + grens; "],':r');"
PRINT #1, "plot(["; x - grens, x + grens; "],["; y + yp, y + yn; "],':r');"
PRINT #1, "plot(["; x + grens, x - grens; "],["; y + yp, y + yn; "],':r');"
PRINT #1, "plot(["; x - grens, x + grens; "],["; y - yp, y - yn; "],':r');"
PRINT #1, "plot(["; x + grens, x - grens; "],["; y - yp, y - yn; "],':r');"

PRINT #1, "xlabel('Is1(A)');"
PRINT #1, "ylabel('Is2(A)');"
PRINT #1, "axis('equal');"
PRINT #1, "print -dmeta word\"; file$; ".wmf"
PRINT #1, "print -deps word\"; file$; ".eps"

CLOSE
fileopen = 0
LOCATE 22, 1: PRINT " ";

RETURN
REM *****Deltah*****

deltah:
IF diadt = 0 THEN RETURN
IF o = 1 THEN deltahoek = ATN(dibdt / diadt) * 180 / 3.14 + 60
IF o = 2 THEN deltahoek = ATN(dibdt / diadt) * 180 / 3.14
IF o = 3 THEN deltahoek = -ATN(dibdt / diadt) * 180 / 3.14 + 60
IF o = 4 THEN deltahoek = 60 + ATN(dibdt / diadt) * 180 / 3.14
IF o = 5 THEN deltahoek = ATN(dibdt / diadt) * 180 / 3.14
IF o = 6 THEN deltahoek = ATN(dibdt / diadt) * 180 / 3.14 - 60
RETURN

```

## **Appendix F**

**Program to transfer measured data from a Nicolet Oscilloscope to a Personal Computer.**

```

CLS
PRINT "Scope, versie 1.11"
PRINT "Com 2"
PRINT "Instellingen RS232-poort:"
PRINT "Baudrate=9600"
PRINT "Parity off"
PRINT "Stop bits=1"
PRINT

PRINT "Zoeken naar scope op com 2....."
DIM n(11)
OPEN "com2:9600,n,8,1" FOR RANDOM AS #1

PRINT #1, CHR$(17);
REM leeghalen van de pijplijn
T = TIMER
1 IF TIMER > T + 1 OR LOC(1) > 0 THEN ELSE GOTO 1

xon = 1
2 IF LOC(1) > 50 AND xon = 1 THEN PRINT #1, CHR$(19); : xon = 0
IF LOC(1) < 20 AND xon = 0 THEN PRINT #1, CHR$(17); : xon = 1
IF LOC(1) = 0 THEN T = TIMER ELSE k$ = INPUT$(1, 1): GOTO 2
3 IF LOC(1) > 1 THEN GOTO 2
IF TIMER < T + 1 THEN GOTO 3

PRINT #1, "C,13,13"; CHR$(10)
INPUT #1, E$

PRINT #1, "C,8,1,13"
INPUT #1, E$

PRINT #1, "C,4,1,13"
INPUT #1, E$

T = TIMER
5 IF TIMER > T + 1 THEN ELSE GOTO 5

10 IF EOF(1) THEN ELSE INPUT #1, A$: GOTO 10

REM***** Hold on
*****
REM PRINT #1, "Z1"
REM INPUT #1, E
REM PRINT #1, "H,2,0"
REM INPUT #1, E
REM PRINT #1, "Z0"
REM INPUT #1, E

CLS

DIM wafe(35, 5)
PRINT "Gevonden signalen:"

PRINT #1, "W"
INPUT #1, E
INPUT #1, NWF
FOR i = 1 TO NWF
INPUT #1, number
INPUT #1, E

```

```

INPUT #1, NORMSET
INPUT #1, E
INPUT #1, channel
wafe(number, 1) = NORMSET
wafe(number, 2) = number
wafe(number, 3) = 1
INPUT #1, E
INPUT #1, E
PRINT "Signaal"; number; " -> Kanaal"; channel + 1
NEXT i
INPUT #1, E

INPUT "Welk SIGNAAL uitlezen"; channel
channel = channel

IF wafe(channel, 3) = 0 THEN PRINT "Geen geldig kanaal": CLOSE : RUN

PRINT #1, "N,"; wafe(channel, 1)
INPUT #1, E

FOR i = 1 TO 11
INPUT #1, n(i)
NEXT i
INPUT #1, E$

x = 15872 / 2 ^ n(2)

PRINT "Wafeform heeft"; x; " data punten."
PRINT "Tijd per punt="; n(6); "sec"
PRINT "Totale tijdsduur van de opname="; n(6) * x; "sec"
PRINT "Voltage range="; n(5) * 32000; "Volt"
PRINT "Oversturen van data naar PC.";
stap = 1
REM IF x > 6000 THEN stap = 2
REM IF x > 9000 THEN stap = 3
REM IF x > 15000 THEN stap = 4

PRINT #1, "D,6,"; wafe(channel, 2); ",0,"; MID$(STR$(INT(x / stap)),
2, 10); stap
INPUT #1, E$
PRINT #1, CHR$(19);
xon = 0
DIM D(x)
J = 10
FOR i = 1 TO INT(x / stap)
IF LOC(1) > 50 AND xon = 1 THEN PRINT #1, CHR$(19); : xon = 0
IF LOC(1) < 10 AND xon = 0 THEN PRINT #1, CHR$(17); : xon = 1
H$ = INPUT$(1, 1)
l$ = INPUT$(1, 1)
IF LOC(1) > 50 AND xon = 1 THEN PRINT #1, CHR$(19); : xon = 0
D(i) = CVI(H$ + l$)
IF LOC(1) > 50 AND xon = 1 THEN PRINT #1, CHR$(19); : xon = 0
NEXT i
PRINT
INPUT #1, E

PRINT "Klaar."

hz = n(8) * 65636 + n(9)

```



```

terug:

INPUT "Filename: "; file$
ON ERROR GOTO fout
filebestaad = 1
OPEN file$ FOR INPUT AS #5
CLOSE
verder:
ON ERROR GOTO 0
IF filebestaad = 1 THEN BEEP: PRINT "File bestaat reeds!!": GOTO
terug

OPEN file$ FOR OUTPUT AS #2
FOR i = 1 TO INT(x / stap)
PRINT #2, (i - hz) * n(6) * stap, (D(i) - n(7)) * n(5)
NEXT i
CLOSE
PRINT
PRINT "Geef toets voor volgende sessie, escape is stoppen";

LOCATE , , 1
k$ = INPUT$(1)
LOCATE , , 0
IF k$ = CHR$(27) THEN END ELSE RUN

fout:
CLOSE
filebestaad = 0
RESUME verder

```